TIME DOMAIN REFLECTOMETER IRREGULARITIES IN OPTICAL FIBRES

Thesis

The Open University

BACHELOR OF PHILOSOPHY DEGREE

TIME DOMAIN REFLECTOMETER IRREGULARITIES IN OPTICAL FIBRES

P. S. ROGERS

BACHELOR OF PHILOSOPHY DEGREE

TIME DOMAIN REFLECTOMETER IRREGULARITIES IN OPTICAL FIBRES

Author's number: M 7022334
Date of submission: 21 August 1989
Date of award: 1 February 1990

P. S. ROGERS

CONTENTS

SUMMARY

The aim of this thesis is not to present any new information but to critically review work carried out on optical fibre measurements with a particular interest in irregularities or perturbations present using the backscatter technique by Optical Time Domain Reflectometry.

Optical fibre structure, principles of operation and manufacture are examined as are the principles and practicalities of the various characterising optical fibre measurements.

An in-depth review of the most pertinent of the references considered is also included. Finally the practical work undertaken is described and conclusions presented.

EX12

HIGHER DEGREES OFFICE

LIBRARY AUTHORISATION FORM

STUDENT: P. S. ROGERS SERIAL NO: M7022334

DEGREE: B Phil

TITLE OF THESIS: TIME DOMAIN REFLECTOMETER IRREGULARITIES IN OPTICAL FIBRES

I confirm that I am willing that my thesis be made available to readers and maybe photocopied, subject to the discretion of the Librarian.

SIGNED: _____ DATE: 12/4/81

INTRODUCTION

In the late 1970's and early 1980's, STC Submarine Systems were involved in setting up and operating an optical fibre manufacturing unit in Harlow, Essex. The technology necessary for this plant came from the STC Research Laboratories, also in Harlow, where some years earlier Optical Fibres had been invented by Kao and Hockham (1).

My position in the manufacturing unit in 1982 was as a Senior Engineer responsible for the development and implementation of Test Methods and Test Equipment to enable fully qualified and documented Optical Fibres to be released and eventually cabled at the STC cable factory in Newport, Gwent.

Initially all the throughput was tight jacketed multimode fibre (both step and graded index) whose nominal dimensions were 50um core, 125um cladding, 250um elastomer primary coating and finally a nylon secondary coating of 0.8mm or 1mm. However single mode fibres with a nominal core diameter of 8um (other dimensions remaining the same) were soon introduced. Chapter 1 describes the structure, principles of operation and manufacture of the various types of fibre and the necessary theoretical support.

In qualifying a fibre, a number of key parameters are measured and at that time 100% testing was utlised on fibres whose nominal length was 1km. These measurements included cross-sectional dimensions using standard glass lens microscopy, attenuation (both monochromatic, 850nm and 1300nm, and spectral), dispersion (for bandwidth calculations), NA (spot on the wall and far field

radiation) length (by direct measurement during drumming) strength (by proof testing) temperature vs attenuation (on a batch sample basis) and backscatter. In addition, for single mode, (1300nm), mode field diameter or radius (spot size) and mode cut off. Note dispersion measurements of single mode fibres were only made during initial qualification confidence testing and on a sample basis, not on a regular production basis. These measurements were performed using a Raman laser (Nd:YAG). Chapter 2 describes these tests in more detail with any necessary theoretical support.

Of all the measurements made on fibres at that time the most subjective was back scattering or OTDR (Optical Time Domain Reflectometry) and it led to much debate, disagreement and fibre rejection. It was also considered by purchasers of fibre not to be accurate enough for length measurement. I was therefore tasked to put forward proposals for pass-fail criteria using OTDR equipment techniques that could be repeated and demonstrated to customers' Quality Assurance representatives. It was during this review that certain perturbations were observed that were not easily identifiable and warranted more in-depth investigation. With the financial support of STC this follow up investigation was performed and is described in Chapter 4.

The first task undertaken was a literary review. This was not only to gain general background information concerning OTDR techniques and practical experimentation but also to determine whether similar perturbations and backscatter signatures to those discovered were catalogued.

Approximately fifty references were obtained, some rejected immediately as not being specifically relevant, some superficially studied (1-21) and some reviewed in depth (22-31). All of these papers deal with conventional OTDR's however investigations were attempted using a coherent OTDR (32).

Of the references studied in depth, Chapter 3 is a resume of the salient points and possible indications to the observed perturbations.

CHAPTER 1

OPTICAL FIBRE STRUCTURE, PRINCIPLES OF OPERATION AND MANUFACTURE

1.1 Optical Fibre Structure

An optical fibre whether single mode or multimode has the same basic structure. Figure 1 shows the mechanical parameters of a fibre ie. the core, cladding, elastomer or acrylic primary coating and nylon secondary coating (which may not be tight fitting if the `loose tube' principle is adopted). The various regions are of a coaxial arrangement with the core and cladding consisting of homogeneous glasses (figure 1a). In this case the refractive index of the core is fixed and higher than that of the cladding to enable `guiding' of the light wave and is termed `step-index' due to the step-like function of the regions. Where the core of the fibre has a refractive index distribution that is not constant (inhomogeneous) but varies as a function of the radial co-ordinate it is termed `graded-index' (figure 1b). Single mode fibres are always of the step-index construction where as multimode fibres may be either step or graded index.

1.2 Optical Fibre Principles of Operation

1.2.1 Refractive Index and Propagation

According to geometrical optics, when light passes from an optically dense to a rarer medium total internal reflection without transmission occurs for angles of incidence on the interface which are greater than the critical angle c, given by $\sin c = n_2/n_1$, where n_1 is the refractive index of the denser medium and n_2 of the rarer. However, more

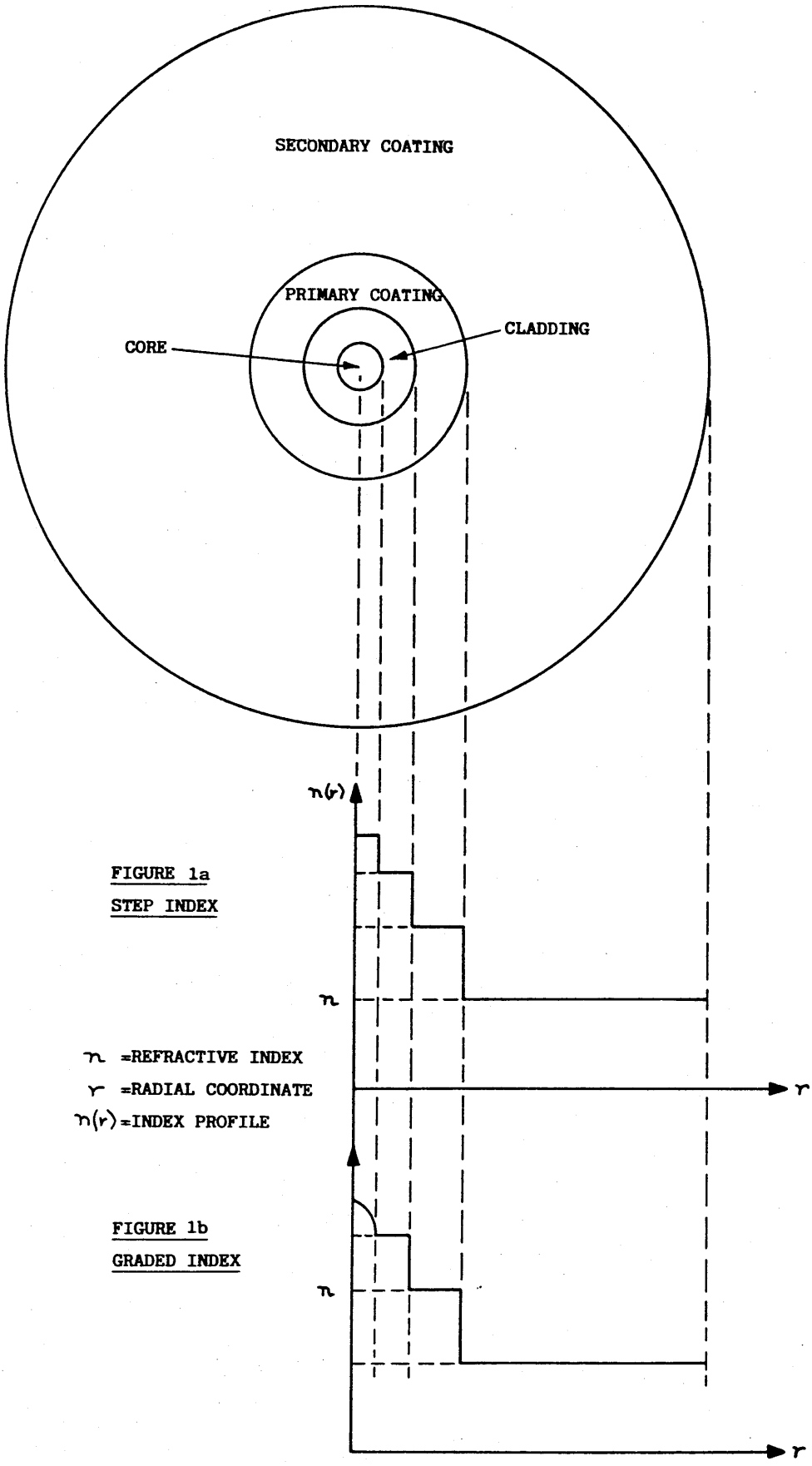

FIGURE 1a
STEP INDEX

n =REFRACTIVE INDEX
r =RADIAL COORDINATE
$n(r)$=INDEX PROFILE

FIGURE 1b
GRADED INDEX

Figure 1

detailed analysis using wave theory indicates that some penetration of the second medium does in fact occur. This penetrating wave, known as the `evanescent wave' has an exponentially decaying amplitude and is a standing wave. Within two or three wavelengths of thickness, this wave decays to negligibly small values and although energy is stored in this wave it is not propagated. If a second boundary however, is placed within two or three wavelengths of the first so that the evanescent wave reaches it with some finite amplitude, then propagation occurs and is known as `frustrated internal reflection'. Hence if a fibre makes perfect contact with some other material or with another fibre, transmission will occur with consequent light loss from the first fibre. Even if this contact is not perfect but exists with a wavelength or so separation, frustrated internal reflection will cause losses. To prevent this, fibres are coated with a material of lower refractive index. This coating not only helps to reduce surface scattering but with a suitable good quality material will keep the evanescent wave absorption low. Naturally the refractive index vs the source wavelength is an important consideration.

1.2.2 Guided Modes

Optical fibres can support a number of guided waveforms called modes. Single mode fibres, as the name suggests, support only one mode which can exist in two mutually orthogonal polarisations whereas multimode fibres support hundreds to thousands of modes. The total number of modes that can be

carried depends on the parameter known as the V number where $V = n_1 ka \sqrt{2\Delta}$, where n_1 is the maximum value of the core index, k is the propagation constant of a plane wave in free space and may be expressed as $2\pi/\lambda$ where λ is the vacuum wavelength of the source injected into the fibre, a is the core radius and Δ is the relative difference between the maximum refractive index and the cladding value n_2.ie.

$\Delta = (n_1^2 - n_2^2)/2n_1^2$. For step-index fibres the total number of guided modes of both polarisations is $N = \frac{1}{2}V^2$.

1.2.3 Numerical Aperture (NA)

As the angle of incidence at the fibre wall must exceed the critical angle in order for light to be propagated along the fibre without significant losses, this places a constraint on the angle of incidence and hence brings to the fore the importance of the parameter known as the numerical aperture (NA). As well as being related to the maximum angle at which radiation can be introduced in the fibre core it also dictates the angle at which it radiates into space when escaping from the end. By using Snell's law it can be shown that the entry or exit light beam $NA = n_0 \sin \theta$ where n_0 = refractive index of air which approximates to 1 and θ is the half angle of the light beam cone. This relates to the fibre $NA = n_1 \sin \theta_c$ where θ_c is the angle of the (limiting) ray that can just be guided by the core. Also it can be shown that, $NA = n_1 \sqrt{2\Delta}$ and hence $= \sqrt{n_1^2 - n_2^2}$.

1.2.4 Cladding Modes

If the refractive index of the primary coating is less than that of the cladding then rays which escape into the cladding may be internally reflected and thus also propagated (figure 2). These so called `cladding modes' may appear to contribute to the transmitted power, but they are generally very lossy and may, if not eliminated, give misleading results in measurements of fibre attenuation. Hence for some measurements the use of cladding mode `strippers' is made by removing the low index coating and replacing it with high refractive index fluid in a trough.

1.2.5 Fibre loss

The intensity of light passing through any medium decreases exponentially with distance. Transmission losses are usually quoted in terms of decibels per kilometre by comparing optical input power P_i to output power P_o over 1 km length of fibre hence the loss = $10 \log_{10} (P_i/P_o)$ dB/km. There are a number of mechanisms that cause losses viz:

1.2.5 (i) Absorption losses.

These occur when the frequency of the light waves is such that oscillations are set up in atoms or molecules in the glass, thus converting optical energy into energy of motion (heat). This absorption can become quite high when the frequency of light is equal to the fundamental frequency or an overtone frequency of the mechanical oscillator (resonance) which can occur in the molecular structure of the glass or is associated with electron

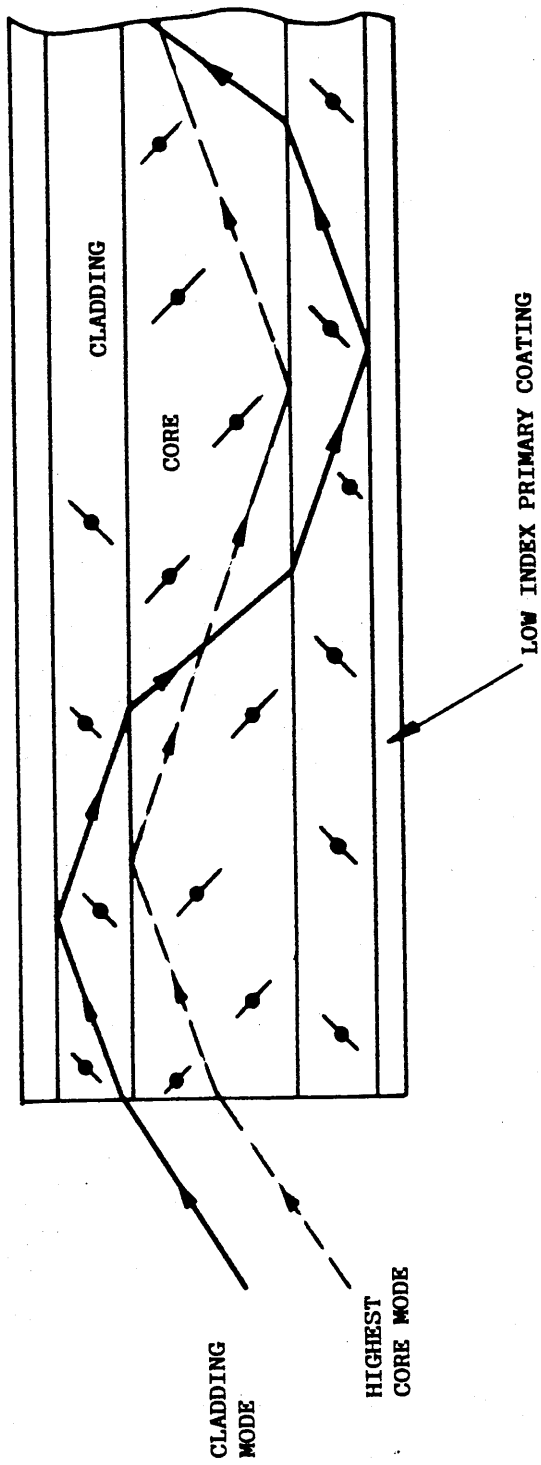
CLADDING
CORE
LOW INDEX PRIMARY COATING
CLADDING MODE
HIGHEST CORE MODE

Figure 2

transitions. A low intrinsic absorption window exists between 0.8 and 1.7 um (infra red region). More important are absorption losses due to impurities such as hydroxyl groups contributed by small traces of water, which are very hard to remove completely. These have stretching vibrations which resonate at 1.38 um, 0.95 um and 0.72 um hence it is desirable to use a source wavelength which avoids these resonances. Unless the fibre material is purified to a high degree, traces of metal ions such as iron, copper, cobalt and nickel can contribute significant absorption lines in the following regions respectively, 1.1 um, 0.8 um, 0.7 um and 1.2 um. Keeping the fibre materials free of such contamination is an expensive and demanding task.

1.2.5 (ii) Scattering Losses

Any kind of geometric imperfection or refractive index fluctations (inhomogeneities) that varies along the fibre axis causes modes to couple among each other or for energy to be completely lost from the guided mode. Coupling among guided modes does not cause losses however, not all of the modes are guided ones and are not all confined to the fibre core eg. cladding modes, hence imperfections of the fibre can couple guided modes to cladding and radiation modes that carry power away from the core and are thus associated with loss.

(a). Linear (Scattering without change of frequency)

(i) Rayleigh Scattering occurs at inhomogeneities which have dimensions much smaller than the source wavelength such as density variations, which cause refractive index fluctuations, and compositional fluctuations associated with the cooling of the glass. The attenuation is proportional to $1/\lambda^4$ so it is beneficial to operate at the longest possible wavelength. It should be noted that Rayleigh scattering sets the ultimate loss limit for an optical fibre.

(ii) Mie scattering occurs at inhomogeneities comparable in size to the source wavelength such as bubbles, strains, variations in diameter and irregularities in the core-cladding interface. These can be reduced to insignificant levels by careful manufacture.

(b) Non-linear (Scattering with changes of frequency)

(i) With Stimulated Brillouin Scattering, incident photons react with the glass lattice to produce phonons of acoustic frequency and scattered photons of a different frequency, which are lost from the system. This scattering occurs mainly in the backward direction.

(ii) Stimulated Raman Scattering is similar to Brillouin scattering but phonons have an optical frequency. This is mainly a forward scattering process. Both of these scattering processes occur only when a certain threshold optical power is exceeded and in practice this can be avoided.

From all of the above fibre loss mechanisms it can be seen that single mode fibre loss is intrinsically lower than multimode fibre loss.

1.2.5 (iii) Bend losses.

These occur because part of the mode on the outside of the bend must travel faster than that on the inside to maintain the wavefront perpendicular to the direction of propagation. If this requires a speed greater than that of light, energy will be radiated away (Einstein's Theory of Relativity).

There is a critical radius of curvature for a fibre in normal use dependent on the source wavelength and the refractive indices of the core and cladding. For single mode fibres operated at long wavelengths the value is approximately 1 mm which is easily avoidable in practical systems.

An associated problem is microbending losses due to irregular changes in the direction of the fibre axis which may be caused by strains induced by the secondary coating or the cabling process. These microscopic bends therefore have a very small radius and hence result in radiation losses. Microbending is minimised by controlled coating and cabling.

1.2.5 (iv) System losses

These losses are associated with fibre coupling to the source and detector, jointing etc. Light is lost between source and fibre due to their differences in

size and shape and if the light acceptance cone (dependent on NA) of the fibre is exceeded. For example a flat geometry LED acts as a Lambertian radiator ie. a point source with a cosine intensity distribution, hemispherical LED's are equivalent to an isotropic (light emitted in all directions) point source over $\pm 45^{o}$. Hemispherical emitters lose 3 dB more than flat emitters, however, the useful light emitted is 10 dB more producing overall gain. Also high NA fibres collect more light than low NA fibres. Fresnel reflections occur at every interface between media of different refractive indices causing loss. Misalignment or mismatch of fibres due to concentricity errors etc and in connectors, causes loss. If the sensitive area of the detector is less than the fibre emergence cone (opposite of the acceptance cone at the input of the fibre) then losses will occur.

Because of the different causes of loss in a system the system loss budget is important. In this way an assessment of the loss in a system can be ascertained by the addition or the individual losses and with a suitable margin for error built in, adequate transmission can be maintained.

1.2.6 Dispersion

Most optical fibre communication systems employ pulses of light to convey information from one end to the other. If the input pulses arrived at the fibre end unchanged, except for a decrease in pulse energy, the pulses could be detected unambiguously as long as they carry sufficient energy. The maximum repeater spacing would then only be limited by attenuation. However, pulses increase in length (if we look at them at one instance in time) or in duration (if we look at them at one point in the fibre). This increase in pulse length with distance of travel in the fibre is caused by dispersion. There are different physical reasons for pulses to increase in length and hence are categorised into material, waveguide and intermodal dispersion as follows.

1.2.6 (i) Material Dispersion

This is the most fundamental type. It is caused by the wavelength dependence of the refractive index of glass and is related to resonances in the dielectric material. If the light source generating the pulse was strictly monochromatic, the spectral width of the light signal would only depend on the shape of the pulse. However, as most optical light sources have a spectral source width in excess of the spectral width of the pulse itself the pulse is produced by a large number of monochromatic sources each with a slightly different frequency hence the pulse will spread out over a time

interval due to the wavelength dependence of the refractive index.

If the dispersive properties of the dopant material used to give the waveguide its properties differ from those of the host glass then the group velocity of light is different at different radial positions in the fibre core. This is known as profile dispersion and it can be compensated for by shaping the refractive index profile of the core to take it into account.

1.2.6 (ii) Waveguide dispersion

The waveguiding mechanism itself in a fibre contributes to the overall pulse broadening ie. the group velocity varies with wavelength for a given mode. Waveguide and material dispersion are not additive.

1.2.6 (iii) Intermodal dispersion

Fibre imperfections cause coupling among all the different kinds of modes of the fibre. Coupling among guided modes has a beneficial effect on intermodal dispersion. Since this dispersion is due to differing propagation velocities for different modes and hence different arrival times of the modes at the detector thus some improvement results if power is coupled among the guided modes. A portion of the pulse, which may have been travelling at more than the average speed can couple to slower modes that retard its progress. Averaged over all the modes the spreading of the pulse width is much reduced if the modes are tightly coupled.

Unfortunately, it is very hard to cause effective coupling among all guided modes without coupling guided core modes to cladding and radiation modes. Improved pulse performance due to mode coupling is thus bought at the price of increased losses.

Intermodal dispersion is high in step index fibres, however it is much reduced in graded index fibres.

1.2.6 (iv) Characteristic Dispersion mechanisms in single and multimode fibres.

As single mode fibres only support one mode, albeit in two mutually orthogonal polarisations, they do not suffer from intermodal dispersion. However, in the case of ellipitical deformation of the nominally circular fibre cross section, the two orthogonal polarisation states would travel at slightly different velocities causing an intermodal delay problem. Both types of fibre experience material dispersion and waveguide dispersion.

If lasers are used as the source, chromatic dispersion is usually less pronounced than intermodal dispersion giving single mode fibres the potential for much larger bandwidth (which is directly dependent on dispersion) compared with multimode fibres. In fused silica, material dispersion vanishes at a wavelength near 1.3 um. The point of overall vanishing (first order) dispersion is shifted by the contribution of waveguide dispersion. If desired, the zero dispersion wavelength

of single-mode fibres can be shifted into the vicinity of 1.5 um to coincide with a loss minimum. If operated at the minimum dispersion wavelength single-mode fibres can achieve bandwidths of thousands of GHz.

1.3 OPTICAL FIBRE MANUFACTURE

1.3.1 Introduction

Optical fibres are commonly manufactured from either plastics, silica or silicate glasses. Those constructed from a transparent polymeric material have the advantages of large diameter (e.g. up to 1 mm) flexibility and ease of termination and jointing. Set against this is the high intrinsic absorption in polymeric materials and their considerable temperature sensitivity which limits their application to short distance communication and telemetry systems.

Silicate glass has been the traditional material used in the manufacture of optical fibres but it suffers from the drawback of high attenuation at the wavelengths used which are in the near infrared. Special glasses are therefore produced which are low in the absorbing ions of the transition metals (Cu^{2+}, Fe^{2+}, Ni^{2+}) and are also low in lead. A typical glass composition is 70% SiO_2, 24% Na_2O and 6% CaO by weight.

1.3.2 Optical Fibre Core and Cladding

For many years, fibres have been manufactured by the `rod and tube' method in which a concentric glass rod and glass tube of different refractive index are heated in a furnace and then drawn out into a thin fibre. During drawing the core and

cladding glasses maintain their respective geometrical relationships even though the fibre is drawn down through a diameter reduction of 300:1. Alternatively, glass fibres can be extruded directly from concentric platinum crucibles containing the core and cladding glasses in a molten state. Glass rods are first drawn from purified batch materials of core and cladding compositions and then these are used as a feedstock for the two crucibles. Fibres are drawn from the concentric orifices at the lower end of the crucibles. This technique is rarely used nowadays as it is too difficult to control the respective diameters of the concentric fibres.

Silica (SiO_2) exhibits very low intrinsic optical loss which makes it an ideal candidate for the manufacture of optical fibres. It has some serious drawbacks however, since its softening point is approximately 1400°C as compared to 700°C for glass and it has a very low refractive index so that its cladding requires a still lower index. As a result of these natural obstacles, various special manufacturing techniques have been developed. In all cases a `preform' is made and then is subsequently drawn down in diameter using the pulling technique. This entails clamping one end of the preform and heating the other end in a furnace. The melted glass is drawn into a hairlike thread by winding onto a drum driven at constant speed with feedback from the fibre diameter measuring equipment. It is an important characteristic of this pulling process that the shape of the refractive index profile of the preform is preserved and can be found in the

fibre core (except for a scale transformation of the radial co-ordinate).

Preforms are usually produced nowadays not from two concentric rods but from a rod or tube coated internally or externally with a dopant which alters its refractive index. Dopant deposition is normally from the vapour phase utilising the decomposition of metal or semi-metal halides. GeO_2 is the dominant dopant for increasing the refractive index of SiO_2 so the decomposition of $GeCl_4$ is frequently utilised. The addition of P_2O_5 via the decomposition of $POCl_3$ increases the refractive index of the glass and also reduces the viscosity of the hot glass. F^- ions will reduce the refractive index of SiO_2 when used with P_2O_5.The thermally decomposed halide mixture which is deposited on the silica is frequently called a `soot'. There are three basic vapour phase processes as follows.

1.3.2 (i) Inside vapour decomposition (IVD)

This involves the deposition of soot layers on the inside of a tube of pure silica or high silica glass. The rotating tube is heated externally by a repeatedly traversing oxy-hydrogen burner to thermally decompose the gases which are flowing down the tube. A mixture of $SiCl_4$ and O_2 is continuously passed and initially this is mixed with CCl_2F_2 (di-chloro,di-fluoro, methane) to produce F^- dopant ions so as to lower the refractive index and make the cladding. Subsequently this dopant gas is changed to $GeCl_4$ and $POCl_3$

whilst still retaining $SiCl_4$ to deposit the matrix material. Germanium raises the refractive index to form the core and P_2O_5 reduces the softening point of the glass. The next step is that the tube is heated under vacuum and it collapses on itself. The lower melting point core fuses together very readily. After cooling the fibre is drawn from the preform.

1.3.2 (ii) Outside vapour deposition (OVD)

This technique consists of building up a coating of soot on the outside of a solid silica rod by thermal decomposition of vapours passing through a burner. The burner traverses a rotating rod and deposits soot to the required thickness in a semi-sintered state. Upon completion, the rod is removed and zone sintered and although the cladding is still porous, it is used in this state for fibre drawing. One distinct advantage of this technique is the ability to manufacture large diameter preforms from which 100 km or more of 125 um diameter fibre may be drawn.

1.3.2 (iii) Vapour axial deposition (VAD)

A variation in the multistep OVD process is for the soot for the core and sometimes for the cladding to be simultaneously deposited to form a rod-like soot preform, on the end of a silica rod.

1.3.3 Primary and Secondary Coating and Cabling

Once the core and cladding have been manufactured it is important that they are protected from surface damage or even atmospheric attack which can rapidly affect the considerable tensile strength of the bare fibre. This is prevented by the primary coating which is applied immediately after fibre drawing and is usually an `on-line' process, and the addition of the secondary coating as an extruded tight jacket or as a loosely fitting sleeve in the loose tube design. To improve handling and for ruggedisation the secondary coated fibres can be cabled which would feature some form of tensile strength member and a tough outer sheath to provide the necessary mechanical and environmental protection.

The failure of fibres generally occurs as a result of microscopic surface flaws which occur infrequently and at random intervals. Resistance to crushing and impact loads is provided primarily by the cushioning effect of the outer cable sheath, although even secondary coated fibres exhibit considerable tolerance to physical abuse. Resistance to bending failure is important as the cable will probably be subjected to a considerable degree of bending during its life on the reel and its installation. Cables will usually accept a minimum bend radius of 20 diameters although some may be bent down to 5 diameters. Current cable designs show very little attenuation change over the temperature range -15° C to +60° C and are unaffected by humidity. Primary coated fibre is stable over a very wide temperature range, however high temperature cables require expensive fluoropolymers as sheathing.

CHAPTER 2

OPTICAL FIBRE MEASUREMENTS

As stated in the introduction, to qualify an optical fibre a number of parameters are measured, each with its own pass/fail criteria set either by the manufacturer or the customer. This chapter will briefly describe the measurement techniques of the most important parameters.

2.1 Mechanical and Geometrical Properties

2.1.1 Fibre geometry

A short length of fibre is taken from each end of the fibre under test. One end of each short length is illuminated by a quartz-halogen light box and the other end viewed by a shearing glass-lens microscope connected to a video camera. By using the shearing effect and a video screen the following parameters can be examined.

2.1.1 (i) Average Core, cladding and primary coating radii.

The accuracy of these measurements depends on how well each individual boundary can be determined. These parameters are important to maximise transmission and to minimise launching and splice losses.

2.1.1 (ii) Ellipticity.

Ellipticity of the normally circular fibre cross section can cause intermodal delay problems and splice losses.

2.1.1 (iii) Concentricity.

Concentricity of the core to cladding will again affect splice and connector losses.

2.1.2 Proof testing

This is important as an indication of fibre strength particularly when fibres are to be used for cabling. If any physical deformities are present eg. bubbles or hairline fractures then the fibre will break under the stress of this test. The test is performed by winding the whole length via 5 pullies arranged into a 'W' shape which are all travelling at the same speed, however the lower 2 are of a slightly larger diameter, thus a controlled, calibrated, strain can be applied to the fibre over its complete length. Secondary coated fibres can withstand strains of up to 3%.

Before and after proof testing the fibre is backscattered using an OTDR to investigate any fractures or anomolies along the whole length.

2.1.3 Fibre length

2.1.3 (i) OTDR

Fibre length can be measured using an OTDR providing it is calibrated and the refractive index is known to sufficient accuracy. In this case the distance L from the fibre launch to any particular point (including the opposite end) is given by $L = (C/n_1)(t/_2)$ where c = speed of light in a vacuum, n_1 = refractive index of the fibre core and t = time delay from the oscilloscope/display (see section 2.2.1 (ii)). Accuracy of $\pm$5 m is typical. A number of examples of OTDR traces are included in Chapter 4.

2.1.3 (ii) Drumming

The most accurate method of measuring length is by winding the fibre from one bobbin to another (drumming), allowing the fibre to pass over a calibrated wheel connected to a counter giving a direct length reading. Accuracies of $\pm$0.1% are common however, recoverable stretching can cause problems if the winding tension is too high.

All of the above measurements/tests on the mechanical and geometrical properties can be performed on single and multimode fibres.

2.2 Transmission Properties

2.2.1 Attenuation

2.2.1 (i) The `cut-back' method.

The most accurate measurement of fibre attenuation is by the cut-back method. Referring to figure 3, the power emerging from the fibre at B is measured and then the fibre is cut to a length of about 3m, without disturbing the launch conditions, and then the power emerging from A is measured. If L is the length of fibre between A and B then the attenuation = $(1/L)\ 10\ \log_{10}(P_A/P_B)$ dBm^{-1}.

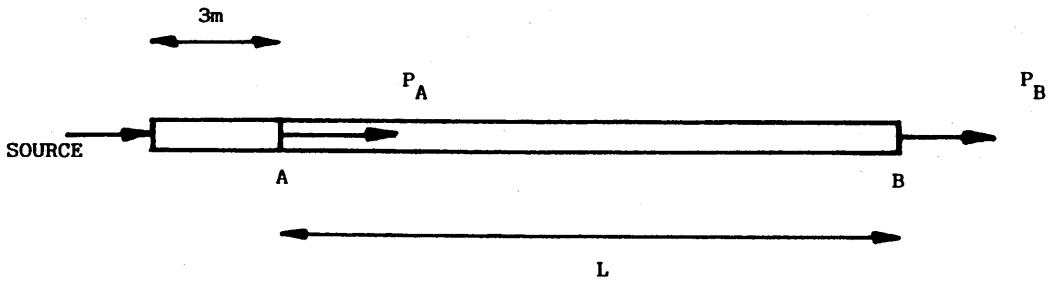

Figure 3

A block diagram of the necessary equipment is shown in figure 4. The source is usually a tungsten halogen lamp which is then chopped at approximately 200 Hz and the lock-in amplifier detects only this frequency thus eliminating the effects of background light. For monochromatic measurements at 850 nm and 1300 nm, the appropriate wavelength filter is introduced between the chopper and the focussing lens. For spectral attenuation measurements, eg. 750 nm to 1600 nm, the filter is replaced by a monochromator driven by a stepping motor with increments of 10 nm. The vacuum chuck holds the fibre in a fixed position and this may be secured to an XYZ manipulator for fibre alignment.

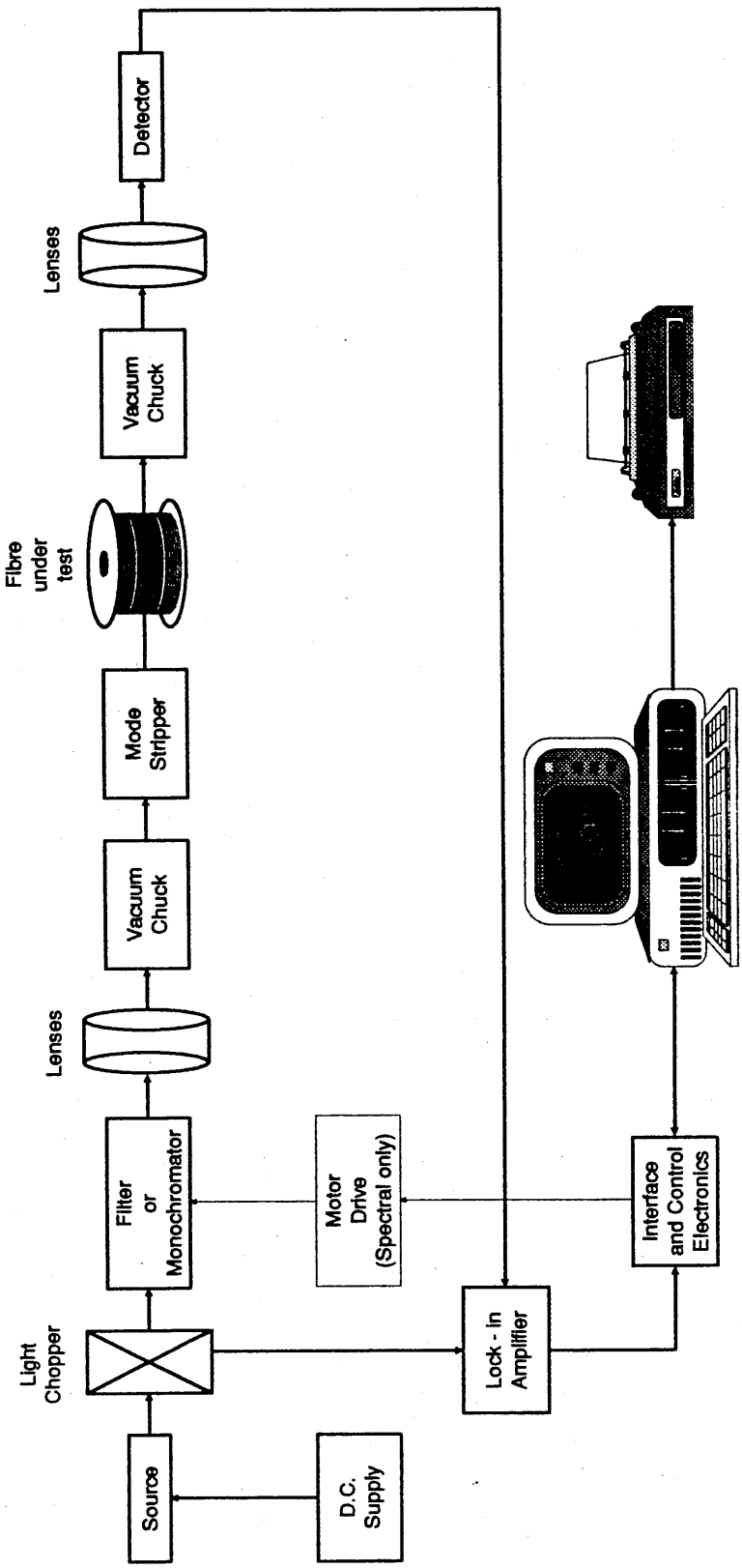
Detector
Lenses
Vacuum Chuck
Fibre under test
Mode Stripper
Vacuum Chuck
Lenses
Filter or Monochromator
Motor Drive (Spectral only)
Light Chopper
Source
D.C. Supply
Lock - in Amplifier
Interface and Control Electronics

Figure 4

Before the fibre is placed in the chuck, approximately 30 cm of secondary and primary coating is stripped off and the end is cleaved using a scribe or cleaving tool. The bare fibre is held in a trough of index matching fluid in order to strip out cladding modes which could cause measurement error. The other end of the fibre under test is then cleaved and positioned in front of the detector using a split-ferrule arrangement. The detector is fed to the lock-in amplifier and the necessary interfaces, mini computer and printer connected. Once the power signals have been recorded for the reel of fibre under test, the fibre is cut back, repositioned in front of the detector and the new power readings recorded. For spot wavelength measurements, the attenuation value is displayed on the computer screen, however, if spectral measurements are performed then the mini computer calculates the attenuation values at each wavelength and the printer delivers a trace of loss (dB) vs wavelength (nm or um). Figure 5 shows a typical example.

Cut-back attenuation measurements are also employed for temperature vs attenuation tests (single wavelength). This entails temperature cycling secondary coated fibre in a climatic chamber and recording power levels on a chart recorder during cycling to detect anomolies with the secondary coating extrusion process. The cut back is performed at the end of the test and hence

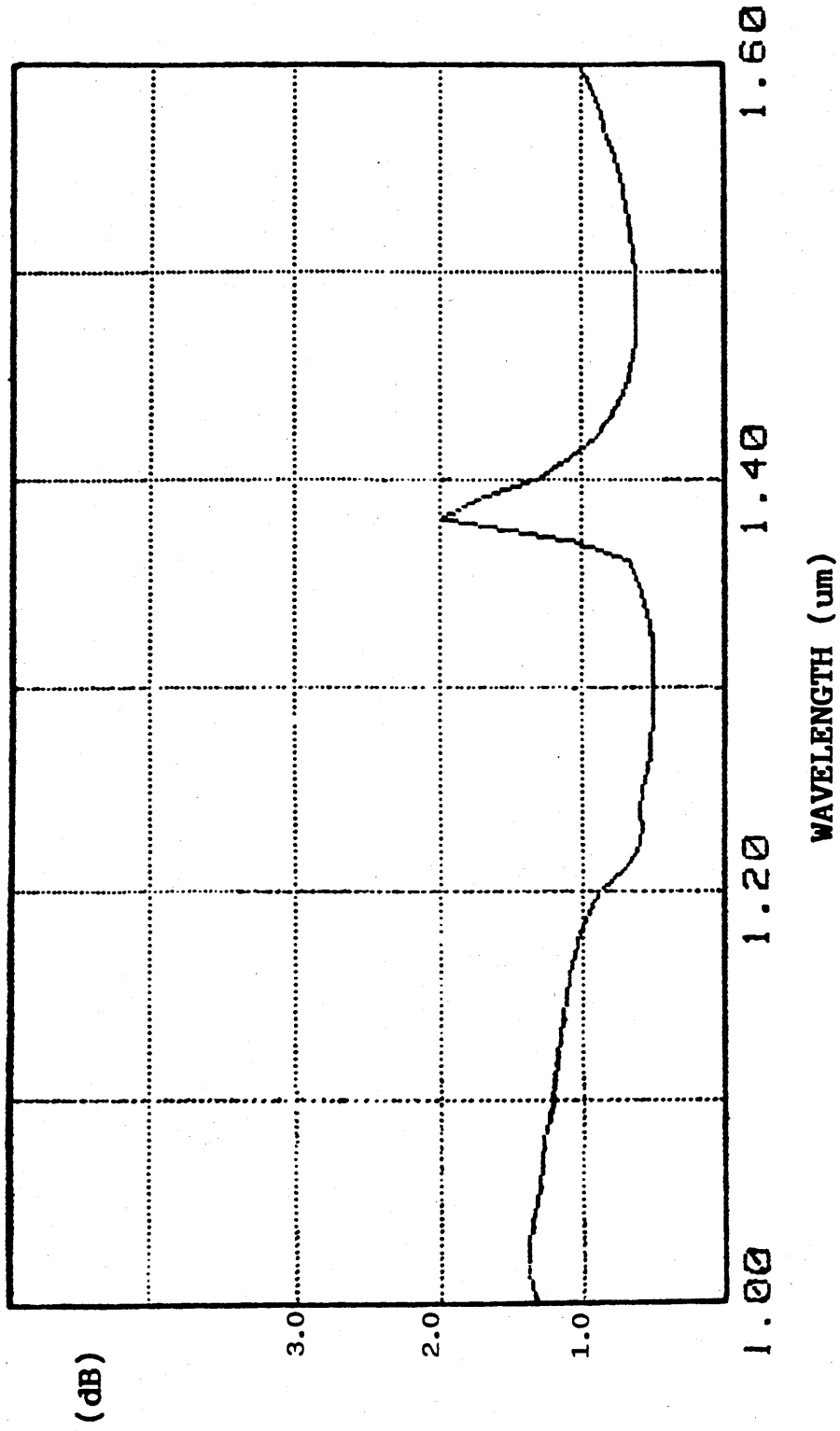

Figure 5

attenuation at any point on the cycle can be calculated. This is only performed on a batch sample basis with the pass/fail criteria applied at specific points on the temperature cycle.

The advantage of this method of attenuation measurement is its accuracy. The disadvantages are that it is destructive and only a single measurement for the whole fibre length is available (without further destruction).

2.2.1 (ii) The backscatter method by OTDR.

Time domain reflectometry makes use of the fact that the microscopic fluctuations of the refractive index and small flaws in the fibre cause light to be reflected. An isolated scatterer reveals its presence as a sharp spike in the back reflected signal and Rayleigh scattering, which is present everywhere, causes a continuous reflected signal of very low amplitude with a characteristic trace that is exponential in nature. Referring to figure 6, a pulsed laser source ranging from 5 to 200 nsec in width (AlGaAs injection laser or Q-switched Nd.:YAG laser) at a fixed wavelength, is injected into the fibre via a coupler. The backscattered light (scattering angle = 180°) re-emerges at the coupler and is fed to the detector, whose bandwidth is typically of the order of 20-40 MHz, processed (known time delays) and displayed on an oscilloscope or internal CRT. The received power is nominally 40 dB down on the injected power and its

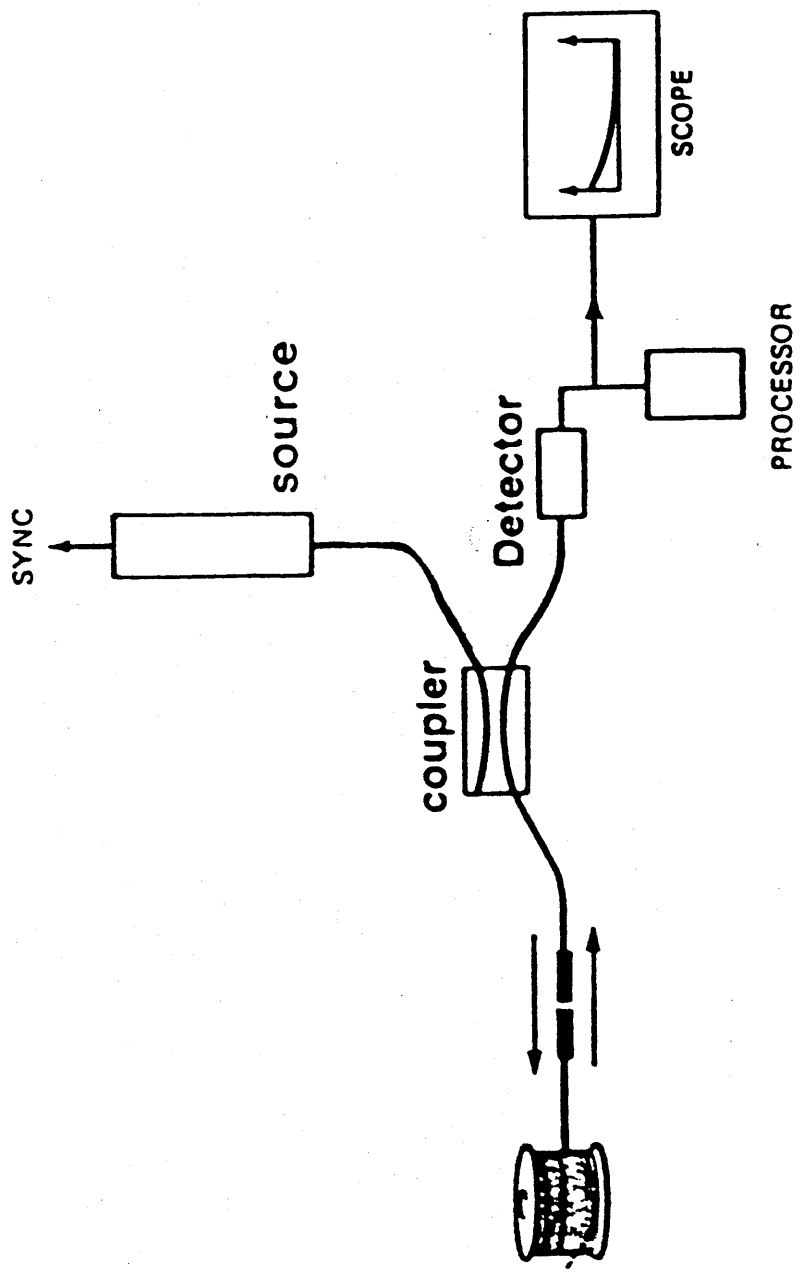

Figure 6

detection requires special electronics capable of identifying periodic signals that are buried in noise. An instrument of this kind is the boxcar integrator which samples the signal repeatedly in a narrow time slot and rescues the signal from the large background noise by summing over all the samples. Randomly phased noise cancels during the summation process while the signal adds coherently and builds up. The time slot used for taking the samples is slowly moved across the entire temporal range that is to be examined. Suppression of the undesirable reflection from the fibre end during laser injection (which, naturally, is very much larger than the received low level backscattered signal) is achieved by index matching or more commonly by using electronic gating of the detector to prevent it from overloading. Figure 7 shows the shape of various loss regions in diagramatic form that may be encountered when measuring a fibre.

One method of determining attenuation is from an experimental fit to the exponential decrease of the backscatter power. The usual method is to use a `least-squares' curve fitting routine to fit an exponential function to the backscatter signal. This gives a `best-fit' decay constant which is simply related to the attenuation under certain restrictive conditions. Where the fibre consists of two or more regions of different, but uniform, loss characteristics

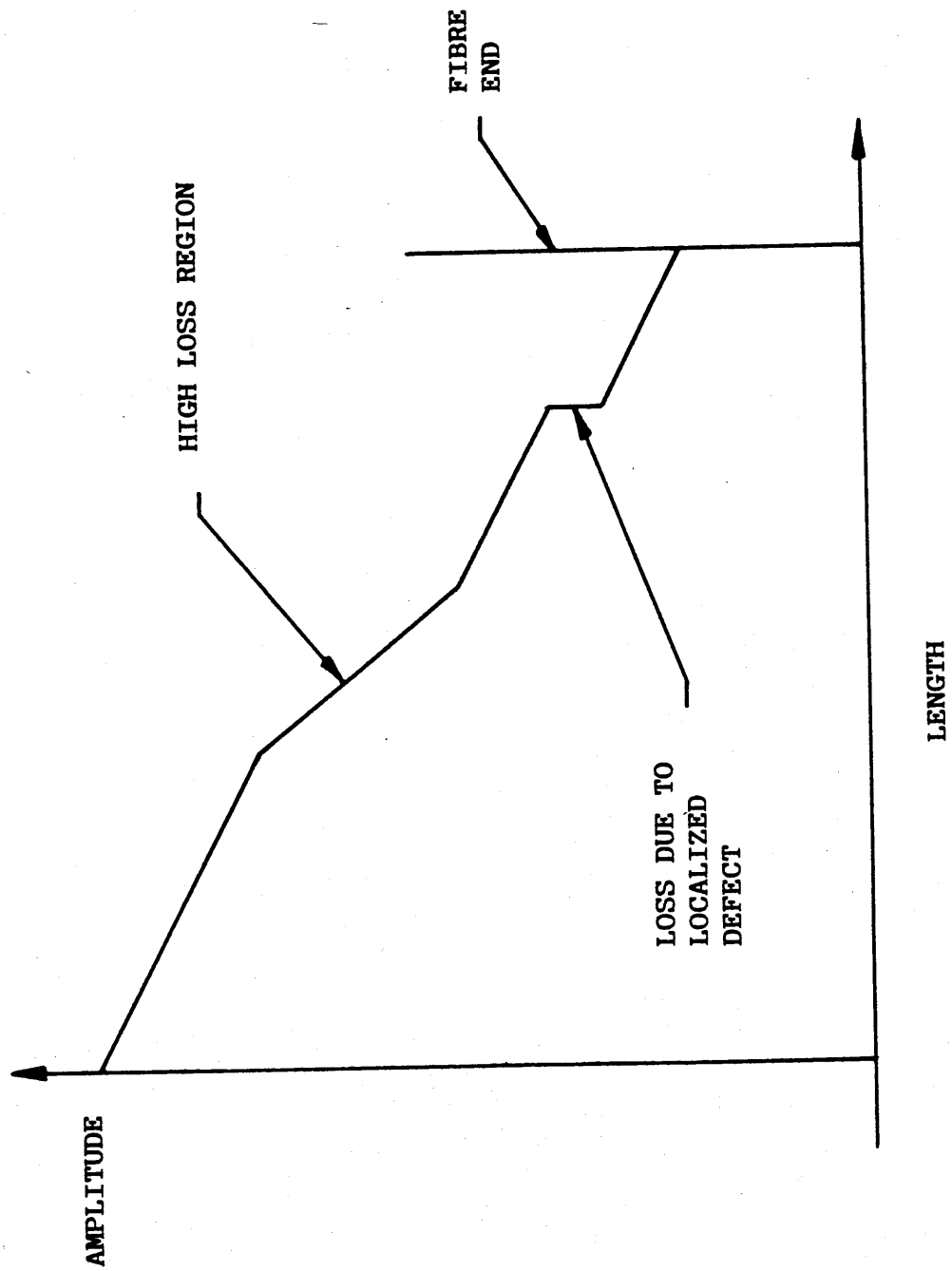
FIBRE END
HIGH LOSS REGION
LOSS DUE TO LOCALIZED DEFECT
LENGTH
AMPLITUDE

Figure 7

then a piecewise least-squares fitting can be performed over each region separately. It can be shown that for the least-squares fit situation, attenuation = 5(log e) $<\alpha>L$ dB where $<\alpha>$ is the best fit to the exponential decay and L is the length of fibre under consideration.

Another method is similar to the direct cut-back method of determining attenuation and is known as the `two point' method. In this case, the backscatter signal (P_A) from the input end at L = 0 is compared with the backscatter signal (P_B) from the point under consideration and the attenuation = 5 $\log_{10}$ (P_A/P_B) dB. Under certain conditions it can be shown that this approach gives closer agreement with the direct cut-back attenuation measurement than is obtained from least-squares curve fitting.

The advantages of the backscatter method of attenuation measurement are that it is non-destructive, can measure attenuation at any desired point on the fibre, thus enabling localised faults to be identified and cut out, and for field work it may be important that access to only one end of the fibre is necessary. The main disadvantage is that it is single wavelength. Reference 24 describes the principles of operation and individual components in more detail.

Although the above attenuation measurements can be performed on both single and multimode fibres it is important to note that where multimode fibre measurements are concerned, to prevent inaccuracies due

to non-equilibrium mode distribution, where losses are unpredictable, a mode scrambler may be incorporated.

The mode scrambler artificially mixes the modes and may consist of short lengths of fibre distorted by clamping between two pieces of rough sandpaper of by splicing together two short lengths of step index fibre and one short length of graded index fibre (step-graded-step). This scrambler is `butt jointed' between the fibre under test and the source. Mode scrambling can also be introduced directly into the fibre under test at the launch end by winding a few turns around a mandral of an appropriate diameter and clamping it in place. This is known as the `mandral wrap' method.

2.2.2 Single mode Fibre Cut-off Wavelength

The cut-off wavelength test is to ensure that the fibre under test is actually or sufficiently single mode. If the trace obtained from the spectral attenuation plot of a short length of fibre is examined then a marked drop in attenuation is visible in the 1150-1270 nm region (figure 5 (which is the plot for a long length of fibre) shows this to a lesser extent). This drop indicates where second order modes are no longer of importance and providing this cut-off is sufficiently far away from the source wavelength (commonly 1300 nm for communication systems) then no multimode characteristics will come into play. It is important to note that the cut-off is not sharp and a low attenuation `tail' is usually still present hence a 0.1 dB level is employed (see figure 8) for measuring purposes.

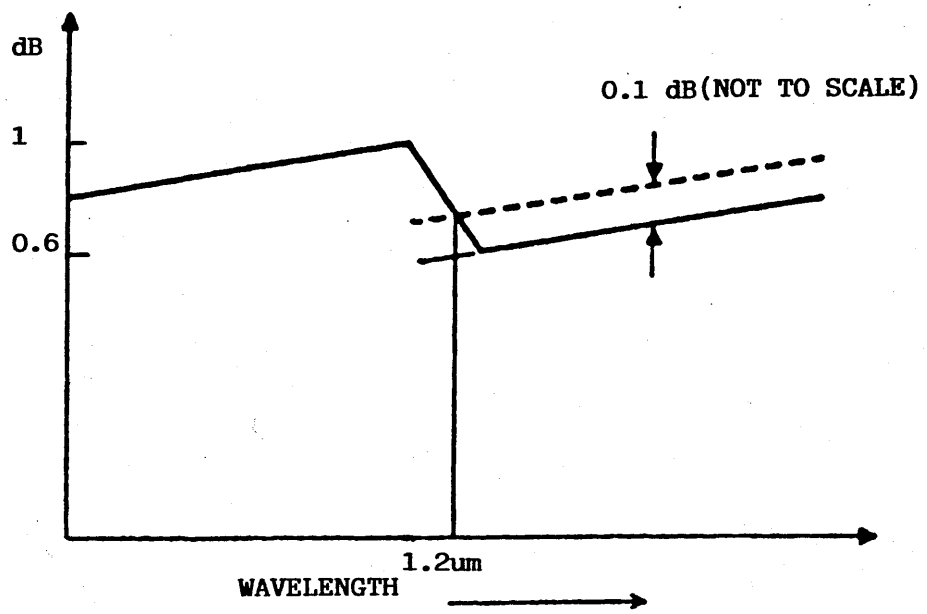

Figure 8

The same equipment as in section 2.2.1 (i) (as used for spectral attenuation measurements) is employed. A short length (2m) of fibre is used as the fibre under test and it is bent to form a loosely constrained loop in order to remove higher order modes thus giving good repeatability. The monochromator is then set for wavelengths around the expected cut-off wavelength. Once the power signals have been recorded they are compared with the transmission through a reference

fibre whose cut-off wavelength is significantly above or below that of the fibre under test. If the 0.1 dB point is difficult to compute then the wavelengh can be determined by drawing best-fit lines on the attenuation curve. Figure 9 illustrates an example of the cut-off region for a single mode fibre.

2.2.3 Single mode Fibre mode Field Diameter (spot size)

Due to the propagation characteristics of single mode fibres, (see Chapter 1) light travels in the cladding (even after cladding modes have been stripped out) and hence the diameter of light emerging from a fibre is not just the core diameter but also part of the cladding diameter. It is this emerging beam diameter that is known as the spot size and is commonly 9.2 um compared to a core diameter of 8 um at 1300 nm. The spot size is therefore important when splicing fibres or jointing to lasers, detectors etc.

The test equipment is similar to that used for spot attenuation measurement (see section 2.2.1(i)) and is performed with the 1300 nm filter in place and mode stripping at the detector end as well as the launch end. A short length of fibre (2 m) is used as the fibre under test and it is bent to form a loosely constrained loop in order to remove higher order modes. However, once the power reading has been recorded, the fibre is then cut in half and the 2 halves held in vacuum chucks which are fitted to motor driven butt stages. The halves are then `re-joined' by butting

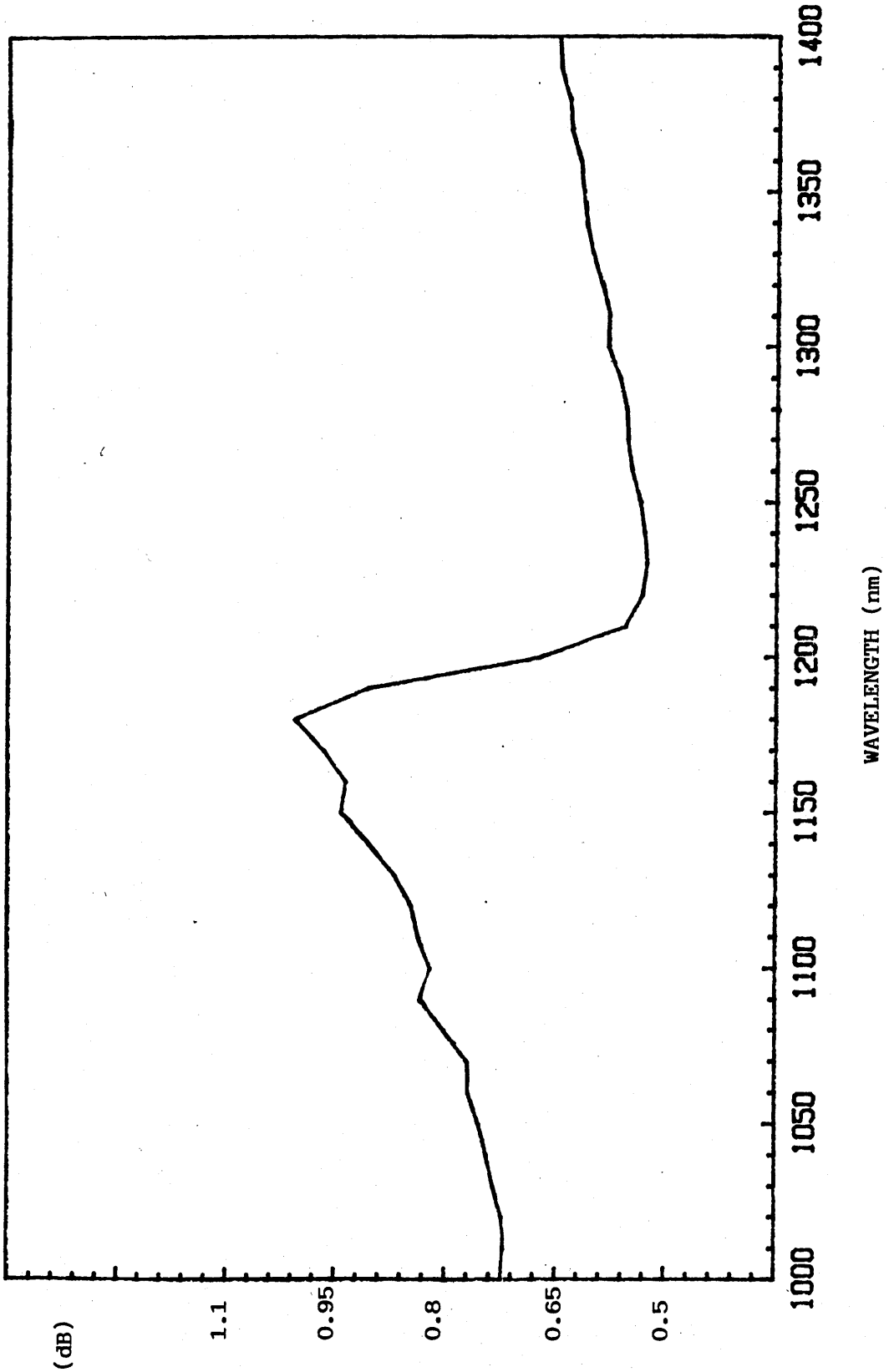
(dB)
1.1
0.95
0.8
0.65
0.5
1000
1050
1100
1150
1200
1250
1300
1350
1400
WAVELENGTH (nm)

Figure 9

together, maximised to greater than 90% of the previously recorded power reading, separated by a few microns and a drop of index matching fluid placed between them. The butt stages are driven by a precision controller capable of 0.1 um resolution such that the joint is offset in discrete steps. The optical power transmitted through the traversing joint is then measured and recorded. An approximate Gaussian distribution results and the distance traversed by the butt stages between the 1/e points (referenced to the maximised signal) is recorded This measured distance is the mode field diameter or spot size.

On a batch sampling basis spectral spot size is performed where the filter is replaced with the monochromator and the mode field diameter vs wavelength is calculated.

The pass fail criteria is decided by the application.

2.2.4 Dispersion

2.2.4 (i) Multimode fibre dispersion

As stated in Chapter 1, there are a number of contributing factors to dispersion or pulse broadening. Figure 10 indicates how the transmitted pulse is broadened to the received pulse. Dispersion can be thought of either as a line broadening (Time Domain characterisation) or a frequency broadening (Frequency-Domain characterisation) and the two are linked through Fourier transforms.

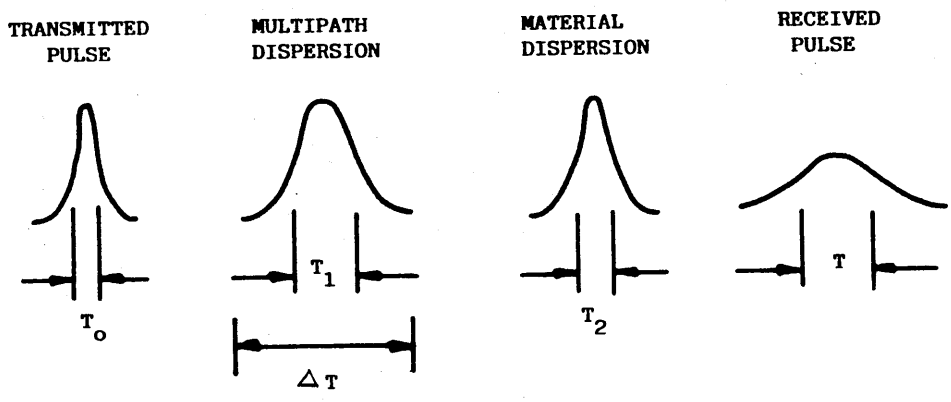

Figure 10

Dispersion is usually quoted as the pulse broadening in time per unit length (ns/km). The bandwidth of the fibre and hence its `communication capacity' is derived directly from the dispersion. Measurements are most commonly made in the time domain and referring to figure 11, the source is a laser with pulses of 100-400 pico second duration. A signal from the laser is fed via a digital delay generator to the trigger of a sampling oscilloscope. The delay generator compensating for the pulse delay in the fibre under test. The laser is fed to the fibre under test through a mode scrambler (to ensure repeatability) and the necessary lenses.

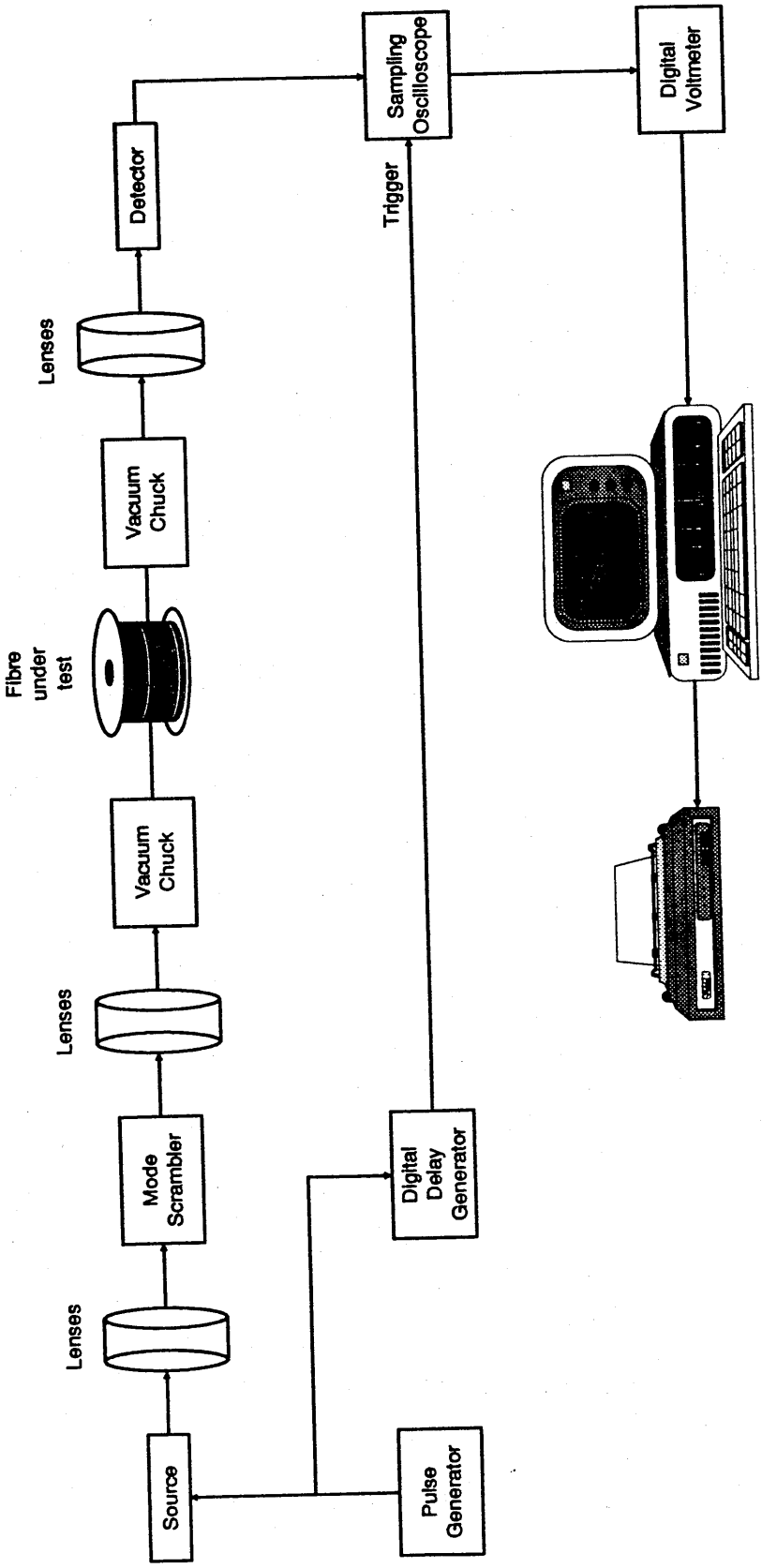
Source
Lenses
Mode Scrambler
Lenses
Vacuum Chuck
Fibre under test
Vacuum Chuck
Lenses
Detector
Pulse Generator
Digital Delay Generator
Trigger
Sampling Oscilloscope
Digital Voltmeter

Figure 11

One end of the fibre is cleaved and held in a vacuum chuck which may be secured to an XYZ manipulator for fibre Alignment. The other end is also cleaved and positioned using a vacuum chuck. This end of the fibre is aligned with the avalanche photo diode detector using a lens arrangement and the diode output is fed to the oscilloscope. The mini computer stores the pulses, which are digitised by the digital voltmeter, and averages. The fibre is then cut back to approximately 2 m and the operation repeated, with the mini computer storing and averaging the input pulses. The computer will then compare the input and output pulses and calculate the dispersion, D, from the following, $D = (T_0^2 - T_1^2)^{\frac{1}{2}} \; 1/L$ ns/km where T_0 is the full width at half height of the output pulse, T_1 is the full width at half height of the input pulse and L is the length of the fibre in km. Also computed, by Fourier transform, is the 3 dB Bandwidth in MHz.km. Figure 12 shows examples of typical time and frequency plots for multimode fibre.

This test method is appropriate for both of the common multimode fibre operating wavelengths viz 850 nm and 1300 nm.

2.2.4 (ii) Single mode fibre dispersion

Tests on single mode fibre dispersion are usually only conducted on a type approval basis or on a sample basis where very long lengths are to be employed between

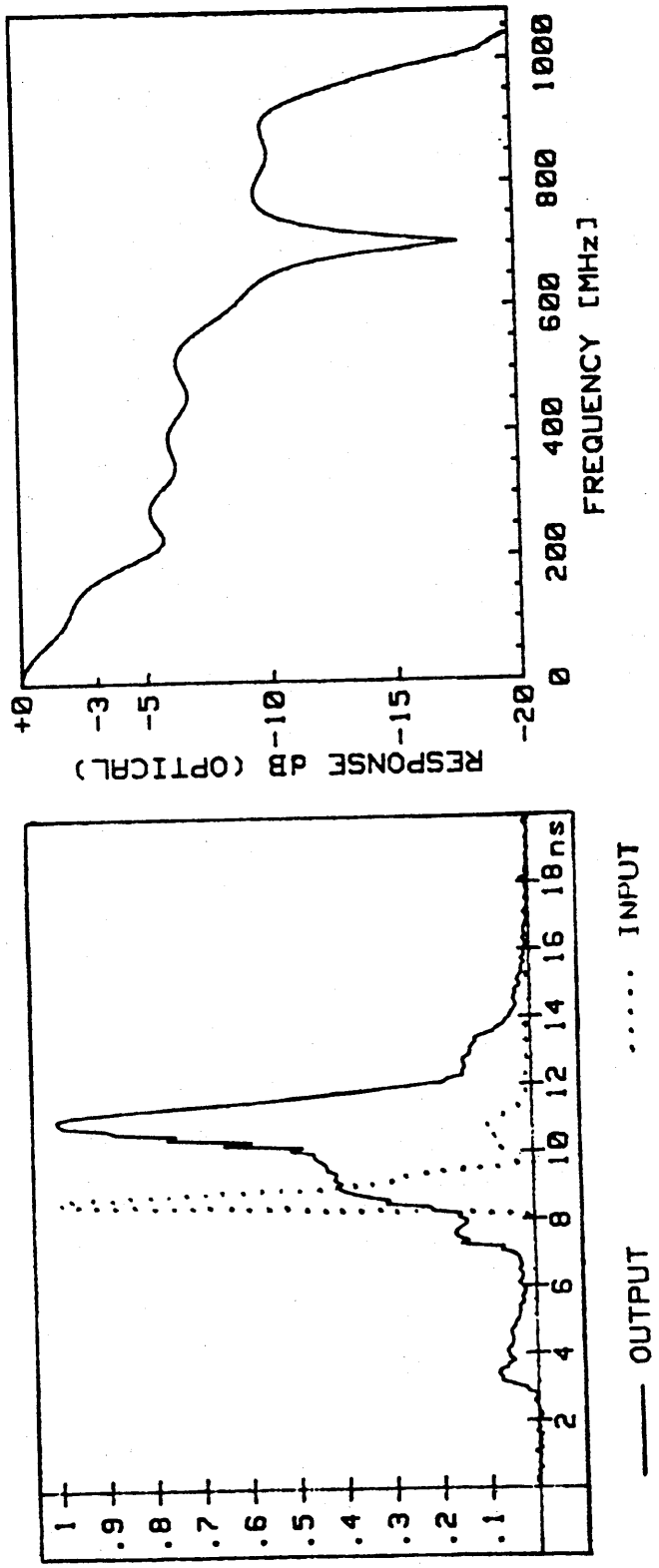
RESPONSE dB (OPTICAL)
+0
-3
-5
-10
-15
-20
0
200
400
600
800
1000
FREQUENCY [MHz]
1
.9
.8
.7
.6
.5
.4
.3
.2
.1
2
4
6
8
10
12
14
16
18ns
OUTPUT
INPUT

Figure 12

transmitter and receiver and hence dispersion is important. The measurement configuration is similar to the multimode case except it is chromatic dispersion that is being measured i.e. delay vs wavelength as material dispersion is now the dominant feature with the lack of intermodal delay. The laser source in this case is a Q-switched Nd: YAG unit operating at 1.06 um wavelength which supplies approximately 1 kW of pulse power to a single mode, low loss, specially doped `Raman fibre' of 176 m length enabling a tunable optical source to be obtained. The high power is necessary to stimulate the Raman fibre thus obtaining a series of peaks or lines at 1.12, 1.18, 1.24, 1.31 and 1.44 um and at the maximum power these lines shift into each other giving a continuous spectrum, of varying amplitude, from 1.18 um to 1.7 um.

By using a monochromator, individual wavelength pulses are fed to the fibre under test which are detected and displayed in a similar way to the multimode case as is the necessary delay for triggering. Again the cut-back process is undertaken to obtain the input reference pulses and the same equation employed, however as a number of wavelengths are involved the chromatic dispersion is expressed in ps/(nm.km). This leads on to the important chracteristic in single mode fibre dispersion measurements which is the `zero-dispersion wavelength' ie. that wavelength at which the chromatic dispersion vanishes (see section 1.2.6(iv)).

2.3 Optical Properties

2.3.1 Numerical Aperture (NA)

2.3.1 (i) The `spot on the wall' method (for multimode fibre)

In this measurement a short length of fibre is mode stripped and launched at one end with a He-Ne laser via lenses. The other end is held in a split ferrule and clamped to an optical bench such that the emerging light is displayed on a target screen and the distance from fibre end to screen can be measured. The screen consists of three concentric circles whose diameters are 8, 10 and 12 cm. The fibre end is traversed along the optical bench and positioned each time so that the cone of light fills each of the three circles in turn. The distance from the fibre end to the screen is noted in each case. One definition of NA is the sine of the half angle of the cone of rays leaving a short length of fibre (under conditions where the highest order guided modes are launched) ie, NA =sin $(\tan.^{-1}(D/2d)$ where D = circle diameter and d = distance from the fibre end to the screen. The NA value for the three circles must fall within a specified pass/fail band.

2.3.1 (ii) The far field radiation method (for multimode fibre)

The test equipment is similar to that used for spot attenuation measurement (see section 2.2.1(i)) and is performed with the 1300 nm filter in place. A short length of fibre (2 m) is used as the fibre under test and the launch end is identical. The detector has a pin

hole placed in front of it (or a small area detector can be used) and the receive end of the fibre is attached to a goniometer such that the fibre can be scanned in front of the detector in an arc. The goniometer is adjusted until a maximum signal is obtained and this is recorded by the mini computer. The optical power detected by scanning across the pin hole is recorded and an approximate Gaussian distribution results. The angle subtended by the goniometer between, typically, the 5% signal points (referenced to the maximised signal) is recorded and the NA is calculated from its definition as the sine of the half angle.

NA measurement is not so accurate and to some extent not so important for single mode fibre and hence is not usually performed. It is replaced by the spot size measurement which produces sufficient information on the entry or exit light beam for accurate splicing and jointing etc.

CHAPTER 3

LITERARY REVIEW

This section is the in depth review of 11 references, undertaken to gain background information concerning OTDR techniques and practical experimentation as well as to determine whether general OTDR perturbations had been investigated and catalogued. The reference numbers refer to the listing in Appendix A.

3.1 Reference 22

Characterizing Optical Fibres with an OTDR

This work showed graphical information pertaining to backscatter signatures however it appears that this was drawn rather than being actual photographs. It was useful by indicating that non-uniformities are caused by diameter variations, area mismatch losses due to splices and interconnections and numerical aperture variations. Also mentioned was uncertainties due to temperature effects and the Author was of the opinion that backscatter measurements are generally fraught with uncertainties but intelligent use of the technique can provide good results.

3.2 Reference 23

Backscattering measurements in optical fibres: separation of power decay from imperfection contribution

This author also makes the point that there is a lack of reliability in the interpretation of results using backscattering. This being due to the fact that the pulse shape contains information pertaining to power decay along a fibre and

also spatial imperfections or fluctuations of the optical and geometrical parameters. Because of this mixture, ambiguity in the interpretation of results can arise. The technique proposed is to remove ambiguity in the interpretation of results by launching succesively from the two ends of the fibre.

Actual results are presented and a simple rule is suggested, namely the actual attenuation constant of a fibre can be obtained as the arithmetic mean between the attenuation constants carried out from the backscattering signals detected at each end of the fibre. From the results, the technique appears to be effective however reproduction in practice is likely to be a problem.

3.3 Reference 24

Backscatter measurements on optical fibres

The OTDR and its individual components are described in detail as is the system performance of the unit. Some computer simulated figures have been used within the report. Measurements with 'Unperturbed' fibres are described. It was noted that the degree of agreement between backscatter - derived loss measurements and those determined by the 'Cut-back' method (see chapter 2) is dependent on measurement procedures as well as the intrinsic properties of the fibre i.e. if the properties of a fibre under test were uniform (not a function of length) and reciprocal (the same in both forward and backward directions) then the losses determined from the 'Cut-back' and backscatter methods should be equal. Naturally in practice these conditions are not fulfilled indicating the importance of

having an insight into the various perturbations that may be present in fibres under test.

Initial reported scans of concentric core fibres indicate consistent fluctuations of the trace, these are most likely due to diameter changes arising in manufacture. However system noise can also introduce random irregularities that will manifest themselves independently during each scan. By scanning a number of different fibres it becomes apparent that some fibres have smaller variations than others and they appear real.

The types of scattering mechanisms are described viz Rayleigh and non-Rayleigh. Rayleigh scattering originates in intrinsic spatial variations in the refractive index and in the dopant material which are small compared with the wavelength used. Non-Rayleigh scattering manifests itself from such processes as micro-bending, core-cladding interface scattering, mie scattering, macro-bending and scattering/reflections from fibre imperfections. Most of these mechanisms scatter radiation predominantly in the forward direction. By plotting the spectral loss as a function of λ^{-4}, the Rayleigh scattering co-efficient can be determined by a least - squares fit by ignoring the wavelengths where water absorption is prevalent (OH Peaks).

A number of practical points were then examined, namely, a) mode excitation, b) fibre-end preparation and c) mode strippers.

a) With multimode fibre measurements it is necessary to flood the fibre with laser radiation to excite all possible modes. b) For the best results it is essential to have the fibre ends cleaved so that they are perfectly reflecting mirror surfaces.

If cleaving is performed by the 'scratch and pull' method then the fibre face can be composed of three regions viz the mirror, the mist and the hackle zones. If properly cleaved, the surface almost entirely consists of a mirror zone. In addition to being smooth and flat, the end surface must be perpendicular to the fibre axis. c) Due to the isotropic nature of the Rayleigh scattering it is possible for some of the rays to be captured by the fibre cladding, however experimentation showed no perceptable change in backscatter signal with or without mode stripping, indicating a negligible amount of backscattered power propogating in the cladding. Hence mode strippers do not have a significant effect on backscatter signal levels thus making OTDR fibre launching a simple process.

Measurements on fibres with local perturbations are also considered. These perturbations which generate a change in the background Rayleigh response may be either extrinsic e.g. bends or intrinsic e.g. an impurity region of high loss. Signatures obtained can be divided into two categories viz absorption-like and scatter-like signal returns. Scatter-like signatures are defined as those, for example, where spikes are formed on a descending trace and hence the increase in backscatter signal is larger than the associated decrease on the descending trace. Absorption-like signatures are defined as those, for example, where there are rapid increases in local attenuation such as splices. The most general form of signature, however, is a combination of both.

3.4 Reference 25

Backscatter Signature Simulations

The author has attempted to catalogue various backscatter signatures by presenting a collection of digital computer-generated replicas of signals that can be encountered in OTDR systems. Signatures originating from localized and distributed imperfections are superimposed on uniform traces. Details of the effects of fibre perturbations are illustrated and the emphasis is placed on the correct interpretation of OTDR signals as well as pointing out sources of error which can arise in characterizing optical fibres.

The presented simulations are intended to be an aid in interpreting fibre anomalies in backscatter signatures thus enhancing the qualitative nature of the signals and also to assist in enabling the OTDR to be used for acceptance testing and Quality Control.

Mention is made of the modelling required for simulation, the digitizing and the 'ground rules'. The types of graphic displays used in signature analysis are also described namely direct detector output, logarithm of the detector output and differential logarithm of the detector output with the abscissa as time along the fibre axis.

Examples of the various simulated signatures are offered (141 in total) covering the following groups of conditions: 1) Point Defects, a) a scatter-like defect (as defined in reference 24) is simulated and the effect on this by various combinations of

source pulse width and shape illustrated. 15 different displays are recorded giving an insight into how the OTDR source can affect the signature of the same defect and thus influence its interpretation in practical experimentation. b) an absorption-like defect (as defined in reference 24) is simulated and the effect of the same 15 variations in source illustrated. c) a composite point defect (defined as a perturbation where impulse response shows features which are both scatter-like and absorption-like in nature, that is, it exhibits a pronounced increase in backscatter signal followed by a pronounced decrease in signal level) is simulated and again the effect of the same 15 variations in source illustrated. This set of simulations above all indicate how difficult interpretation of the same defect can be under various conditions and reinforces the vigilance necessary in practical situations. All of the examples so far were on a logarithmic display, the author then procedes to illustrate 13 simulations of a composite imperfection with a differential display showing the effect of varying the delay $\triangle$ T in the differential display. Except for magnitude, only very slight variances of the initial imperfection were noted.

A number of conclusions are drawn by the author viz: the magnitude of the distributed Rayleigh component is approximately proportional to the energy in the source pulse. Unlike Rayleigh signatures, the magnitudes of scatter-like signatures do not increase with pulse duration i.e. the defect structure tends to broaden out. Reflection from these localized regions returns a basically unaltered pulse in the backward direction and from

extended regions involves a convolution process of the input pulse with the scattering medium. With absorption-like defects, a signature is provided from which the loss can always be inferred even with pulse widths that would have completely obliterated a scatter-like signature under similar conditions. The main effect of increasing the input pulse width is to cause a relative decrease in the higher frequency components of the trace. Transient effects appear at the beginning, end and at discontinuities in the fibre which are apparent signatures from finite width pulses. They can appear over time intervals equal to the pulse width duration and during these periods problems in signature interpretation are foremost if the defect response occurs in this non equilibrium region. Apparent time-shift becomes prevalent as the pulse duration increases affecting the appearance of the most prominant defect signature features, however the location of the defect is still governed, correctly, by the leading edge of the defect signature. Location precision of a defect is determined more by the rise time of the source pulse than its duration.

2) Extended Defects. Where a fibre has regions of anomalous properties which occur on a length scale less than or comparable to the physical length of the input pulse in the fibre the response will differ in a qualitative way from that due to point defects. In general this means that the backscatter signature will be broadened when compared with the input pulse duration. 4 simulated signatures are presented describing the effects of various input pulse conditions.

3) Symmetry and Length-Dependent Effects. These two types of effect can cause error and uncertaintities. One source of error originates in distributed fibre properties (scattering absorption, NA, diameter) which are a function of length, another relates to the lack of fibre symmetry with respect to the forward and reverse directions of propagation of radiation. Several examples are then given of signature distortion when non-uniform and non-reciprocal fibre properties are encountered. A series of 3 figures are illustrated showing the capture fraction dependence on fibre length. In the case of the logarithmic plot a slight curvature can be detected. This curvature is more apparent in the plot of residuals where residuals are defined as:- Residual (dB) = Actual Attentuation (dB) - Predicted Attenuation (dB) where the predicted attentuation is given by a linear least-squares fit. When the same fibre is reversed end for end, the curvature of the resulting signature and residuals, surprisingly, is the same. The measured attentuation is, as expected, different. Similar series of 5 figures are shown for scattering loss and absorption loss. Splices and Couplers in fibre links are the most important examples of situations which can exhibit symmetry and length-dependent anomolies. Extreme examples of unsymmetric splices are given where a very sharp step is shown, i.e. a high level of local attenation over a minute distance in the forward direction however, when the fibre is reversed, end for end, an apparent 'gain' is noted. This has also been demonstrated experimentally. The conclusion of this is that these losses can

only be accurately determined by measuring from both ends and averaging i.e. only round-trip splice loss can be determined exactly using the backscatter technique.

4) Di Vita Technique. This was described earlier under reference 23, and is a generalised approach of providing a means for separating the distributed loss of the fibre from the backscatter contributions due to any imperfections.

5) Wavelength Dependence. Of the various mechanisms that cause attenuation in a fibre, Rayleigh Scattering is the dominant loss term at the source wavelength, even in fairly high loss fibres. On the other hand, many localized imperfections will have defect signatures that are largely independent of wavelength, and backscatter structure due to diameter fluctuations appears to be approximately constant. The magnitude of the background Rayleigh Signature varies as the inverse fourth power of the wavelength λ^{-4} Hence the qualitative nature of most signatures containing localized defects will change with wavelength in a predictable way. 2 examples of this are demonstrated. By simulating fibres whose loss consists entirely of Rayleigh scattering and whose composite defect is wavelength independent and introducing source wavelengths of 800nm and 900nm it can be seen that the zero time scattering level is higher in the 800nm case by a factor of $(800/900)^{4}$ or about 2dB, but the shape at this time period is greater. Also, the features of the defect signature are altered somewhat even though the defect parameters are unchanged.

6) Noise Considerations. Besides the effect that perturbations of the fibre have on the backscatter response other influences incidental to the data acquisition process may also cause distortions of the signature. A major limitation of the OTDR technique is the limited dynamic range over which adequate signal to noise ratio may be obtained. Backscatter signals are inherently very small hence system noise is always going to be a problem. Significant amounts of noise are contributed by thermal noise, background radiation, avalanche photodiode and laser diode noise and power fluctuations. A number of 'noisy' displays are contructed. Where a logarithmic display is used, it tends to skew the average values towards higher loss values hence averaging in the logarithmic space will therefore contain a bias when low signal to noise ratios are encountered. So the simple rule is, averaging noisy signals in the logarithmic domain should be avoided.

7) Point Defects in Close Proximity and Their Resolution. Signatures of localized defects in close association always present special problems. These can be due to the uncertainty in interpreting the resultant structure or the input pulse characteristics which are required to identify defects. Again signatures can be a function of the properties of the defect in question, the magnitude of the backscatter signal generated, as well as the input pulse width, shape and type of graphic display. It had been assumed in the next set of simulations that the resolution is determined exclusively by the input pulse i.e. that dispersion is negligible and the response of the receiver

and processing electronics do not contribute appreciably to the shape of the defect signatures. Note that resolution is defined as the ability of the OTDR system to distinguish between defects which are in close proximity in the fibre.

a) resolution of scatter-like defects. 33 simulated examples are given which are based on two adjacent point scatterers which are stimulated in various ways.

b) resolution of absorption-like defects. 19 simulated examples are given which are based on two adjacent absorbing defects which are stimulated in various ways.

c) resolution of composite defects. As previously mentioned, the scatter-like and absorption-like features of a composite-type defect will approximately add in the resultant signature hence any conclusions drawn from the two previous analyses are valid for the composite situation. Only 2 simulations are described for this case.

Conclusions and Recommendations. The examples described by this author, although only simulations, enable various pitfalls to be avoided and gives pointers when interpretation of backscatter signatures are undertaken. These examples clearly demonstrate the complexity of the backscatter response when defect responses appear with time separations comparable to the source pulse width. The situation is complicated by the number of types of possible defect signatures, relative magnitude of the backscatter signals, launched pulse characteristics and graphic display techniques. For example scatter-like defects are often easier to resolve visually than absorption-like defects under

similar conditions. Also, it appears that the conventional definition of resolution is not really an adequate measure of the ability of the OTDR system to distinguish between all types of defects in close proximity and in some cases adjacent imperfections are completely unresolved using this criterion.

3.5 Reference 26

Optical fibre characterisation: Backscatter, time domain bandwidth, refracted near field and interlaboratory comparisons.

Initial discussion in this work encompasses the theory and practical implementation of OTDRs and includes an expanded description of the unit used for the described experiments. Points of note are a) effects of different types of beam splitter and illustrations of the variations in coupling loss as a function of angle of incidence for different degrees of polarization of the incident beam b) the description of the fibre launcher which appears to be used in most commercial equipments and c) the importance of signal to noise ratio and how noise affects the recorded trace. Various examples of different types of fibre both unperturbed and perturbed are shown as are descriptions of loss and length measurements and error analysis.

The article then goes on to discuss bandwidth considerations and pulse broadening which is important in multimode fibres particularly when used in communication systems. With single mode fibres there is less pulse broadening and its importance

only becomes apparent when many kilometres of fibre are employed between transmitter and receiver/repeater. A practical system for measuring bandwidth is described and examples of measured fibres illustrated.

The third part of the article describes the implementation of a refractive index profiler. Description of the different types of scanning are described viz near field scanning which depends on the existence of a local acceptance angle (or numerical aperture) at any point on the entrance face of the fibre, i.e. the vertex angle of the cone that can enter the fibre and be guided depends on the index of the core at the point of illumination and refracted ray scanning, where a fibre is illuminated with a focused beam where vortex angle greatly exceeds the acceptance angle of the fibre and observation is made of the rays that are refracted at the core-cladding interface rather than the rays that are trapped by the fibre. Various examples of scanned multimode and singlemode fibres are shown and data used to calculate the core-cladding index differences.

Qualitative information can also be derived from these scans such as contamination in the original preform from which the fibre was drawn.

Finally a comparison of measurements made at a number of U.S establishments (government and industry) was undertaken. Various fibres were used as examples and measured for attentuation, bandwidth, NA and core diameter. This was to investigate any measurement variations discovered on particular fibres over a different set of measuring equipments. The

following conclusions for attentuation measurements were noted, a) measurement agreement has improved industry-wide since the last time this exercise was undertaken b) uncabled fibres can exhibit good stability if proper attention is given to buffering and winding configuration c) restricted and overfilled launching conditions for attentuation measurements yield similar standard deviations for comparisons on some types of graded index fibre d) appropriately specified beam optics and mode filter approaches can give virtually the same results for restricted launch attentuation on many types of long length graded index fibre e) some differences in results arising for one particular fibre indicates that non-modal effects such as failure to completely strip cladding light, non-linear detection, incorrect wavelength etc. can alter the precision dramatically f) the outcome of measurement comparisons is likely to depend on the magnitude of test fibre Differential Mode Attentuation (DMA) g) comparisons using a large number of fibres would be beneficial.

The first part of this work was written by the same author as references 24 and 25 and hence much of this section has been previously discussed. The second and third parts do not directly deal with OTDR measurements however they were useful in ascertaining how imperfections etc affect measurements other than attenuation. The final section demonstrates that even under laboratory conditions the same fibres can exhibit differing results over and above the usual measurement tolerances indicating that repeat measurements even on a single piece of equipment, particularly where subjective results are involved, should be undertaken.

3.6 Reference 27

Optical fibre diameter variations and their effect on backscatter loss measurements

This reference closely investigates observed features in multimode fibre local attenuation plots obtained by backscattering associated with fibre diameter fluctuations. The two distinct observations are that propagation through a contracting taper produces a reduction in observed attenuation and an expanding taper exhibits a positive loss of similar magnitude. On consideration these appear to be the opposite of what is expected. This phenomenon is caused by attenuation of the backscattered signal which is sensitive to mode conversion and DMA since it contains high order modes.

This article then goes on to describe the theory involved for each type of tapered fibre. The backscattered power received by the detector is affected by both the forward loss of the input pulse and the reverse attentuation of the scattered light. However, the following assumptions are made: the fibre baseline loss α is equal in both directions and thus the returned power $P_R = P_0 e^{-2l\alpha}$ where l is the distance to the scatter point and P_0 the received power from the start of the fibre. Also that the forward propagating pulse only partially excites the guide so that it is able to negotiate small diameter changes without loss.

Three cases in point are described, a) expanding taper, where the diameter of the fibre increases steadily, here the returned light from a scatter point within or beyond the taper region has

additional losses as the high order modes of the larger waveguide are lost by radiation. As a rule of thumb, the magnitude of the loss is given simply by the reduction in area of the waveguide. b) contracting taper, with DMA, where the diameter of the fibre decreases steadily, is more complex. Light scattered into high order modes from a point after the taper is converted to lower order modes on traversing the taper, since it appears to be an expanding taper to reverse-propagation light. Thus light from beyond the taper returns to the source as lower order modes, whereas that from a point prior to the taper fully excites the waveguide. Since the fibre has a lower loss when partially excited, a greater proportion of light from beyond the taper arrives at the detector than from before the taper, giving an apparent reduction in loss. If the DMA is due to a reduction in fibre diameter between the point of interest and the detector then the effect of the contracting taper is to recoup returning power which had previously been lost at the diameter reduction. If the DMA is introduced by a prior diameter reduction then the rule of thumb is that the received power on traversing a contracting taper will increase in proportion to the area change. c) contracting taper with cladding effect, experiments undertaken by the authors have shown that an increase in backscatter power is evident for a contracting region even when no diameter reduction is present between the source and taper hence some other mechanism must be at work. A scatter point that follows the taper region will cause backscattered light to excite both the core and

cladding of the fibre and the returning light in the cladding will see the fibre as an expanding taper. This light will then enter the core as the taper expands and the mechanism similar to case a) is evident hence the power that can enter core is proportional to the area change. There is now no requirement for DMA in the reverse path. In practice, cladding modes suffer a higher loss than power in the core and this provides a means whereby the two power increasing mechanisms can be distinguished. Schematic examples of the three mechanisms are displayed in the article with calculated local attentuation curves. Where cladding modes are involved (case c)) the increase in backscattered power fades back to the normal level for scatter points that follow the taper causing an overshoot in the attenuation signature, however in practice cases b) and c) usually appear together.

The authors verified case c) above experimentally by manufacturing a fibre that had a controlled taper with the following features: initial core diameter of 60um tapering to 53um gradually over 75m. The fibre was silicone clad graded index and the source a semi-conductor laser operating at 904nm. The results obtained for this contracting fibre are remarkably similar to the schematic diagram and the fading back to the normal expected backscatter level occurs after a distance of 100m indicating a cladding attenuation of approximately 100db/km which is common for silicone-clad fibres.

The experiment was repeated for propagation in the reverse direction i.e. into an expanding taper and is very similar to

schematics shown for case a). However, one big difference was noted, the magnitude of the effect is apparently half that calculated earlier and the reason put forward by the author is that light scattered from a pulse which only partially excites the waveguide does not fully excite the guide in the reverse direction.

To further verify the effect of cladding modes the experiment on case c) was repeated with the primary silicone coating removed with acid in the taper region. A large number of sharp peaks appeared in the trace over this region probably as a result of scattering of the cladding modes at the boundary between the cladding and acid. When propagation in the reverse direction was repeated, the result was exactly as before, i.e. it remained totally unaffected by the silicone coating removal.

To eliminate the effect of this interface scatter, the fibre was immersed in index matching liquid and case 3) experiment repeated. The reduction in local attenuation was then much less apparent however, it could not be removed completely emphasising the persistence of low order cladding modes contributing to the effect.

For multimode fibre backscatter signature interpretation this reference is probably one of the most useful as tapering of fibres during manufacture must occur due to the methods of core/cladding diameter control.

3.7 Reference 28

High resolution Measurement of Diameter Variations in optical fibres by the backscatter method

This reference is a continuation of the previous reference. Here, more complex diameter variations are examined with high resolution equipment. Again a fibre was drawn with known diameter variations. This was accomplished by adding analogue signals to the error feedback loop which is part of the diameter control system used on the fibre pulling tower during manufacture. Hence known diameter changes can be induced into the fibre and accurately recorded on the standard diameter monitoring equipment. Backscatter signals from a 904nm laser source were acquired using a transient recorder interfaced to a digital computer with the attenuation obtained by differentiation.

The profile of the 1260m multimode fibre was such that the diameter changed as follows. From a nominal 125um for the first 210m, reducing to 123um then 121um and increasing to 129um all over 40m, reducing to 125um and finally down to 110um over 30m. The only other diameter variation present was a reducing taper located at 390m from the beginning. The spatial resolution of the backscatter system is approximately 2.5m allowing the effects to be readily observed. The curves illustrated from backscattering both ends of the fibre are largely symmetrical with one another despite the fact that measurements performed from the end whose 125um diameter lasted for 210m would not be significantly affected by DMA whereas those from the other end

would involve considerable DMA resulting from the taper located prior to diameter changes under consideration. Increases in power where decreasing tapers are present are clearly visible on the figures and where the initial decreasing tapers are present i.e. 125um to 123um to 121um at the beginning of the fibre, no significant prior DMA can exist (no prior tapers) hence this supports the mechanism involving cladding modes previously described. When the diameter increases to 129um a very sharp drop in backscatter power is evident with a local increase at the 129um to 125um boundary. Again, as described in reference 27, close examination reveals that the magnitude of individual signal variations is approximately half that expected from theoretical calculations, the reason being that the backscattered light does not fully excite the waveguide, but excites a subset of high-order modes. Experiments were then performed to further verify this by varying the fibre excitation conditions, the results showing only a small variation in magnitude. Also radiation of forward travelling light at a contracting taper could be induced only by highly exciting the fibre hence verifying the assumption of no forward loss under normal circumstances. This forward radiation loss was observed as a sudden increase in local-attenuation at a point along the taper.

Further experiments were then described where a 1km fibre had sinusoidal diameter variations over the central 500m section. The fibre diameter was a nominal 120um with four cycles of a 5um peak-to-peak sinusoidal variation. A further unprogrammed diameter variation spike also appeared 50m further down the

fibre from the sinusoids. The amplitude of the backscattered power measured from each end reproduced the variations in diameter with the expected increase in scatter return for a decrease in diameter. When plots of local attenuation were drawn they were precisely anti- correlated both for the 4 sinusoids and for the unprogrammed feature. Again the amplitude is slightly smaller than the expected theoretical curves. After the diameter variations, the backscatter power curve returns to the expected exponential decay and the local attenuation curves are symmetrical about the fibre median loss which in this case was 2.5 dB/km thus indicating that no forward loss was caused by the diameter fluctuations. Experiments on fibres manufactured with up to 4um RMS bandlimited Gaussian diameter random variations similarly showed no excess loss.

3.8 Reference 29

Determination of structural parameter variations in single-mode optical fibres by time-domain reflectometry

Further to references 27 and 28 this work goes on to investigate single-mode fibre structural variations by introducing a known diameter change. Also presented is a means of performing backscatter measurements on single-mode fibres with sufficient precision to enable the structural parameters to be deduced from the signature. The 850m single-mode fibre used had an initial diameter of 110um increasing to 125um over a 20m region, 280m from the beginning. It is important to note that elsewhere the diameter was constant to better than 1um. The measuring

equipment consisted of a Q-switched Nd:YAG laser with pulses of 200ns duration at a wavelength of 1060nm. By careful design, the equipment was such that polarisation sensitivity was eliminated and non-linear effects avoided. Scattered light was detected by a silicon APD and the signal amplified, digitized, then fed to a microcomputer for averaging and processing. The fibre was backscattered from both ends and the diameter change showed up clearly in the traces as a change in the power level, as before, increasing power with decreasing diameter. Local attenuation plots (obtained by differentiating) clearly show the diameter variations as a large fluctuation of opposite sign depending on which end is backscattered. However, other large fluctuations in local attenuation were present (which also anti-correlated) in regions where the diameter of the fibre is very constant and were found to be stable and reproducible. They appear to be due to variations along the fibre length of the backscatter factor which is the ratio of the backscattered power to the pulse energy and is signified by the symbol η. Such fluctuations in η are often found in multimode fibres due to random diameter variations causing re-distribution of power amongst the modes and consequently affecting the backscattered power. This cannot be the case in single-mode fibres where only one mode exists or where the diameter has been accurately controlled. By separating the fibre attenuation from the backscatter factor variations, the true local attenuation can be obtained and this plot is relatively constant. However the backscatter factor trace illustrated shows the fluctuations

which caused the above mentioned features in the local attenuation plots. Variations in η are caused by fluctuations in NA, Rayleigh scatter coefficient and core diameter, with NA being predominant. The observed fluctuations in local attenuation not attributable to diameter variations are therefore most likely to be caused by variations in NA. However in practice there are inter-relations as for example a change in NA is associated with an alteration in the dopant concentrations during preform manufacture prior to fibre drawing which will affect the Rayleigh scatter coefficient etc. The conclusion is that attentuation of a single-mode fibre cannot be reliably determined over a short length from the backscatter signature obtained only from one end. (This fact was then further illustrated using a 470m fibre whose backsacatter factor was steadily decreasing from one end to the other. In one direction an average loss of 1.7 dB/km was indicated whereas in the other directions the fibre appeared to have no loss over most of its length).

3.9 Reference 30

On the theory of Backscattering in single-mode Optical Fibres

The authors have presented a theory of backscattering in single-mode fibres allowing backscatter waveforms to be predicted for fibres of any refractive-index profile or scattering-loss distribution. Where quantitative measurements are of interest, for example the determination of variations of fibre parameters along the length, it is essential to have an accurate model of the dependence of the backscatter signal on

the fibre parameters to enable accurate interpretations to be made for minute changes in power. Unlike the case for multi-mode fibres, where the theory is well established, this paper has set out to clarify the situation by using a different and more general approach from those previously proposed.

Firstly, time dependence of the backscatter signal is reviewed. It is assumed that the pulse launched into the fibre is a Dirac function with a finite energy and of vanishingly narrow width. The effect of a finite pulsewidth is to limit the distance resolution of the measurement, for a constant input energy, varying the pulse-width will not alter the backscatter signal level. The expression stated in this section for the power received at the launch end of the fibre at time t equals $2z/vg$ where z = a position along the fibre length and vg = group velocity in the fibre and its derivation is virtually the same as for multimode fibres. Secondly, the backscatter capture fraction is evaluated. Rayleigh scattering is classically described in terms of electric dipoles driven by an e.m. wave travelling through the waveguide material. In a homogeneous medium, interference between the radiation patterns of the dipoles results in cancellation of the secondary waves in all but the forward direction. A localised inhomogeneity of the refractive index, however, results in a dipole moment where radiation is not cancelled by adjacent dipoles. A portion of the incident wave is then radiated in all directions and power is lost to Rayleigh scattering. The scattering process may, therefore, be represented by a large number of dipoles

oscillating with a fixed phase relative to the incident wave, but whose amplitude is proportional to the random local deviation of the electric susceptibility from its mean value. With coherent illumination the phase relationship between the light scattered by separate dipoles is fixed. The scattered light, therefore, suffers interference.

Assuming that the source used is sufficiently incoherent that such interference effects are eliminated, the contribution of all dipoles to the scattered light can, therefore, be added in intensity and the calculation of the backscatter capture fraction is then reduced to the evaluation of the power coupling between the electric dipoles and the fundamental mode of the fibre.

Assuming linearly polarized mode fields and for weakly guiding fibres there is no loss of generality since an arbitrary state of polarisation may be described as a combination of linearly polarized waves, and the orientation of the electric-field vector of the backscattered wave at the point of capture is that of the dipole moment. In order to calculate the power coupled to the fibre mode, one direction of propagation only is considered and a coupling overlap integral in the far field is performed over a hemisphere centred on the fibre axis. The final expression derived is a general expression for the capture fraction for arbitrary refractive index profiles and scattering-loss distributions, thus enabling the backscatter factor (ratio of the backscattered power to the energy launched into the fibre) to be evaluated from the near field of the mode and the radial scattering-loss distribution directly.

Finally, previous single mode backscattering theory was based on the Gaussian approximation and within the limitations of the Gaussian approach the derivations in this paper confirm the validity. However in some cases use of the Gaussian approximation could lead to errors in the interpretation of features in backscatter waveforms. Having a theory that is applicable to any refractive-index profile or distribution of scattering loss, if the backscatter waveform of a fibre exhibits departures from the simple exponential decay, one or more of the structural parameters must be a function of position hence it would be useful to determine which of the fibre properties are non-uniform in order to provide feedback to the manufacturing process. Experimentally, the backscatter factor is obtained by combining backscatter waveforms measured from each end of the fibre (see reference 29). In general, it is not possible to interpret this information unambiguously in terms of the fibre properties, since the backscatter factor depends on all the major fibre parameters, even under the simplifying Gaussian near-field distribution assumption. For step index fibres (core scattering loss is different from the cladding) the parameters which affect the backscatter factors are the core radius/diameter, the index difference and the scattering loss in the core and cladding. Since all of these parameters are potentially length dependent, further information is required if individual contributions are to be distinguished. In order to calculate the backscatter factor it is first necessary to obtain the near-field distribution and this can be

performed in one of the following three ways: direct measurement on the fibre, calculation from the Refractive Index Profile or adopt one of the equivalent step-index approaches. The authors have then assumed that a non-uniformity of interest in a particular fibre is a perturbation of one or more fibre parameters about their nominal values. The sensitivity of the backscatter factor to changes in fibre parameters was calculated and the results plotted for 5 particular fibres with a range of Rayleigh scattering-loss coefficients, relative sensitivity the core radius on the left-hand axis, relative sensitivity to numeral aperture on the right-hand axis vs Normalised Frequency, V, on the X-axis. Also plotted was a graph of the same 5 fibres with the same x-axis, however the single Y-axis was relative sensitivity of the backscatter factor to core scattering loss. The first graph shows that the NA curves are identical to the core radius ones except that there is a constant offset of 2 (due to $(NA)^2$ appearing in resultant equations). From the second graph it can be seen that for values of V greater than approximately 1.5, the backscatter factor is sensitive to variation of the scattering loss in the core but largely unaffected by changes of Rayleigh scattering-loss coefficient occuring in the cladding region. The important conclusion is that as the relative sensitivities of the backscatter factor to the different fibre parameters vary in markedly different ways as the value of V changes, by performing backscatter measurements at 2 or 3 well spaced wavelengths comparison of the behaviour of the measured features, with the parameter

sensitivities predicted by the theory for the nominal fibre characteristics, will then reveal which parameters are changing at the observed backscatter features.

3.10 Reference 31

Operation manual - optical pulse echo tester, Anritsu MW 97A/98A

During my investigations, the majority of measurements were made using the MW 97A/98A. The operational manual was very useful not only as a guide to the various functions but also because many examples of various measurements are included, these being prints of actual photographs of plots.

A fibre tail is supplied with the instrument which has an optical connector mounted on one end which screws into the laser output socket. For the majority of measurements the free end of the tail was connected to the fibre under test via a plastic precision butt-joint. However, for the repeat measurements the tail was spliced to a 1km fibre tail, the other end being clamped on an XYZ manipulator used to align the fibre under test into a 'butt-joint' situation. Index matching fluid was dropped onto the 'butt-joint' where fibre tail and fibre under test met.

Various plug-in units are available for this instrument depending on whether measurements on multi-mode fibre at 850nm or 1300nm are required or single-mode at 1300nm. These give the instrument great flexibility. All of the plug-ins have a mask function to prevent saturation of the optical and electrical systems by excessive Fresnel reflection at, or adjacent to, splices or connectors in the fibre under test.

Other major features of the instrument are as follows:-

1. Selectable repetition rate of the laser transmitter. Rep. rates of 409.6 us or 204.8 us can be selected.
2. Narrow and wide (switchable) measuring range.
3. Band-limiting low-pass filter for frequency cut-off.
4. Narrow and wide pulse widths (depends onplug-in unit selected).
5. Averaging. When switched on, exponential averaging proceeds. When not in use, the waveform is processed by a simple addition averaging process.
6. For loss measurements, selectable linear approximation methods are available viz Least square approximation or 2-point approximation.
7. Logarithmic or linear vertical scale.
8. A magnification feature, which magnifies the amplitude of the waveform to enable further investigation of visible imperfections.
9. Video output, enabling a video printer to be attached for making hard copies of displays.

The main source of error in distance measurements is where the instrument requires a manual input, this being in the form of the refractive index. In the majority of cases for experimental fibres this value is unknown or is an approximation from

manufacturers data. The more accurate the figure, the better the length measurement accuracy.

3.11 Reference 32

Coherent OTDR for Fault Location in long wavelength optical systems

This reference describes the performance and principles of an OTDR system designed for operation at 1300nm with the use of coherent detection in order to increase its dynamic range without the use of high power sources (usually requiring water cooling) or high sensitivity detectors using PINFETS (which have suffered from dynamic range problems). A semi-conductor laser source with adequately high coherence was developed to enable a system to be constructed.

Figure 6 shows the schematic diagram of the optical system of the more common direct detection OTDR system as used in all the discussions to date. A probe pulse of light is transmitted into the fibre and the backscattered light from the fibre detected, processed and displayed. Figure 13 shows the optical system for a coherent OTDR. Coherent detection is a technique which involves combining a low level signal with a higher power reference signal (local oscillator, LO). Upon detection, a beat signal is produced in the photocurrent at the difference frequency between signal and LO, with a magnitude dependent on the magnitude of the two signal fields. If the LO is made large enough, eventually thermal noise in the receiver becomes negligible in comparison to LO shot noise. The low level signal is also multiplied by the LO field and the resulting

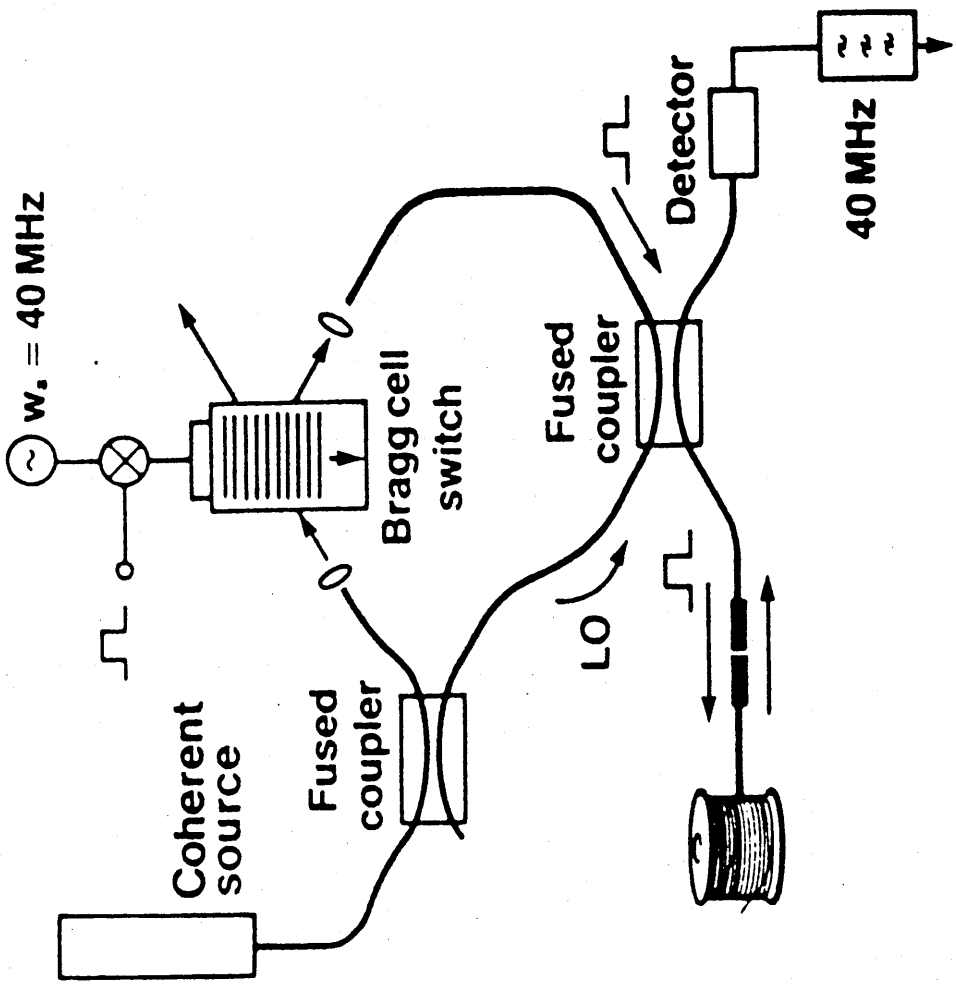
$\omega_s = 40$ MHz
Bragg cell switch
Fused coupler
Detector
40 MHz
LO
Fused coupler
Coherent source

Figure 13

power SNR is the shot noise SNR which is the ultimate limit of sensitivity. The photocurrent is now linearly proportional to the low level received signal rather than the power signal as in direct detection (this reducing the dynamic range of the electrical signal).

In practical systems, it should be noted, only moderate LO power is required, a semi-conductor (non-cooled) laser with sufficient coherence and stability being available using a unique line-narrowing technique. The same laser is used as both source and LO hence any undefined or variable nature of the centre frequency is not critical. This CW light from the source is divided by a directional coupler, optical pulses being produced by passing the signal beam through a Bragg Cell which is operated in a pulsed mode and also provides a 40MHz frequency offset. These pulses are then launched into the fibre and the backscattered return is combined in the second directional coupler with the LO and detected with a PINFET receiver. The voltage at the output of the receiver contains the 40MHz difference frequency carrier, amplitude modulated by the backscatter. The signal is converted to baseband in a tuned, synchronous detector and then digitised. A digital squarer expands the signal to represent the full dynamic range of the backscatter power before it is passed to a fast digital summer and then processed for presentation.

The principle difficulty with coherent detection systems is coherent fading. There are two factors that cause signal fading which add an effectively random noise term to the signal and can

obscure the small incremental losses of splices reducing the characterisation ability The first factor is the inherent bi-refringence of fibres under test and for maximum receiver sensitivity, the received signal and the LO should be in the same state of polarisation. In fact backscattered signals have different states and hence are detected with different efficiences. The second factor is due to the speckle-like nature of coherent backscatter whose resultant intensity depends on the phases of the scattered components and will fluctuate randomly whenever the relative spacing of the scatterers changes or the source frequency is altered. For both types of fading, the noise fluctuations can be reduced by sampling a sufficiently large number of independent Rayleigh and polarisation states. The undefined and variable nature of the source centre frequency enables the fading noise to be reduced as each time it hops to a different frequency, the phases of the returns from individual scatterers are changed, and a different independent sample is taken. Controlled use of this source property overcomes the fading, allowing splices smaller than 0.2dB to be readily resolved. A backscatter single-way dynamic range in excess of 24dB with a 5us pulse corresponding to approximately 60km of 1300nm fibre and detection of Fresnel end reflections up to 70km distant are possible.

Chapter 4

PRACTICAL WORK

4.1 Introduction

This chapter describes the practical experiments undertaken in order to investigate optical fibre perturbations and puts forward conclusions. Some of this data was fed back to the manufacturing unit.

The investigations took the form of three separate activities, namely:

Initial measurements and equipment, sample acquisition, measurements and discussion with Martin Gold from the University of Southampton, and finally repeatability of measurements.

4.2 Initial Measurements and Equipment

4.2.1 Backcatter measurements

In 1982 only relatively unsophisticated OTDR backscatter equipment was available. This fact contributed to the uncertainty of measurement and display and hence one of the reasons why customers questioned its validity and the quality of fibre product. Figure 14 shows a typical multimode fibre trace taken from the then current OFR3 OTDR manufactured by STC opto-electronics division (recorded using a polaroid camera). A break can clearly be seen at a point approximately two thirds along its length and naturally this would result in the fibre being rejected from both this examination and from any cut-back attenuation measurement performed.

Also present is a discontinuity at a point approximately one third along the fibre length which may or may not affect the overall system performance of the fibre and is unlikely to be detected by non-visual attenuation readings.

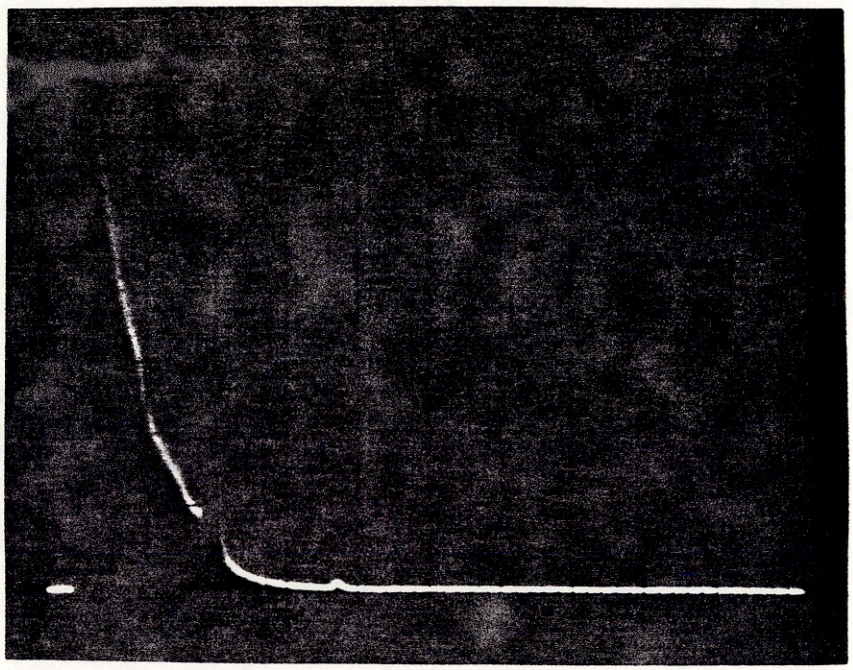

Figure 14

Figure 15 shows a multimode fibre trace (again recorded using a polaroid camera) which has a perturbation at a point approximately one third along its length, however due to the lack of resolution it is extremely difficult to detect. This particular variation is in fact a region of high loss over a relatively short length (probably due to a bubble in the preform prior to fibre drawing, or possibly some impurity)

which would not be detected using the cut-back attenuation method as the remainder of the fibre was low loss. Problems could arise in the field if, for example, the fibre was cut and spliced to another section of high loss fibre or deterioration appeared at that point, resulting in system failure or intermittency, however it is very unlikely that this fibre would have passed proof test.

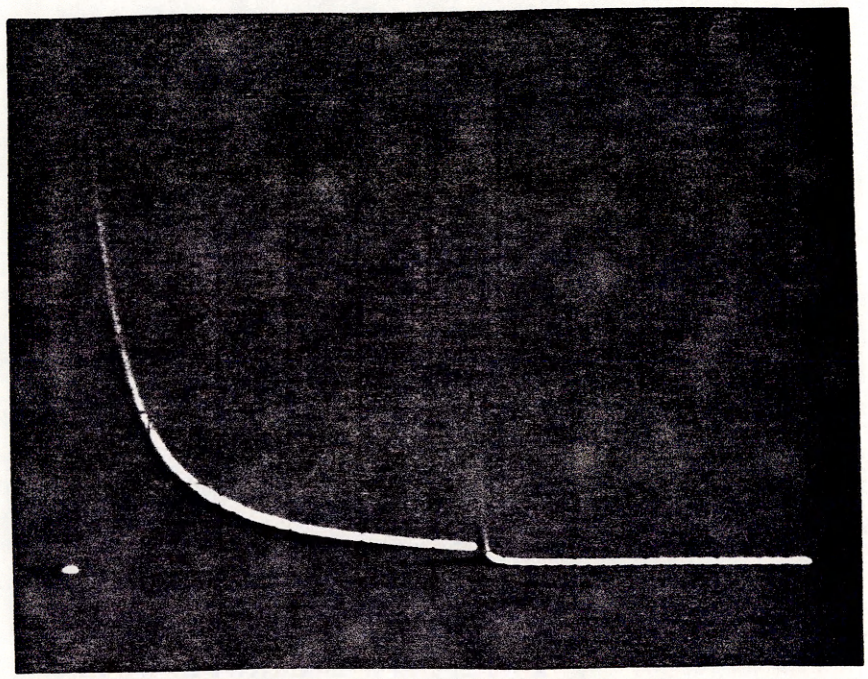

Figure 15

Figure 16 is a repeat measurement of that shown in Figure 15. On this occasion an Anritsu MW97A and an external thermal printer were employed. The perturbation can now be seen quite

clearly and hence decisions on rejection or part discard and/or splicing can be made with firm back-up evidence for quality control and customer audit, even where inexperienced representatives or those unfamiliar with fibre results are involved.

Figure 16

It can therefore be seen that the advent of higher resolution equipment was welcomed and hence the majority of measurements described in section 4.3.2 were made with the Anritsu MW97A or MW98A (advanced HPIB interface capabilities).

4.2.1 (i) Conclusions

The following can be concluded from the above:

a) due to the poor resolution of the equipment available in 1982, discontinuities or perturbations other than breaks that were observed and led to the investigation here-in must have been present over relatively long lengths.

b) where a fibre had passed all other subjective tests i.e. cut-back attenuation, dispersion, geometry and proof-testing (to ensure that mechanical weaknesses were discovered and indicated as breaks on the after-test backscatter measurement) then it is unlikely that system performance would be affected by these 'long-length' visual discrepancies.

c) most observations in 1982 were made on multimode fibre although similar results were obtained when single mode fibres were introduced into manufacture. It is therefore unlikely that these observations were related to the transmission mode.

4.2.2 Scanning Electron Microscope (SEM) measurements

Although an SEM probe for investigating the physical properties of a fibre preform had been designed in 1984, little work had been performed on a drawn fibre. Naturally, the SEM is a tool for 'Surface' structures, however attempts were made to investigate sections below the surface particularly in the region of the core. Various experiments

were performed using gold sputtering, to enable conduction for electron bombardment, and some without where there was little conduction as the natural glass surface remained uncovered. All attempts failed. Figures 17 and 18 respectively (recorded using a polaroid camera) show the results for radial and axial views, and it can be seen that no distinction can be made between core and cladding let alone variations or discontinuities in the said layers.

Figure 17

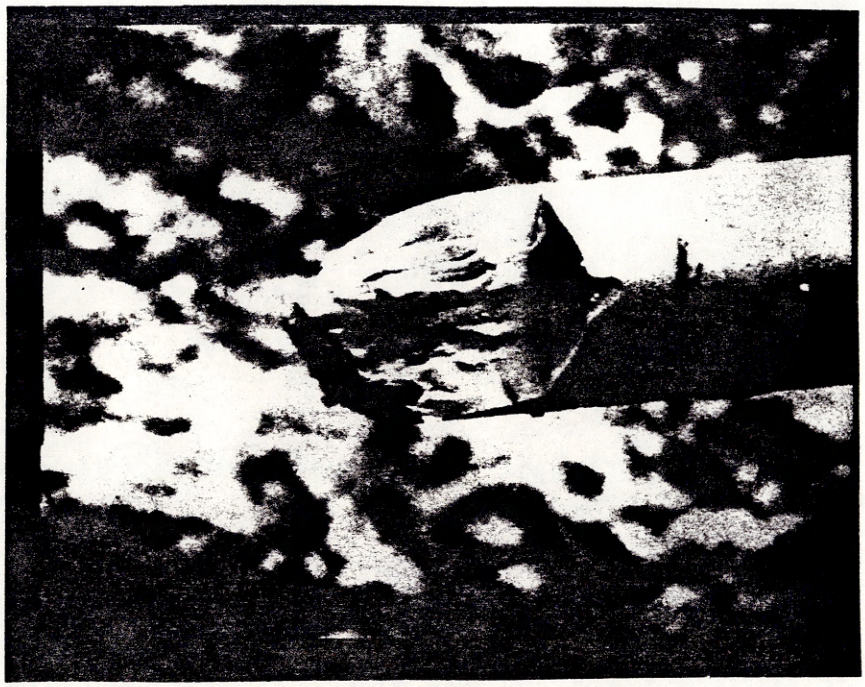

Figure 18

4.2.3 Coherent OTDR measurements

Attempts were made to compare the measurements made with the Anritsu MW97A and a coherent OTDR. Unfortunately the only model available to me for the latter test was an early laboratory model with an 1100nm laser source. The interface from the equipment consisted of a fibre tail of unknown dimensions and it proved impossible to drive a length of fibre and obtain any readings on the display.

4.3 Fibre Sample Acquisition, Measurements and Discussion

4.3.1 Fibre acquisition

Over the period 1984-1987, once the initial foundations had been laid for this overall investigation i.e. planning

background reading, hands-on experience of equipments, collation of relevant papers etc., fibre samples were collected and measured. Unfortunately, I left OCDD Harlow in 1983 and soon after this there was a re-organisation with a consequential loss of staff which made sample collection difficult. Despite this, 67 samples of fibres rejected for OTDR faults were obtained and examined for perturbations and discontinuities. Due to a change in market requirements however, the Harlow manufacturing unit only produced single mode fibre from late 1984 onwards, hence only 3 fibres were multimode. The remainder consisted of 19 tight jacketed, nylon secondary coated single mode fibres and 45 acrylic coated single mode fibres. Lengths varied from 3 to 5 km unlike the standard 1km length manufactured in 1982.

The samples provided had passed through various stages of testing with a high proportion failing at proof test, hence they were rejected for breaks or high attenuation and not necessarily for discontinuities.

4.3.2 Sample measurements

The Anritsu MW97A was used for the measurements and this had the advantage of operating at two different wavelengths, namely 850nm (which is the same as the STC OFR3 used in 1982) and 1300nm, by using the appropriate plug-in module. Experiment showed that there was little difference between the two and as the 1300nm unit was designed specifically for launching into single mode fibre it was decided to use this module.

In all cases the fibre was launched via a 'quick termination'. This is an industry accepted means of connecting an OTDR to a fibre and it consists of a professionally ground and polished optical connector which plugs into the MW97A with a short single fibre cable tail of approximately 0.5m. The free end is stripped back, the bare fibre cleaved and inserted halfway into a plastic tube one cm in length holding a capilliary, containing index matching gel, whose diameter is fractionally larger than the bare fibre. The fibre under test is also stripped back, cleaved and placed in the other end of the capilliary thus making a butt-joint. Figure 19 shows typical examples (Figure 19A is recorded using a polaroid camera and Figure 19B using a thermal printer) of the traces obtained using the MW97A OTDR.

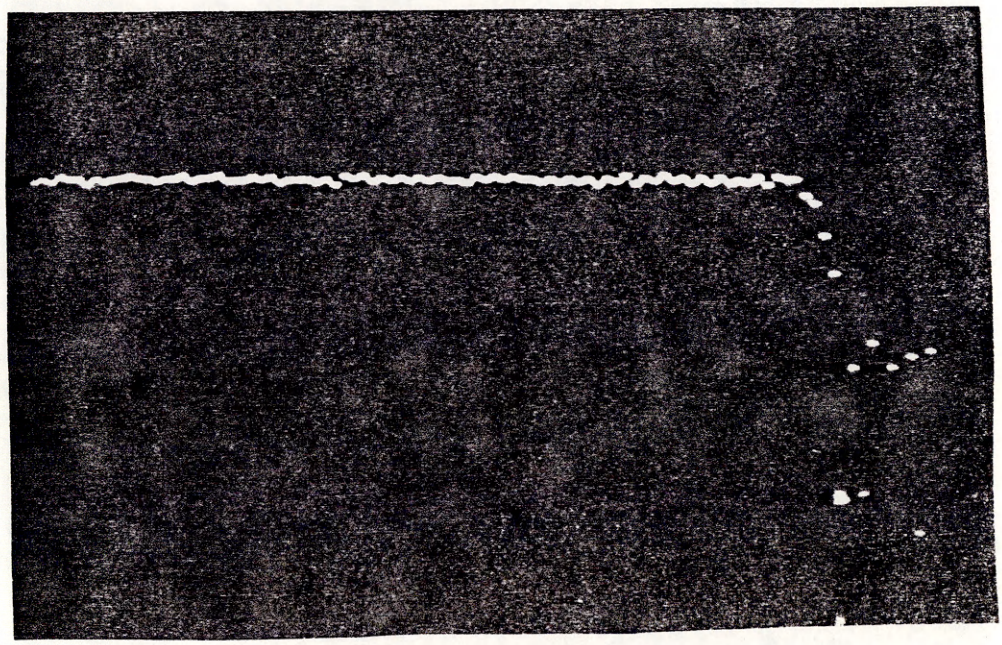

Figure 19A

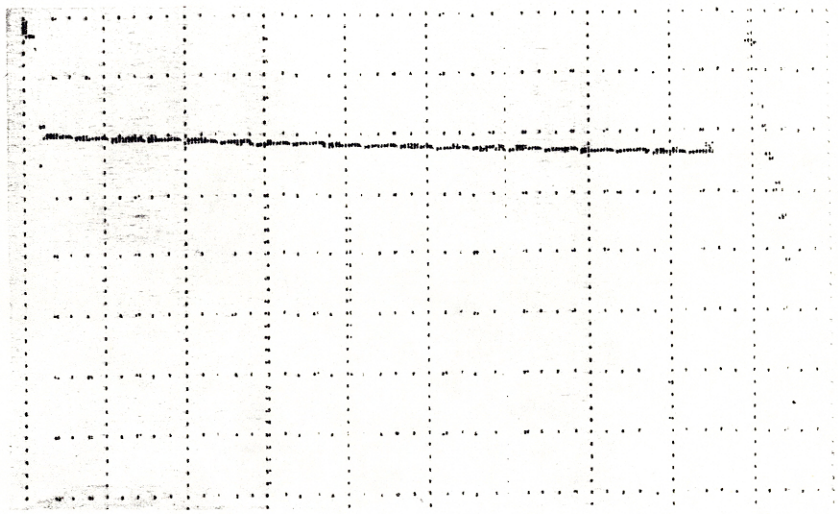

Figure 19B

It had been planned that if any perturbations or discontinuities that had been observed in 1982 manifested themselves in the 67 samples examined, then three measurements would be recorded to ensure that the observation was not just a function of a particular measurement i.e. a quirk of the set-up or test equipment, and that a reasonable correlation between the three readings should be possible. This presented two problems. Firstly, none of the examples appeared to exhibit the perturbations observed in 1982 even at the highest resolution, hence it was not possible to continue the experiments any further. Secondly, there appeared to be a lack of repeatability when taking three consecutive measurements such that fine detail could not be observed even

though the overall shape was constant and naturally a break or high loss region would appear on each example enabling fibre rejection where major faults were exhibited. Figures 20A and 20B show two consecutive readings of a fibre indicating how the overall shape is the same, however the fine detail is different making study of a particular section or point variation difficult. Further investigations of repeatability were therefore performed and these are described in Section 4.4.

Note that no noticeable changes to the overall shape were recorded when fibres were mode stripped using an index matching fluid bath indicating that little cladding light was being propagated.

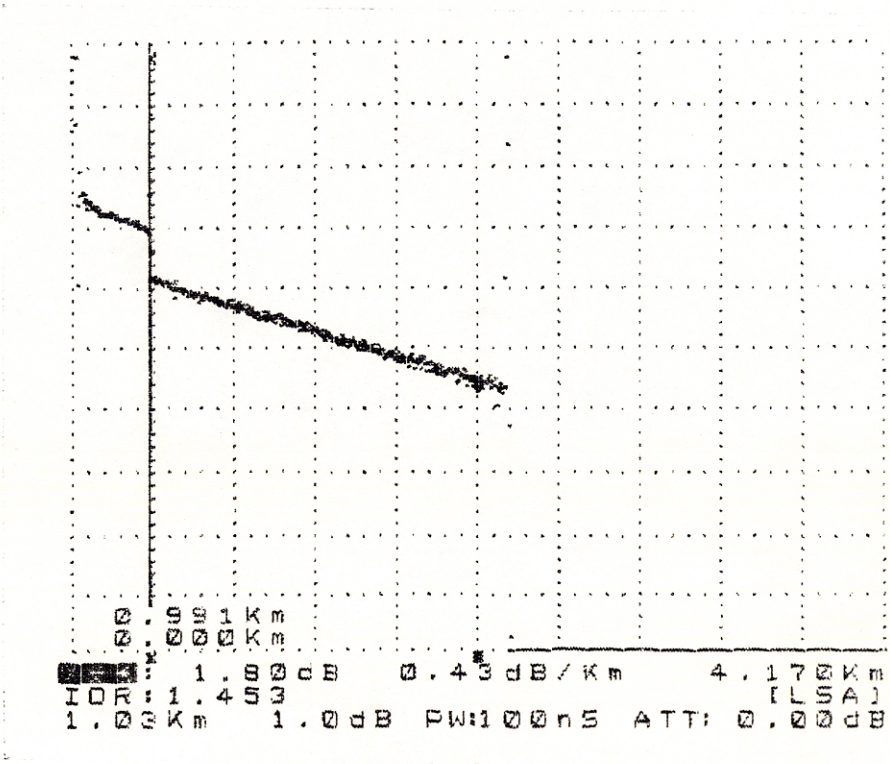

Figure 20A

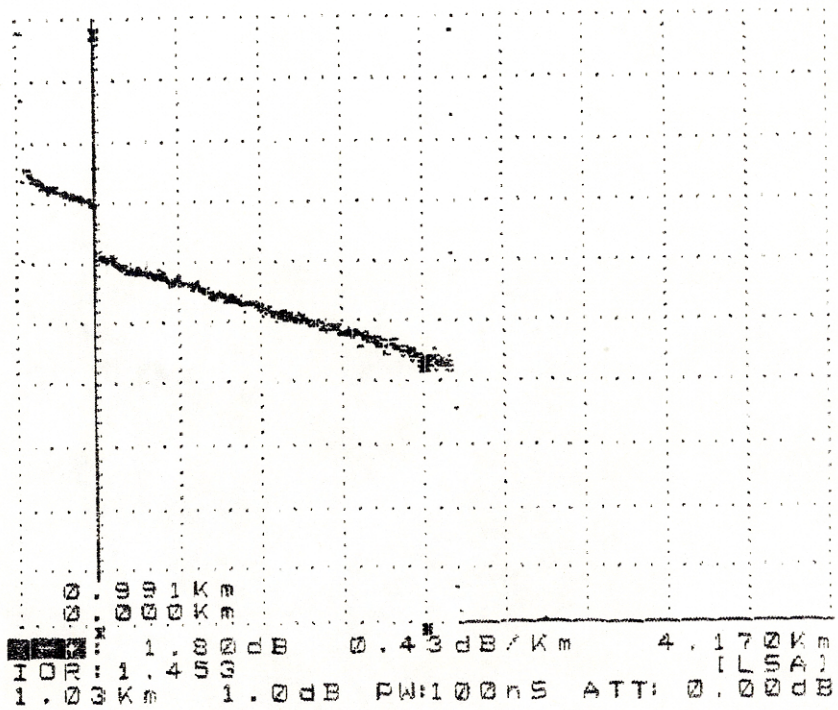

Figure 20B

4.3.3. Discussions

Discussions were held with Martin Gold at the University of Southampton in 1985. At that time, he was heavily involved in examining backscatter features in local attenuation plots, particularly in the field of core and cladding diameter variations in both single and multimode fibres (see references 16, 27, 28, 29 and 30). He showed me some of the fibres and measurement equipment used in his experiments and I concluded that the discontinuities that I had observed in 1982 could have been due to diameter variations or changes in NA as they would have only been visible if present over a relatively long section of the fibre as the resolution of the reflectometer was so poor.

Subsequent to these discussions, an investigation was held into the mechanism for controlling fibre diameter and NA in the Harlow manufacturing unit. Changes had taken place in 1984 in the equipment used to draw fibres with the advent of UV cured acrylic coating and the higher output of single mode fibres. Taller pulling towers (for higher drawing speed) and more sophisticated winding mechanism with digital feedback to the laser diameter control sensors enabled tighter diameter tolerances to be obtained and resultant variations over much smaller lengths despite the higher drawing speed. This was necessary due to the decrease in core size with single mode fibre, i.e. assuming that the core to cladding ratio is fixed in the fibre preform then variations in the cladding diameter would have a much greater effect on an 8um core than a 50um core when the fibre is drawn. There did not appear to be any evidence of changes in NA over the period in question.

4.3.4. Conclusions

The following can be concluded from the above:-

a) The fact that discontinuities observed in 1982 were not observed in the 67 samples recently examined is unlikely to be due to the test equipment, as the resolution in the later OTDR models had increased considerably, and hence was more likely to be due to changes in the fibre itself.

b) It is likely that the variations in fibre attenuation discovered in 1982 were due to fibre diameter changes

for two reasons. Firstly, as stated in Section 4.2.1 (i),due to the poor resolution of the equipment, the attenuation changes and hence the reason for the variations must have been present over relatively long lengths, this would be the case for movements in diameter with poor feedback mechanism to the pulling speed control. Secondly, since 1984 rigid control of fibre diameter variation had been imposed with the introduction of new equipment and since then the fibre samples examined did not appear to show the discontinuities observed in 1982.

4.4. Repeatability of measurements

Due to the problems encountered with repeat measurements, as described in Section 4.3.2, an exercise on the accuracy of repeat measurements was undertaken.

4.4.1 Test set-up

Reels of single mode fibre were individually placed in a temperature stable environment to decrease the possibility of attenuation changes due to temperature variation and launched via approximately 1km of fibre from an Anritsu MW98A OTDR (this being used in preference to the MW97A due to its superior computer interfacing capability). A Hewlett Packard HP85B was used to drive the MW98A for ease of operation and automatic data storage.

The 1km fibre tail was permanently spliced to a short single fibre cable professionaly ground and polished, and connected

to the MW98A. The free end was stripped and cleaved and held in an XYZ manipulator. The fibre under test had one end stripped and cleaved and this held in an adjacent XYZ manipulator such that the two fibre ends held in the manipulators could be brought together as a butt-joint. A microscope was used for alignment purposes and then a drop of index matching fluid was placed on the joint to ensure good optical coupling. The 1km fibre tail was used to enable equilibrium launching thus allowing the whole of the fibre under test to be examined as flooding by the laser will occur on the input to the tail rather than the fibre to be measured. The fibre was measured 10 times over a short period (approximately 45 minutes) ensuring that prior to this, the test equipment had sufficiently 'warmed-up'.

A computer program was written such that the first measurement would act as a reference and only where changes occured at the sample points would the reading be recorded, thus minimising the storage required. Unfortunately due to the variations encountered this proved unsatisfactory and a new program was devised in conjunction with Anritsu. Figures 21 to 35 show the program listing. The program records a maximum of 1000 measurements and stores them in a data file, this being repeated for a total of 10 measurements. The traces can then be plotted out and the actual values printed out by extracting the information from the data file (Figure 36 shows the programme listing to perform this activity).

```
 10 ! DECLARE ARRAY SIZES
 15 DIM S(4),M(4)
 20 DIM Y(1000)
 25 DIM A$[32],B$[32],C$[32],D$[
    10],E$[32],T$[10]
 30 A1=708
 35 !
 40 ! ## ## ## ## ## ## ## ##
 45 ! ON ERROR GOTO 6000
 50 GCLEAR
 55 CLEAR
 60 DISP "  Anritsu MW98A OTDR P
    rogram"
 65 DISP
 70 ! START OF MAIN PROGRAM
 75 ! SELECT I/P DEVICE
 80 DISP "SELECT SOURCE OF DATA"
 85 DISP "[1] OTDR"
 90 DISP "[2] TAPE"
 95 DISP "[3] DISC"
100 INPUT S2
105 IF S2<1 OR S2>3 THEN 80
110 DISP "Select plotter"
115 DISP "[1] Plotter"
120 DISP "[2] CRT (no hard copy"
125 DISP "[3] CRT (with hard cop
    y)"
130 DISP "[4] No output plotted"
135 INPUT P4
140 IF P4<1 OR P4>4 THEN 110
145 IF S2=2 OR S2=3 THEN 500
200 ! OTDR ROUTINE HERE
205 GOSUB 5000 ! GET USER DATA
210 S1=1 ! DEFAULT STORAGE
215 DISP "Select the storage med
    ia for    data files"
220 DISP "[1] Internal tape cart
    ridge "
225 DISP "[2] External disc driv
    e "
230 DISP "[3] OTDR data is not s
    aved"
235 INPUT S1
240 IF S1<1 OR S1>3 THEN 215
242 IF S1=3 THEN 265
245 DISP "Enter the base filenam
    e"
250 DISP "Max no  of 6 character
    s "
255 INPUT F$
260 IF LEN(F$)<1 OR LEN(F$)>6 TH
    EN 250
```

Figure 21

```
265 DISP "Enter the averasins ti
    me in seconds";
270 INPUT D4
275 DISP "Enter the measurement
    no. ";
280 INPUT E$
285 IF VAL(E$)<1 OR VAL(E$)>999
    THEN 275
290 DISP "Enter the no. of measu
    rements "
295 INPUT M2
300 IF M2<1 OR M2>999 THEN 290
302 IF M2=1 THEN T4=0
303 IF M2=1 THEN 350
305 DISP "Enter the time period
    between each measurement"
310 DISP "Enter hours ";
315 INPUT T1
320 DISP "Enter minutes ";
325 INPUT T2
330 DISP "Enter seconds ";
335 INPUT T3
340 T4=(T1*3600+T2*60+T3)*1000
350 GOSUB 7500
355 GOSUB 7700
360 GOSUB 1500 ! GET OTDR DATA
362 GCLEAR 10
365 OUTPUT A1 USING "K,/" ; "AVR
    0"
370 LOCAL A1
375 IF S1=1 OR S1=2 THEN G$=F$&E
    $
380 IF S1=1 OR S1=2 THEN GOSUB 3
    000
385 E$=VAL$(VAL(E$)+1)
390 ! PLOT OUTPUT
395 IF P4=1 THEN GOSUB 2000
400 IF P4=2 OR P4=3 THEN GOSUB 4
    000
405 IF P4=2 OR P4=3 THEN GOSUB 4
    500
410 IF M2=1 THEN 40
412 GOSUB 7500
413 GOSUB 7800
415 M2=M2-1 ! DEC NO OF MEAS.LEF
    T
420 GOTO 350 ! TAKE ANOTHER MEAS
    UREMENT
500 ! DISC & TAPE ROUTINE HERE
505 S1=S2-1
510 IF S1=1 THEN MASS STORAGE IS
     ":T"
515 IF S1=2 THEN MASS STORAGE IS
     ":D700"
520 CAT
525 DISP "Enter base filename to
     be read"
530 INPUT F$
535 IF LEN(F$)<1 OR LEN(F$)>6 TH
    EN 525
```

Figure 22

```
540 DISP "Enter the measurement
    no range "
545 DISP "Start no. ";
550 INPUT S3
555 DISP "Stop no. ";
560 INPUT S4
565 FOR J=S3 TO S4
570 G$=F$&VAL$(J)
575 GOSUB 3500
580 IF P4=1 THEN GOSUB 2000
585 IF P4=2 OR P4=3 THEN GOSUB 4
    000
590 IF P4=2 OR P4=3 THEN GOSUB 4
    500
595 NEXT J
600 GOTO 40 ! RETURN TO START
800 ! ************************
805 ! PPOGRAM VARIABLES
810 ! A1. ..OTDR ADDRESS..708
815 ! A2....ATTEN SETTING DB
820 ! M(0-4) MARKER POS 0-500/10
825 ! S(0-4) MARKER POSITION km
830 ! Y(0-1000) SCREEN DATA
835 ! A$ TITLE
840 ! B$ ROUTE
845 ! C$ OPERATOR
850 ! D$ DATE
855 ! T$ TIME
860 ! E$ MEASUREMENT NO
865 ! D1 DIST. RANGE CODE
870 ! H1 HORIZ. SCALE CODE
875 ! P0 PULSE WIDTH CODE
880 ! H2 HORIZ. SHIFT (km)
885 ! M1 MASK POS. (km)
890 ! I1 REFRACTIVE INDEX
895 ! A2 APPROX. METHOD CODE
900 ! V1 VERT. SCALE CODE
905 ! L1 LOSS MARKER DIFF. (km)
910 ! L2 TOTAL LOSS (dB)
915 ! L3 LOSS (dB/km)
920 ! L4 SPLICE VALUE (dB)
925 ! U1 PLUG-IN UNIT CODE
930 ! F1 FUNCTION CODE
935 ! M CURSOR NO.
940 ! M(0-4) MARKER POS. (0-500/
    1000)
945 ! P1 NO  OF POINTS ACROSS SC
    REEN
950 ! I FOR..NEXT LOOP COUNTER
955 ! X GENERAL PURPOSE VARIABLE
960 ! P2 PLOTTER GP-IB ADDRESS
965 ! D2 SCALING FACTOR
970 ! U$ PLUG-IN UNIT
975 ! H4 HORIZ. SCALE (km/div)
980 ! V2 VERTICAL SCALE (dB)
985 ! F$ FILENAME FOR FILES
990 ! T1 TIMER VALUE (HRS)
995 ! T2 TIMER VALUE (MINS)
1000 ! T3 TIMER VALUE (SECS)
1005 ! T4 TIMER VALUE (mS)
```

Figure 23

```
1010 ! H3 HORZ.SCALE
1015 ! V2 VERTICAL SCALE (dB)
1020 ! D DATE CONVERTED TO SECS.
1025 ! S1 MASS STORAGE SELECT
1030 ! D4 AVERAGING TIME (Sec)
1035 ! S2 I/P DEVIICE CODE
1040 ! P4 PLOTTER/CRT & H.COPY S
     ELECT
1045 ! G$ CONCATENATED FILENAME
     OF F$+E$
1050 ! S3 MEASUREMENT START NO F
     OR FILENAME SUFFIX
1055 ! S4 MEASUREMENT STOP NO FO
     R FILENAME SUFFIX
1060 ! J FILE READIN LOOP VAR
1065 ! X$ GP VARIABLE
1070 ! P9 P.WIDTH SBRT LOCAL VAR
1075 ! **********************
1080 !
1500 ! ************************
1505 ! * ROUTINE TO GRAB ALL   *
1510 ! * THE DATA FROM THE OTDR*
1515 ! ************************
1520 OUTPUT A1 USING "K,/" ; "HL
     D1"
1525 ! ATTENUATOR SETTING
1530 OUTPUT A1 USING "K,/" ; "AT
     TR"
1535 ENTER A1 ; A2
1540 ! DISTANCE RANGE
1545 OUTPUT A1 USING "K,/" ; "DS
     RR"
1550 ENTER A1 ; D1
1555 ! HORIZONTAL SCALING
1560 OUTPUT A1 USING "K,/" ; "HS
     CR"
1565 ENTER A1 ; H1
1570 ! PULSE WIDTH
1575 OUTPUT A1 USING "K,/" ; "PL
     SR"
1580 ENTER A1 ; P0
1585 ! HORIZ SHIFT
1590 OUTPUT A1 USING "K,/" ; "HI
     FR"
1595 ENTER A1 ; H2
1600 ! MASK
1605 OUTPUT A1 USING "K,/" ; "MI
     KR"
1610 ENTER A1 ; M1
1615 ! REFRACTIVE INDEX
1620 OUTPUT A1 USING "K,/" ; "IO
     RR"
1625 ENTER A1 ; I1
1630 ! APPROX METHOD
1635 OUTPUT A1 USING "K,/" ; "AP
     RR"
1640 ENTER A1 ; A3
1645 ! VERT SCALE
1650 OUTPUT A1 USING "K,/" ; "VS
     CR"
```

Figure 24

```
1655 ENTER A1 ; V1
1660 ! LOSS DATA
1665 OUTPUT A1 USING "K,/" ; "LS
     DR"
1670 ENTER A1 ; L1,L2,L3,L4
1675 ! TYPE OF PLUG IN
1680 OUTPUT A1 USING "K,/" ; "UN
     TR"
1685 ENTER A1 ; U1
1690 ! FUNCTION
1695 OUTPUT A1 USING "K,/" ; "FN
     CR"
1700 ENTER A1 ; F1
1705 ! MARKERS
1710 OUTPUT A1 USING "K,/" ; "MK
     SR"
1715 ENTER A1 ; M
1720 OUTPUT A1 USING "K,/" ; "MI
     MR"
1725 ENTER A1 ; M(0)
1730 OUTPUT A1 USING "K,/" ; "MI
     1R"
1735 ENTER A1 ; M(1)
1740 IF F1=0 THEN 1775 ! ONLY 2
     MARKERS FOR LOSS FUNCTION
1745 OUTPUT A1 USING "K,/" ; "MI
     2R"
1750 ENTER A1 ; M(2)
1755 OUTPUT A1 USING "K,/" ; "MI
     3R"
1760 ENTER A1 ; M(3)
1765 OUTPUT A1 USING "K,/" ; "MI
     4R"
1770 ENTER A1 ; M(4)
1775 P1=500 ! POINTS ACROSS SCRE
     EN
1780 IF H1>=0 AND H1<=2 OR H1=5
     THEN P1=1000
1785 OUTPUT A1 USING "K,/" ; "OP
     DR"
1790 FOR I=1 TO P1
1795 ENTER A1 ; X,Y(I)
1800 NEXT I
1805 OUTPUT A1 USING "K,/" ; "HL
     D0"
1810 RETURN
2000 ! ************************
2005 ! * OTDR PLOT TO PLOTTER  *
2010 ! * AT ADDRESS A1        *
2015 ! ************************
2020 GCLEAR
2025 CLEAR
2030 BEEP
2035 DISP "Make sure there is pa
     per in the plotter."
2040 DISP "Press END LINE when r
     eady "
2045 INPUT X$
2050 P2=705
2055 PLOTTER IS P2
```

Figure 25

```
2060 GCLEAR
2065 ! PLOT TO EXTERNAL PLOTTER
2070 LOCATE 0,1.8*RATIO*100,10,1
     55
2075 ! DRAW SCALES
2080 SCALE 0,499,110,249
2085 LINETYPE 1
2090 XAXIS 110,50,0,499
2091 YAXIS 0,25,0,249
2095 FRAME
2100 !
2105 ! PLOT OUT SCATTER TRACE
2110 ! D2=1 IF P1=500, D2=2,P1=1
     000
2115 D2=1
2120 IF P1=1000 THEN D2=2
2125 PENUP
2130 FOR I=1 TO P1
2135 PLOT (I-1)/D2,Y(I)
2140 NEXT I
2145 PENUP
2150 ! MAIN MARKER POSITION
2155 LORG 5
2160 S(0)=FNA(M(0))
2165 S(1)=FNA(M(1))
2170 IF F1=0 THEN 2190
2175 S(2)=FNA(M(2))
2180 S(3)=FNA(M(3))
2185 S(4)=FNA(M(4))
2190 MOVE S(0),Y(INT(S(0)+11.5)*
     D2)
2196 PLOT S(0),0
2197 PLOT S(0),145
2200 MOVE S(1),Y(INT(S(1)+1.5)*D
     2)
2210 IF F1=0 THEN 2235
2215 FOR I=2 TO 4
2220 MOVE S(I),Y(INT(S(I)+100)*D
     2)
2230 NEXT I
2235 PENUP
2240 PLOT S(M),0
2245 PLOT S(M),249
2250 PENUP
2255 IF S(M)<400 THEN LORG 1 ELS
     E LORG 7
2260 MOVE S(M),130
2265 LABEL USING "DD.DDD,K" ; M(
     M)," km"
2270 LOCATE .65*RATIO*100,RATIO*
     100,10,100
2280 SCALE 0,32,0,24
2285 LORG 1
2290 MOVE 1,23
2295 LABEL "Anritsu MW98A OTDR"
2300 GOTO 2330
2301 GOTO 2330
2305 LABEL "Title: ";A$
2310 LABEL "Route: ";B$
2315 LABEL "Operator: ";C$
```

Figure 26

```
2320 IF S2=1 THEN LABEL "Date: "
     ;DATE$;"  Time: ";TIME$
2325 IF S2=2 OR S2=3 THEN LABEL
     "Date: ";D$;"  Time: ";T$
2330 LABEL "Measurement No. ";E$
2331 LABEL
2332 LABEL "Averaging Time. ";D4
     ;"sec"
2334 GOTO 2355
2335 GOSUB 8060 ! PLUG IN TYPE
2340 LABEL U$
2345 LABEL "Distance Range: ";10
     *2^D1;"km"
2350 LABEL
2355 H4=FNH(H1)
2360 IF H4<1 THEN 2375
2365 LABEL USING "K,D.DD,K" ; "H
     orizontal Scale ",H4," km/d
     iv"
2370 GOTO 2380
2375 LABEL USING "K,DDDD,K" ; "H
     orizontal Scale ",H4*1000,"
      m/div"
2380 V3=FNV(V1)
2385 LABEL USING "K,D.DD,K" ; "V
     ertical Scale   ";V3;" dB/d
     iv"
2386 GOTO 2450
2390 LABEL
2395 IF F1=1 THEN 2430
2400 ! LOSS MODE
2405 LABEL "LOSS MARKERS"
2410 LABEL USING "K,DD.DDD,K" ;
     "Distance: ",L1," km"
2415 LABEL USING "K,DD.DD,X,K" ;
      "Loss:      ",L3," dB"
2416 GOTO 2560
2420 LABEL USING "K,DD.DD,X,K" ;
      "Loss/km:   ",L3," dB/km"
2425 GOTO 2445
2430 !
2435 ! SPLICE MODE
2440 LABEL USING "K,MDD.DD,K" ;
     "Splice:    ",L4," dB"
2445 IF A3=0 THEN LABEL "Two Poi
     nt Approximation" ELSE LABE
     L "Least Squares Approximat
     ion"
2450 ! PULSE WIDTH
2455 LABEL USING "K,D.D,K" ; "Pu
     lse Width: ";FNP(P0);" uS"
2456 GOTO 2485
2460 ! REF INDEX
2465 LABEL
2470 LABEL "Refractive Index: ",
     I1
2475 ! ATT SETTING
2480 LABEL
2485 LABEL "Attenuator Setting:
     ";A2;" dB"
```

Figure 27

```
2490 LOCATE 0,100*RATIO,0,10
2495 FRAME
2500 LOCATE 0,180*RATIO,0,10
2505 SCALE 0,500,0,10
2510 MOVE 0,8
2515 LORG 1
2520 LABEL USING "DD.DDD,K" ; H2
     ;" km"
2525 MOVE 250,8
2530 LORG 4
2535 LABEL USING "DD.DDD,K" ; H2
     +5*FNH(H1)," km"
2550 MOVE 250,5
2555 LABEL "Length"
2556 MOVE 155,6.5
2557 GOTO 2405
2560 IF M1=0 THEN 2580
2565 MOVE FNA(M1),1
2570 LORG 1
2575 LABEL "MASK"
2580 RETURN
2585 !
3000 ! ********************
3005 ! * CURRENT SCREEN *
3010 ! * SAVE TO DISC   *
3015 ! ********************
3016 ALPHA 14,1
3018 DISP "SAVING DATA NOW"
3019 OFF CURSOR
3020 IF S1=1 THEN MASS STORAGE I
     S ":T"
3025 IF S1=2 THEN MASS STORAGE I
     S ":D700"
3030 !
3035 G$=F$&E$
3040 CREATE G$,36
3045 ASSIGN# 1 TO G$
3050 PRINT# 1 ; A$,B$,C$,DATE$,T
     IME$,E$,D4
3055 PRINT# 1 ; A2,D1,H1,P0,H2
3060 PRINT# 1 ; M1,I1,A3,V1,U1
3065 PRINT# 1 ; L1,L2,L3,L4
3070 PRINT# 1 ; F1,P1,M,M()
3075 PRINT# 1 ; Y()
3080 ASSIGN# 1 TO *
3085 RETURN
3090 !
3500 ! ********************
3505 ! * READ SCREEN DATA *
3510 ! * FROM DISC        *
3515 ! ********************
3517 CRT OFF
3520 IF S1=1 THEN MASS STORAGE I
     S ":T"
3525 IF S1=2 THEN MASS STORAGE I
     S ":D700"
3530 ASSIGN# 1 TO G$
3535 READ# 1 ; A$,B$,C$,D$,T$,E$
     ,D4
3540 READ# 1 ; A2,D1,H1,P0,H2
```

Figure 28

```
3545 READ# 1 ; M1,I1,A3,V1,U1
3550 READ# 1 ; L1,L2,L3,L4
3555 READ# 1 ; F1,P1,M,M()
3560 READ# 1 ; Y()
3565 ASSIGN# 1 TO *
3567 CRT ON
3570 RETURN
3575 !
4000 ! ********************
4005 ! * PLOT SCREEN DATA *
4010 ! * TO CRT GRAPHICS  *
4015 ! * & ALPHA SCREEN   *
4020 ! ********************
4025 ! PLOT OUT GRAPHICS
4030 P2=1
4035 PLOTTER IS P2
4040 GCLEAR
4045 ! LOCATE 0,RATIO*100,15,100
4050 LOCATE 10,RATIO*90,15,90
4055 SCALE 0,499,0,249
4060 AXES 50,25
4065 FRAME
4070 !
4075 ! PLOT OUT SCATTER TRACE
4080 ! D2=1 IF P1=500, D2=2 IF P
     1=1000
4085 D2=1
4090 IF P1=1000 THEN D2=2
4095 PENUP
4100 FOR I=1 TO P1
4105 PLOT (I-1)/D2,Y(I)
4110 NEXT I
4115 PENUP
4120 ! MAIN MARKER POSITION
4125 LORG 5
4130 S(0)=FNA(M(0))
4135 S(1)=FNA(M(1))
4140 IF F1=0 THEN 4160
4145 S(2)=FNA(M(2))
4150 S(3)=FNA(M(3))
4155 S(4)=FNA(M(4))
4160 MOVE S(0),Y(INT(S(0)+1 5)*D
     2)
4165 LABEL "*"
4170 MOVE S(1),Y(INT(S(1)+1 5)*D
     2)
4175 LABEL "X"
4180 IF F1=0 THEN 4205
4185 FOR I=2 TO 4
4190 MOVE S(I),Y(INT(S(I)+1 5)*D
     2)
4195 LABEL "X"
4200 NEXT I
4205 PENUP
4210 PLOT S(M),0
4215 PLOT S(M),249
4220 PENUP
4225 IF S(M)<400 THEN LORG 1 ELS
     E LORG 7
4230 MOVE S(M),25
```

Figure 29

```
4235 LABEL USING "DD.DDD,K" ; M(
     M),"  km"
4240 LOCATE 0,100*RATIO,0,15
4245 FRAME
4250 SCALE 0,500,0,10
4255 MOVE 0,9
4260 LORG 3
4265 LABEL USING "DD.DDD,K" ; H2
     ;"  km"
4270 MOVE 250,9
4275 LORG 6
4280 LABEL USING "DD.DDD,K" ; H2
     +5*FNH(H1),"  km"
4285 MOVE 490,9
4290 LORG 9
4295 LABEL USING "DD.DDD,K" ; H2
     +10*FNH(H1),"  km"
4300 MOVE 250,6
4305 LORG 6
4310 LABEL "Length"
4315 IF M1=0 THEN 4335
4320 MOVE FNA(M1),1
4325 LORG 1
4330 LABEL "Mask"
4335 IF P4=3 THEN COPY
4340 RETURN
4345 !
4500 ! ****************
4505 ! * PRINTOUT DATA *
4510 ! * TO CRT        *
4515 ! ****************
4520 !
4525 PLOTTER IS 1
4530 GCLEAR
4535 LOCATE 0,RATIO*100,0,100
4540 FRAME
4545 SCALE 0,32,0,24
4550 MOVE 1,22
4555 LORG 1
4560 LABEL "Anritsu MW98A OTDR
       Page 1"
4565 LABEL
4570 LABEL "Title:  ";A$
4575 LABEL "Route:  ";B$
4580 LABEL "Operator:  ";C$
4585 IF S2=1 THEN LABEL "Date:";
     DATE$;"  Time:";TIME$
4590 IF S2=2 OR S2=3 THEN LABEL
     "Date:";D$;"  Time:";T$
4595 !
4600 LABEL "Measurement No.  ";E$
4602 LABEL "Averaging Time.  ";D4
     ;"sec"
4610 GOSUB 8050 ! PLUG IN TYPE
4615 LABEL U$
4620 LABEL "Distance Range:  ";10
     *2^D1;"km"
4625 H4=FNH(H1)
4630 IF H4<1 THEN 4645
4635 LABEL USING "K,D.DD,K" ; "H
     orizontal Scale ",H4,"  km/d
     iv"
```

Figure 30

```
4640 GOTO 4650
4645 LABEL USING "K,DDDDD,K" ; "
     Horizontal Scale ",H4*1000,
     " m/div"
4650 V3=FNV(V1)
4655 LABEL USING "K,D.DD,K" ; "V
     ertical Scale   ";V3;" dB/d
     iv"
4660 IF F1=0 THEN 4685
4665 ! SPLICE MODE
4670 LABEL
4675 LABEL USING "K,MDD.DD,K" ;
     "Splice:        ",L4,"dB"
4680 IF A3=0 THEN LABEL "Two Poi
     nt Approximation" ELSE LABE
     L "Least Squares Approximat
     ion"
4685 IF P4=3 THEN COPY
4690 GCLEAR
4695 LOCATE 0,RATIO*100,0,100
4700 FRAME
4705 SCALE 0,32,0,24
4710 MOVE 25,22
4715 LABEL "Page 2"
4720 MOVE 1,22
4725 IF F1=1 THEN 4760
4730 ! LOSS MODE
4735 LABEL "LOSS MARKERS"
4740 LABEL USING "K,DD.DDD,K" ;
     "Distance: ",L1," km"
4745 LABEL USING "K,DD.DD,X,K" ;
      "Loss:      ",L2," dB"
4750 LABEL USING "K,DD.DD,X,K" ;
      "Loss/km:   ",L3," dB/km"
4755 IF A3=0 THEN LABEL "Two Poi
     nt Approximation" ELSE LABE
     L "Least Squares Approximat
     ion"
4760 ! PULSE WIDTH
4765 LABEL
4770 LABEL USING "K,D.D,K" ; "Pu
     lse Width: ";FNP(P0);" uS"
4775 ! REF INDEX
4780 LABEL
4785 LABEL "Refractive Index: "
     ;I1
4790 ! ATT SETTING
4795 LABEL
4800 LABEL "Attenuator Setting:
     ";A2;" dB"
4805 IF P4=3 THEN COPY
4810 RETURN
4815 !
5000 ! ************************
5005 ! * INPUT MEASUREMENT(S) *
5010 ! * RELATED INFORMATION  *
5015 ! ************************
5020 CLEAR
5025 DISP "Input measurement tit
     le";
```

Figure 31

```
5030 INPUT A$
5035 DISP "Enter route name ";
5040 INPUT B$
5045 DISP "Enter operators name
     ";
5050 INPUT C$
5055 DISP "Date set is ";DATE$;"
      Do you wish to change it?"
5060 DISP "Enter Y or N then pre
     ss ENDLINE"
5065 INPUT X$
5070 IF X$="Y" OR X$="y" THEN 50
     75 ELSE 5090
5075 DISP "Enter date ";
5080 DISP "e.g 05/17/1986 for 17
      May 1986"
5085 INPUT D$
5090 DISP "Time set is ";TIME$;"
      Do you wish to change it?"
5095 DISP "Enter Y or N then pre
     ss ENDLINE"
5100 INPUT X$
5105 IF X$="Y" OR X$="y" THEN 51
     10 ELSE 5140
5110 DISP "Enter current time ";
5115 DISP "e.g 14:22:07 for 2:22
     :07 pm"
5120 INPUT T$
5125 D=MDY(D$)-MDY("12/31/1985")
5130 D=86*1000+D
5135 SETTIME HMS(T$),D
5140 CLEAR
5145 RETURN
5150 !
6000 ! ******************
6005 ! * DISC ERROR SBRT *
6010 ! ******************
6015 BEEP
6020 WAIT 200
6025 BEEP
6030 IF ERRN=60 THEN DISP "Disc
     is write protected, change
     write protect tab on disc"
6035 IF ERRN=62 THEN DISP "Tape
     cartridge out, Please inser
     t a tape correctly"
6040 IF ERRN=63 THEN DISP "File
     already exists with that na
     me, Please use a different
     name"
6045 IF ERRN=65 THEN DISP "Tape
     full, replace with new tape
     "
6050 IF ERRN=67 THEN DISP G$," D
     oes not exist on selected d
     evice,try different filenam
     e"
6055 IF ERRN=73 THEN DISP "Bad t
     ape or tape not initialized
     , only use initialized tape
     s"
```

Figure 32

```
6060 IF ERRN=124 THEN DISP "Disc
      file directory full"
6065 IF ERRN=126 THEN DISP "Plot
     ter is not connected to
      computer"
6070 IF ERRN=128 THEN DISP "Disc
      is full, change disc"
6075 IF ERRN=129 THEN DISP "Stor
     age device damaged, replace
      tape/disc"
6080 IF ERRN=130 THEN DISP "Disc
      is not initialized or disc
      not inserted properly ",
6085 IF ERRN=130 THEN DISP "or d
     isc drive is not present"
6090 DISP "Press END LINE when r
     eady to    continue"
6095 INPUT X$
6100 !
6105 IF ERRN=60 THEN 3000
6110 IF ERRN=62 AND ERRL<3000 TH
     EN 500
6115 IF ERRN=62 AND ERRL<3000 TH
     EN 500
6120 IF ERRN=62 THEN 3500
6125 IF ERRN=63 AND ERRL>3000 TH
     EN 245
6130 IF ERRN=65 AND ERRL>3000 TH
     EN 3000
6135 IF ERRN=67 THEN 525
6140 IF ERRN=124 OR ERRN=128 THE
     N 3000
6145 IF ERRN=126 THEN 2000
6150 IF ERRN=129 AND ERRL=530 TH
     EN 520
6155 IF ERRN=129 AND ERRL>3000 A
     ND ERRL<3200 THEN 3000
6160 IF ERRN=129 AND ERRL>3200 A
     ND ERRL<4000 THEN 3500
6165 IF ERRN=130 AND ERRL>500 AN
     D ERRL<900 THEN 500
6170 IF ERRN=130 AND ERRL>3000 A
     ND ERRL<3200 THEN 3000
6175 IF ERRN=130 AND ERRL>3200 A
     ND ERRL<4000 THEN 3500
6180 DISP "Error cannot be overc
     ome"
6185 !
6190 !
6500 PAUSE
7000 ! AVERAGE TIME WAIT SBRT
7500 ! MEASUREMENT RUN DATA
7515 OFF CURSOR
7516 ALPHA 1,1
7517 CLEAR
7520 DISP "Date: ";DATE$
7525 DISP "Measurement Title: "
     A$
7530 DISP "Route: ";B$
7535 DISP "Operators Name: ";C$
```

Figure 33

```
7540 IF D4>0 THEN DISP "Meas. Av
     erage time: ";D4;"secs"
7545 DISP "Meas. No: ";E*;"  Mea
     s. left: ";M2
7560 IF T4=0 THEN 7590
7565 DISP "Time between"
7570 DISP "measurements: ";T1;"h
     r"
7575 DISP "                ";T2;"m
     in"
7580 DISP "                ";T3;"s
     ec"
7590 IF S1=1 THEN DISP "Data sto
     red on tape cartridge"
7595 IF S1=2 THEN DISP "Data sto
     red on disc"
7600 IF S1=1 OR S1=2 THEN DISP "
     Base Filename: ";F$
7602 OFF CURSOR
7605 RETURN
7700 ! AVERAGE TIME WAIT SBRT
7702 IF D4=0 THEN 7740
7705 OUTPUT A1 USING "K,/" ; "AV
     R1"
7710 ON TIMER# 3,D4*1000 GOTO 77
     35
7715 !
7720 ALPHA 14,1
7725 DISP "  AVERAGING  TIME LEF
     T:";INT(D4+.5-READTIM(3));"
     sec"
7726 OFF CURSOR
7730 GOTO 7720
7735 OFF TIMER# 3
7740 !
7745 ALPHA 14,1
7750 DISP "  DATA READ IN PROGRE
     SS"
7753 OFF CURSOR
7755 RETURN
7800 ! INTERMEASUREMENT WAIT SBR
     T
7805 OFF CURSOR
7810 ON TIMER# 3,T4 GOTO 7850
7815 ALPHA 14,1
7825 DISP "TIME BEFORE NEXT MEAS
     UREMENT:-"
7826 OFF CURSOR
7830 T5=T4/1000-READTIM(3)
7835 T6=INT(T5/3600)
7840 T7=INT((T5-T6*3600)/60)
7845 T8=INT(T5-T6*3600-T7*60)
7850 DISP T6;"HR ";T7;"MIN ";T8;
     "SEC"
7852 OFF CURSOR
7855 GOTO 7815
7860 OFF TIMER# 3
7870 ALPHA 14,1
7875 DISP
7876 OFF CURSOR
```

Figure 34

```
7980 RETURN
8000 ! FUNCTION TO CONVERT HSCAL
     ING TO KM
8005 DEF FNH(X)
8010 IF X=0 THEN H3=4
8015 IF X=1 THEN H3=2
8020 IF X=2 THEN H3=1
8025 IF X=3 THEN H3=.5
8030 IF X=4 THEN H3=.25
8035 IF X=5 THEN H3=.1
8040 IF X=6 THEN H3=.05
8045 IF X=7 THEN H3=.025
8050 FNH=H3*1.5/I1 ! CORRECT FOR
      REFRACTIVE INDEX
8055 FN END
8060 IF U1=1 THEN U$="0.85um Mul
     ti Mode"
8065 IF U1=2 THEN U$="1.3um Mult
     i Mode"
8070 IF U1=3 THEN U$="1.3um Sing
     le Mode"
8075 IF U1=4 THEN U$="1.55um Sin
     gle Mode"
8080 RETURN
8085 DEF FNV(X) ! VERT SCALE
8090 IF X=0 THEN V2=2.5
8095 IF X=1 THEN V2=1
8100 IF X=2 THEN V2= 5
8105 IF X=3 THEN V2=.25
8110 FNV=V2
8115 FN END
8120 DEF FNP(X) ! PULSE WIDTH
8125 IF X=0 THEN P9=.1
8130 IF X=1 THEN P9=.5
8135 IF X=2 THEN P9=2
8140 FNP=P9
8145 FN END
8150 DEF FNA(X) = (X-H2)/(10*FNH
     (H1))*499
8155 END
```

Figure 35

```
 10 OPTION BASE 1
 20 DIM S(4),M(4)
 30 DIM Y(1000)
 40 DIM E$[32]
 50 DISP "WHAT IS FILE NAME"
 60 INPUT F$
 70 DISP "ENTER THE MEAS NO.RANG
    E"
 90 DISP "START NO. ";
 90 INPUT S3
100 DISP "STOP NO.  ";
110 INPUT S4
120 FOR J=S3 TO S4
130 G$=F$&VAL$(J)
140 ASSIGN# 1 TO G$
150 READ# 1 ; A$,B$,C$,D$,T$,E$,
    D4
160 READ# 1 , A2,D1,H1,P0,H2
170 READ# 1 ; M1,I1,A3,V1,U1
180 READ# 1 ; L1,L2,L3,L4
190 READ# 1 ; F1,P1,M,M()
200 READ# 1 ; Y()
205 ASSIGN# 1 TO *
210 PRINT "MEASUREMENT NO",E$
220 PRINT "POINTS ALONG X-AXIS"
230 FOR X=5 TO 550
240 PRINT Y(X);
250 NEXT X
255 PRINT
260 END
```

Figure 36

4.4.2. Test results

Although a number of fibres were measured as described in Section 4.4.1 above, the following is a case in point. A plot representing the whole of the Y-axis (as displayed on the OTDR) is shown in Figure 37. To enable more in-depth investigation the resolution was increased thus only that part of the Y-axis that contains information on the fibre attenuation is shown. Figures 38 to 47 exhibit the ten plots and it can be seen that although the overall shape is constant, the fine detail varies with each measurement. Note only that part of the X-axis that contains information has been reproduced on the above figures.

To make direct comparisons between each plot simpler, Figures 48 to 57 show the contents of the data file for each plot respectively (Note, due to the quantity of data recorded for each plot, the data listing has been split into two halves, hence each figure is marked A and B for each half respectively). On figure 48 the numerical peaks marked 1, 2 and 3 align with the pictorial peaks 1, 2 and 3 respectively in Figure 37. Peak 1 is the initial launch of the 1km fibre tail, with its splice, 2 is the butt-joint between the two fibres and 3 is the end reflection. These peaks can be seen for all ten plots and data lists.

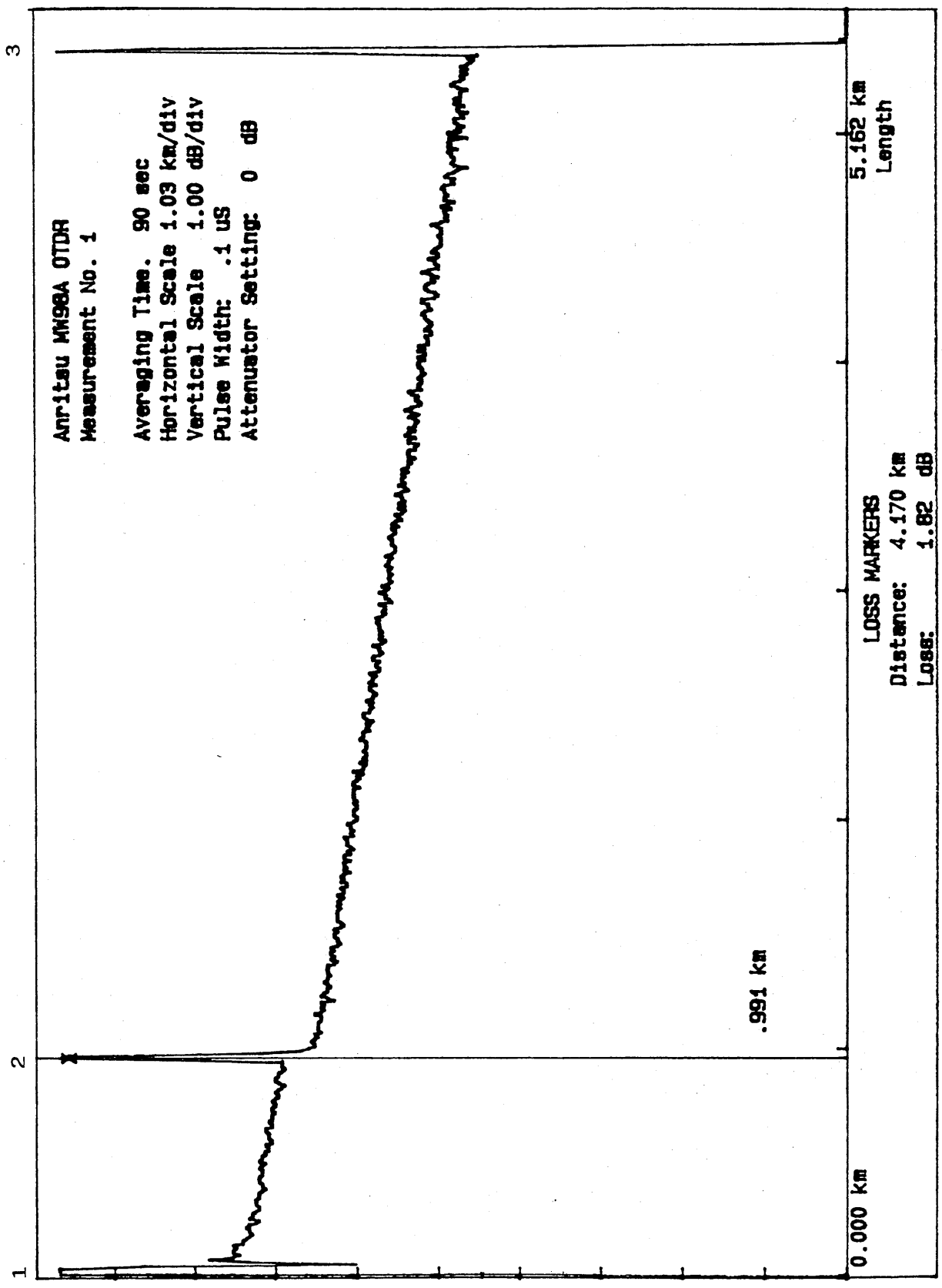
Anritsu MW90A OTDR
Measurement No. 1
Averaging Time. 90 sec
Horizontal Scale 1.03 km/div
Vertical Scale 1.00 dB/div
Pulse Width: .1 uS
Attenuator Setting: 0 dB
.991 km
LOSS MARKERS
Distance: 4.170 km
Loss: 1.82 dB
0.000 km
5.162 km
Length
1
2
3

Figure 37

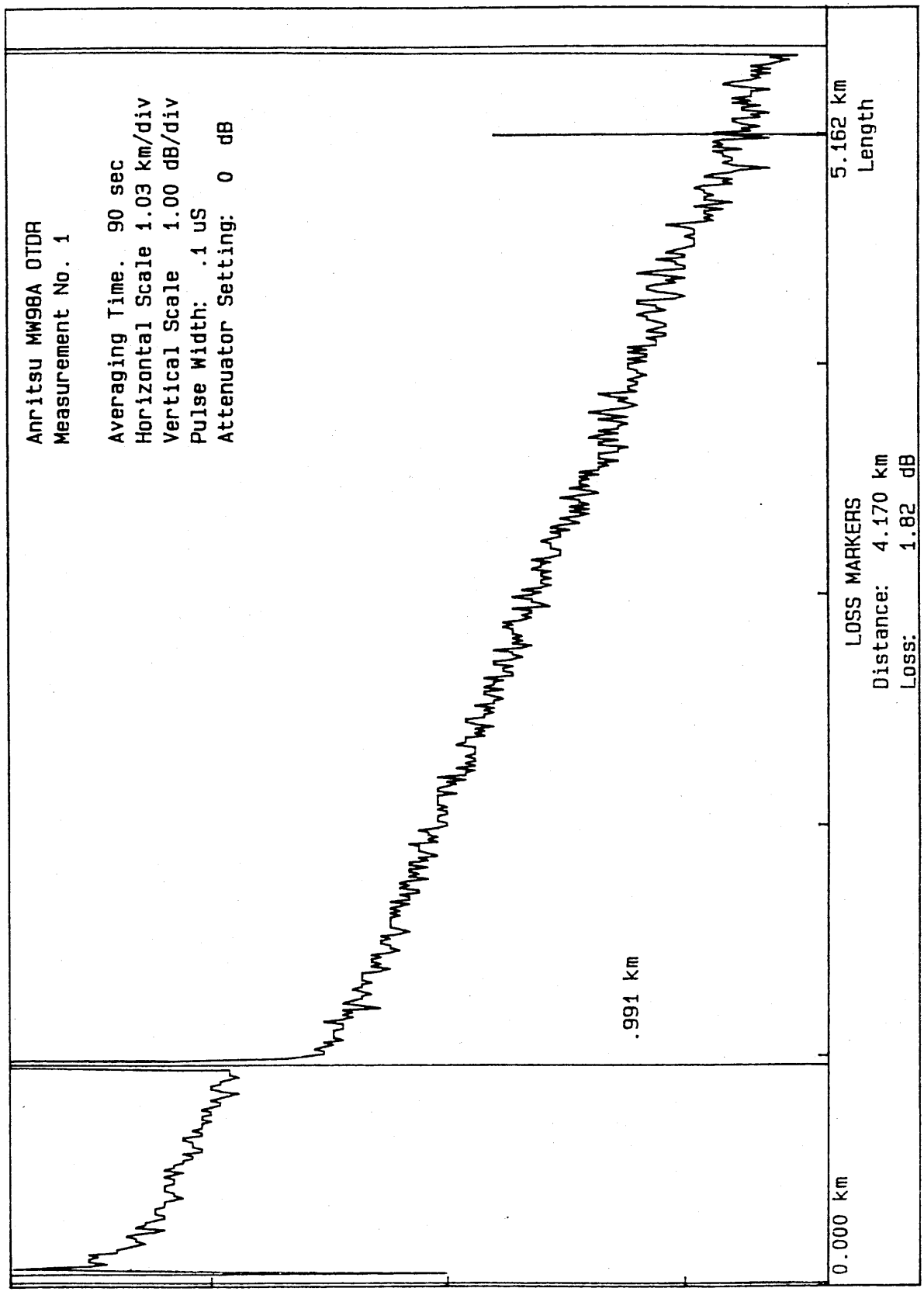
Anritsu MW98A OTDR
Measurement No. 1
Averaging Time. 90 sec
Horizontal Scale 1.03 km/div
Vertical Scale 1.00 dB/div
Pulse Width: .1 uS
Attenuator Setting: 0 dB
.991 km
LOSS MARKERS
Distance: 4.170 km
Loss: 1.82 dB
0.000 km
5.162 km
Length

Figure 38

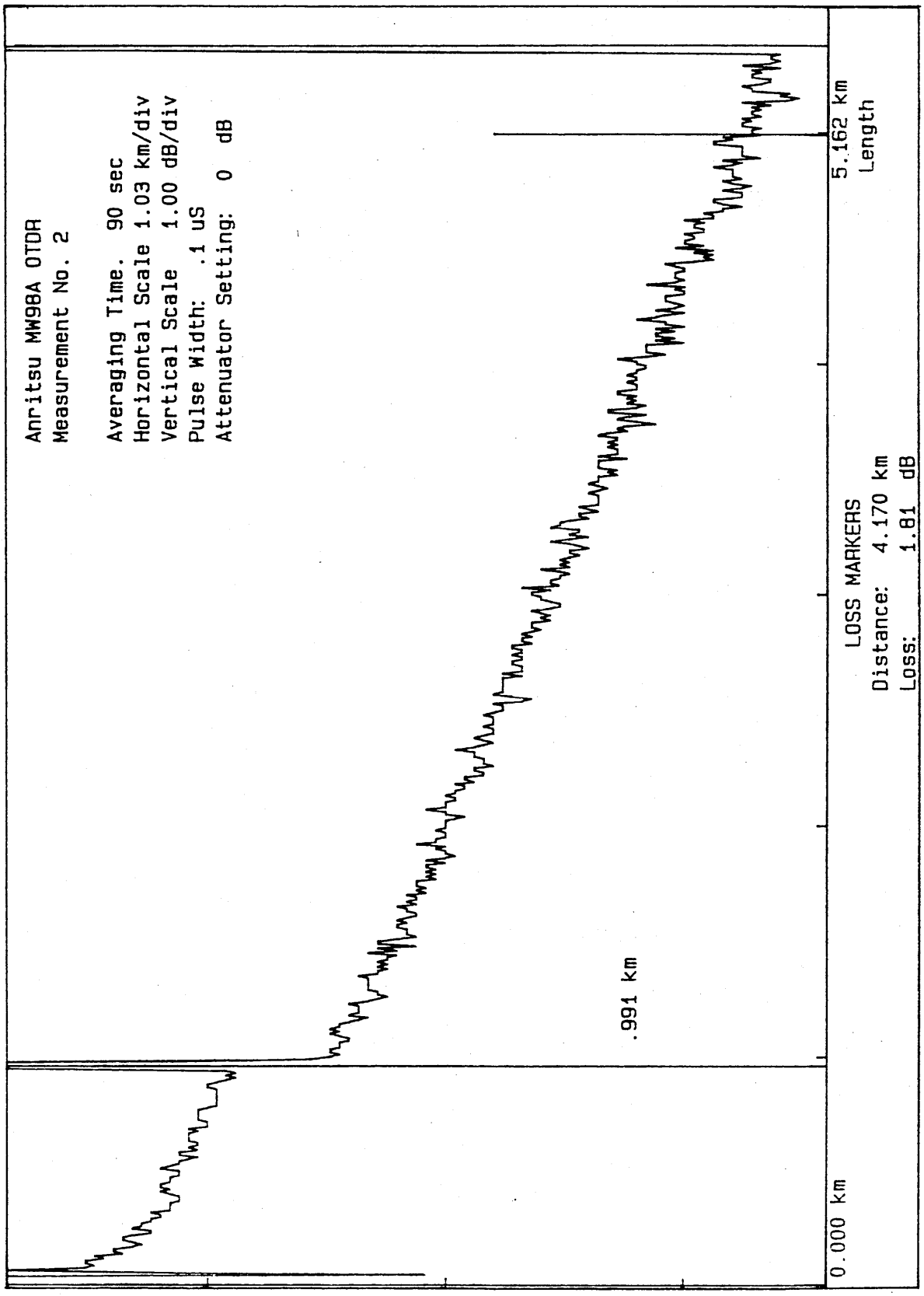
Anritsu MW98A OTDR
Measurement No. 2
Averaging Time. 90 sec
Horizontal Scale 1.03 km/div
Vertical Scale 1.00 dB/div
Pulse Width: .1 uS
Attenuator Setting: 0 dB
.991 km
LOSS MARKERS
Distance: 4.170 km
Loss: 1.81 dB
0.000 km
5.162 km
Length

Figure 39

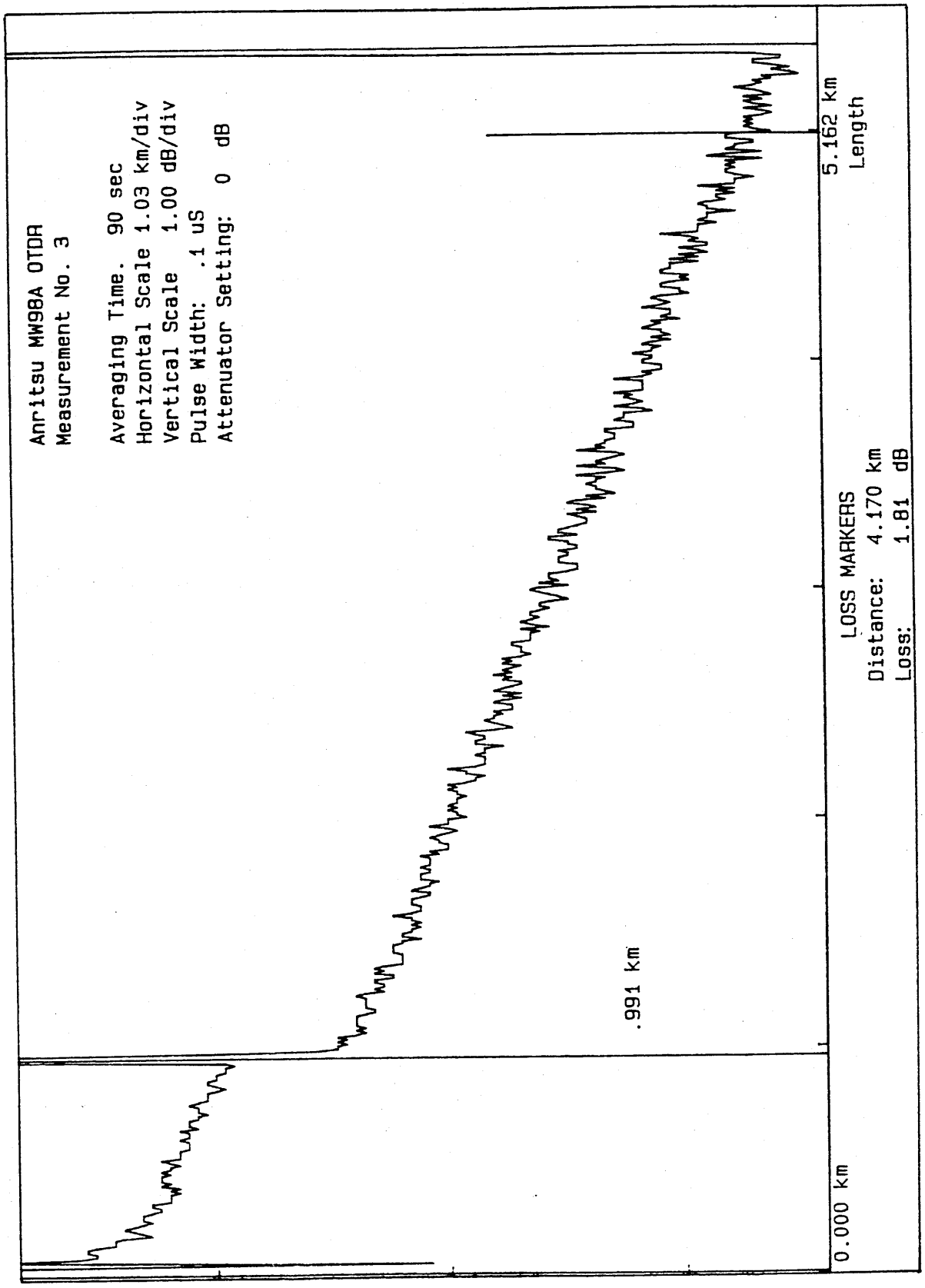
Anritsu MW98A OTDR
Measurement No. 3
Averaging Time. 90 sec
Horizontal Scale 1.03 km/div
Vertical Scale 1.00 dB/div
Pulse Width: .1 uS
Attenuator Setting: 0 dB
.991 km
5.162 km
Length
LOSS MARKERS
Distance: 4.170 km
Loss: 1.81 dB
0.000 km

Figure 40

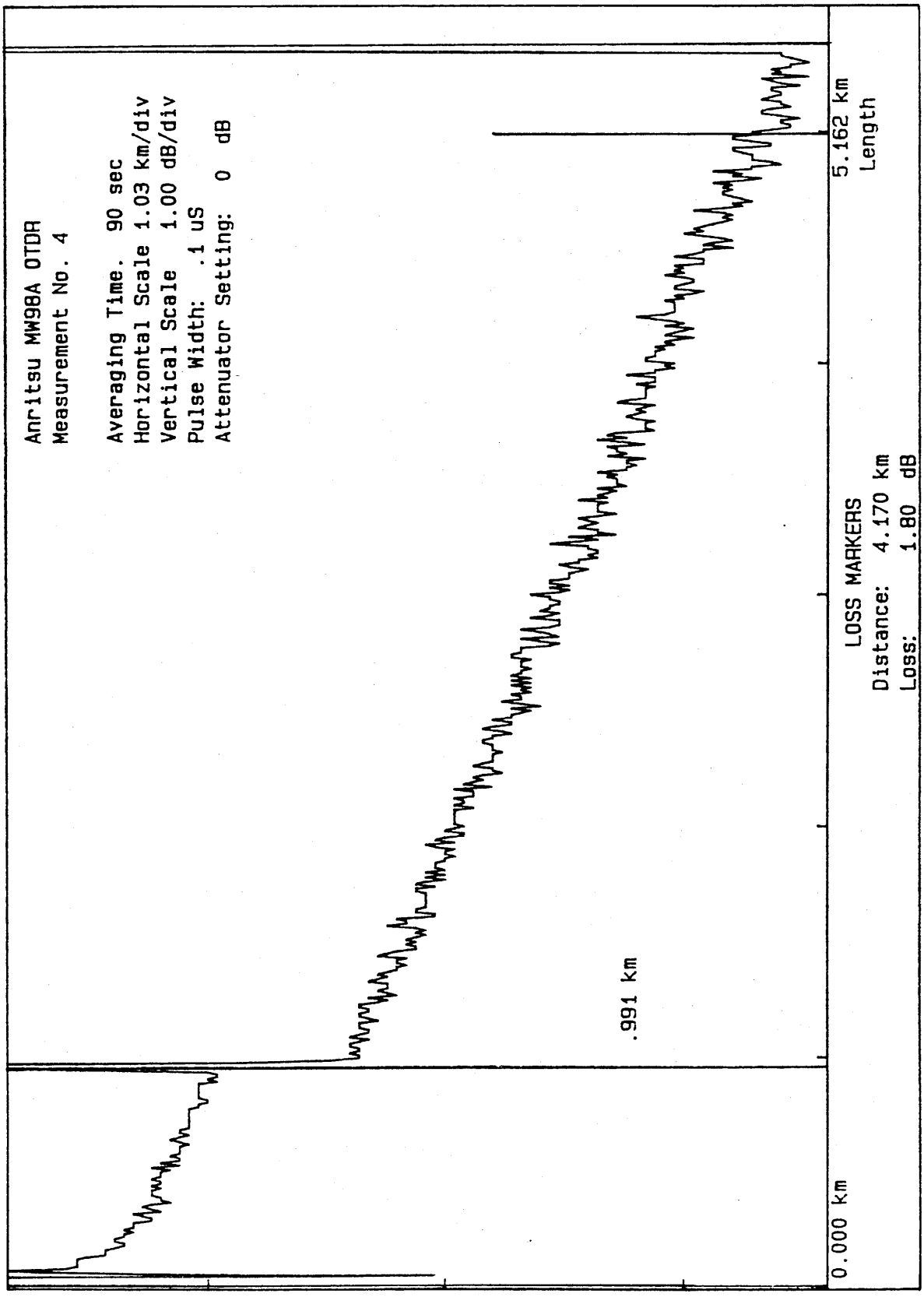
Anritsu MW98A OTDR
Measurement No. 4
Averaging Time. 90 sec
Horizontal Scale 1.03 km/div
Vertical Scale 1.00 dB/div
Pulse Width: .1 uS
Attenuator Setting: 0 dB
.991 km
LOSS MARKERS
Distance: 4.170 km
Loss: 1.80 dB
5.162 km
Length
0.000 km

Figure 41

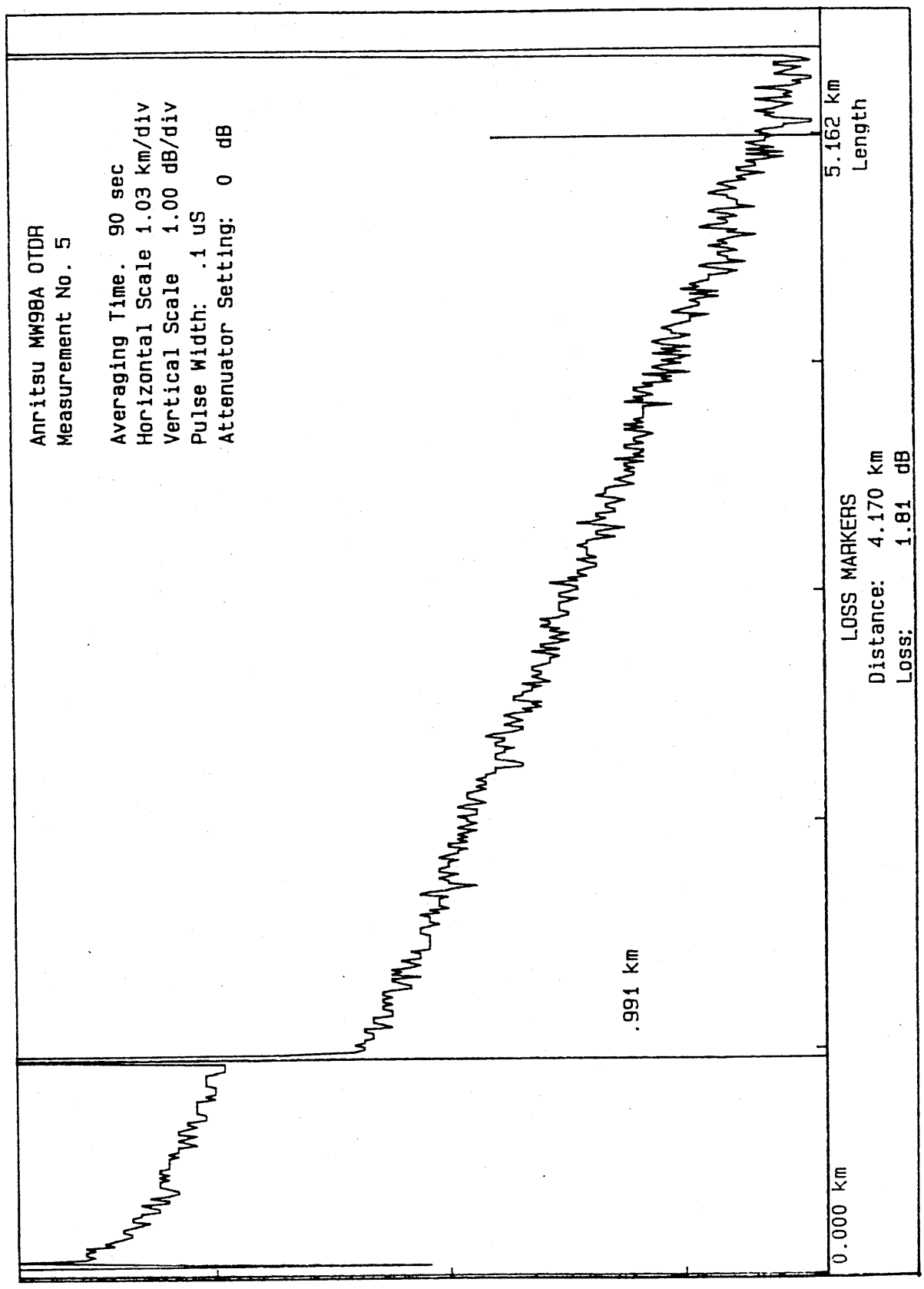
Anritsu MW98A OTDR
Measurement No. 5
Averaging Time. 90 sec
Horizontal Scale 1.03 km/div
Vertical Scale 1.00 dB/div
Pulse Width: .1 uS
Attenuator Setting: 0 dB
.991 km
5.162 km
Length
LOSS MARKERS
Distance: 4.170 km
Loss: 1.81 dB
0.000 km

Figure 42

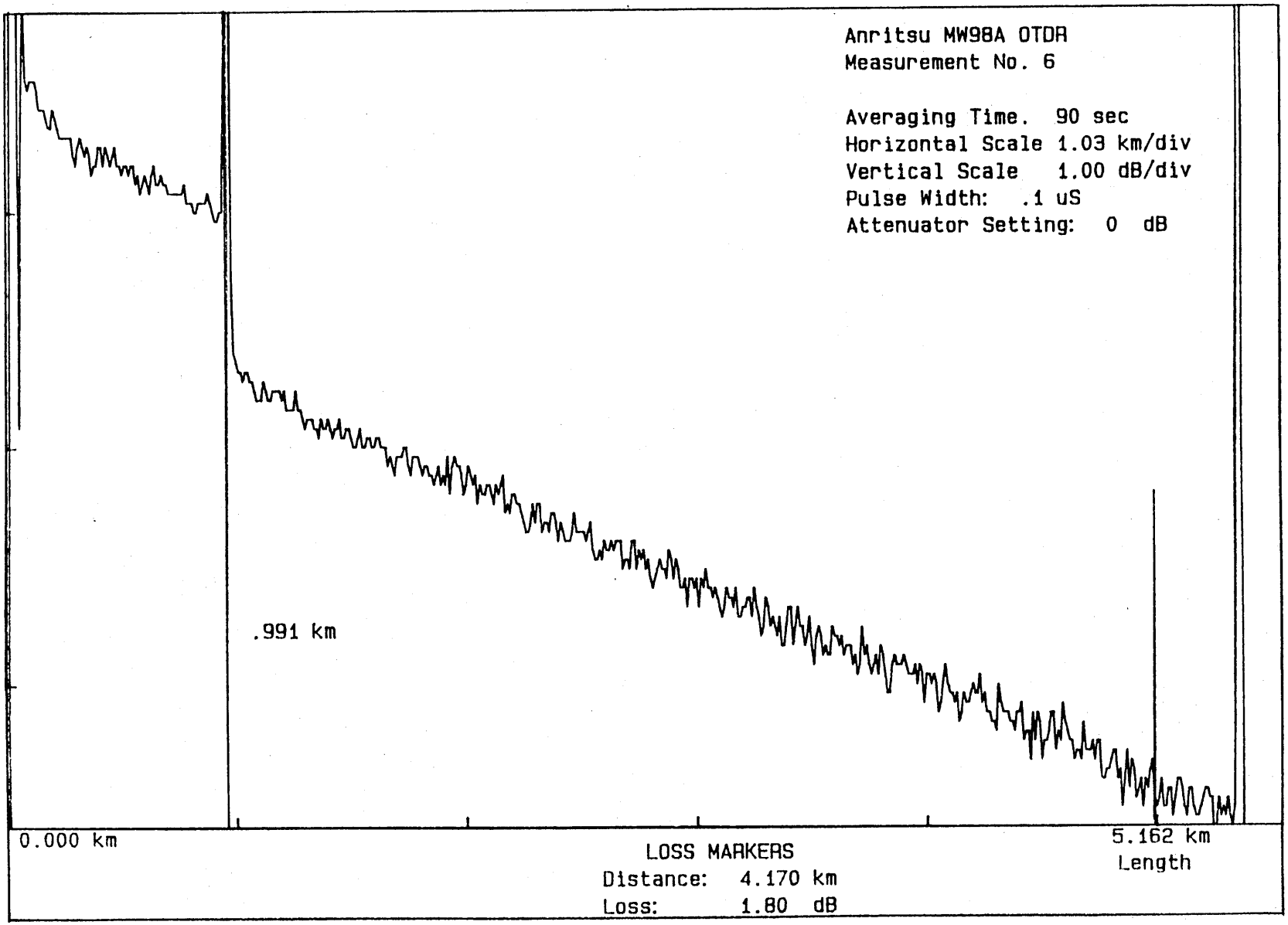
Anritsu MW98A OTDR
Measurement No. 6
Averaging Time. 90 sec
Horizontal Scale 1.03 km/div
Vertical Scale 1.00 dB/div
Pulse Width: .1 uS
Attenuator Setting: 0 dB
.991 km
0.000 km
5.162 km
Length
LOSS MARKERS
Distance: 4.170 km
Loss: 1.80 dB

Figure 43

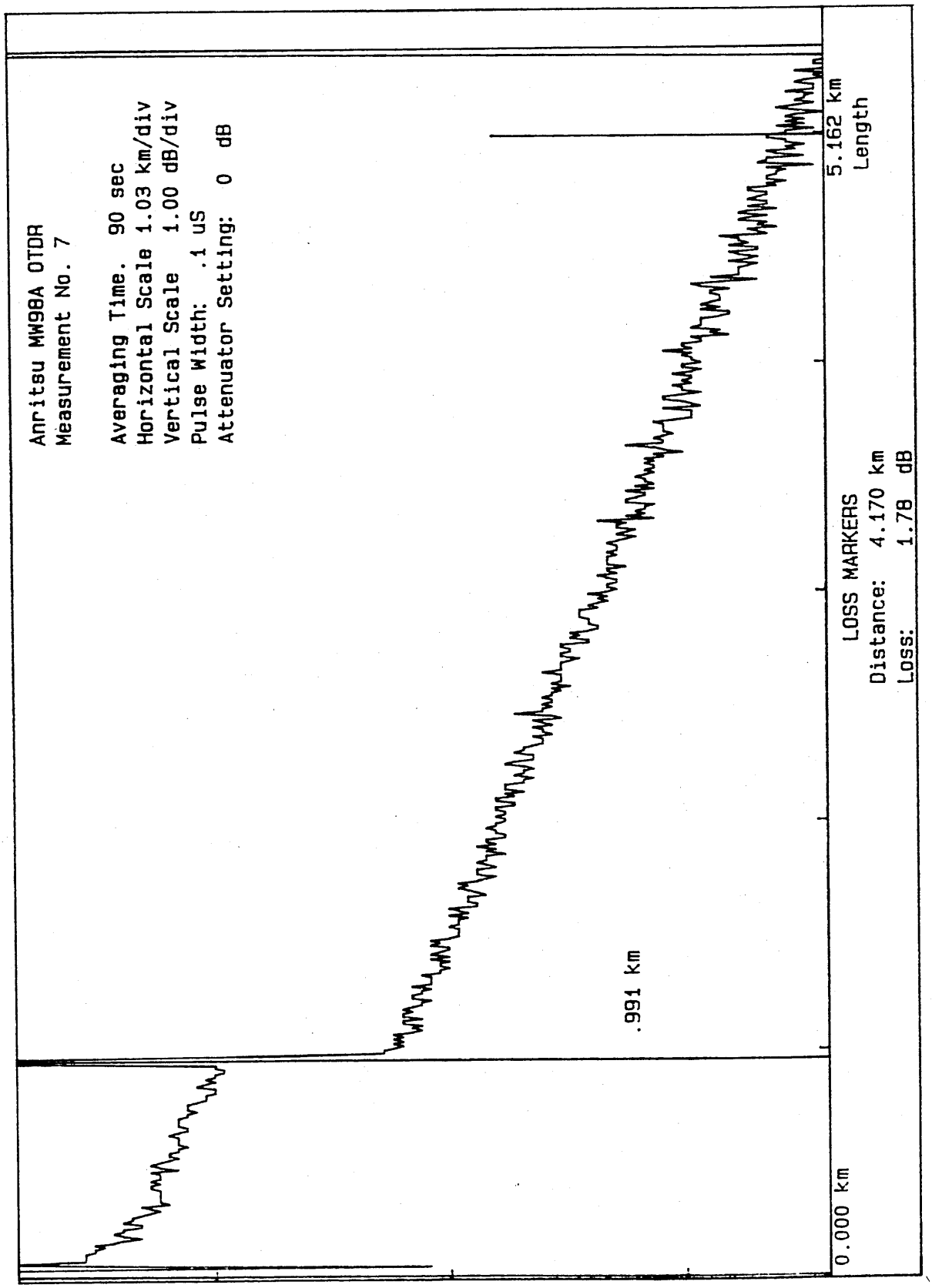
Anritsu MW98A OTDR
Measurement No. 7
Averaging Time. 90 sec
Horizontal Scale 1.03 km/div
Vertical Scale 1.00 dB/div
Pulse Width: .1 uS
Attenuator Setting: 0 dB
.991 km
LOSS MARKERS
Distance: 4.170 km
Loss: 1.78 dB
5.162 km
Length
0.000 km

Figure 44

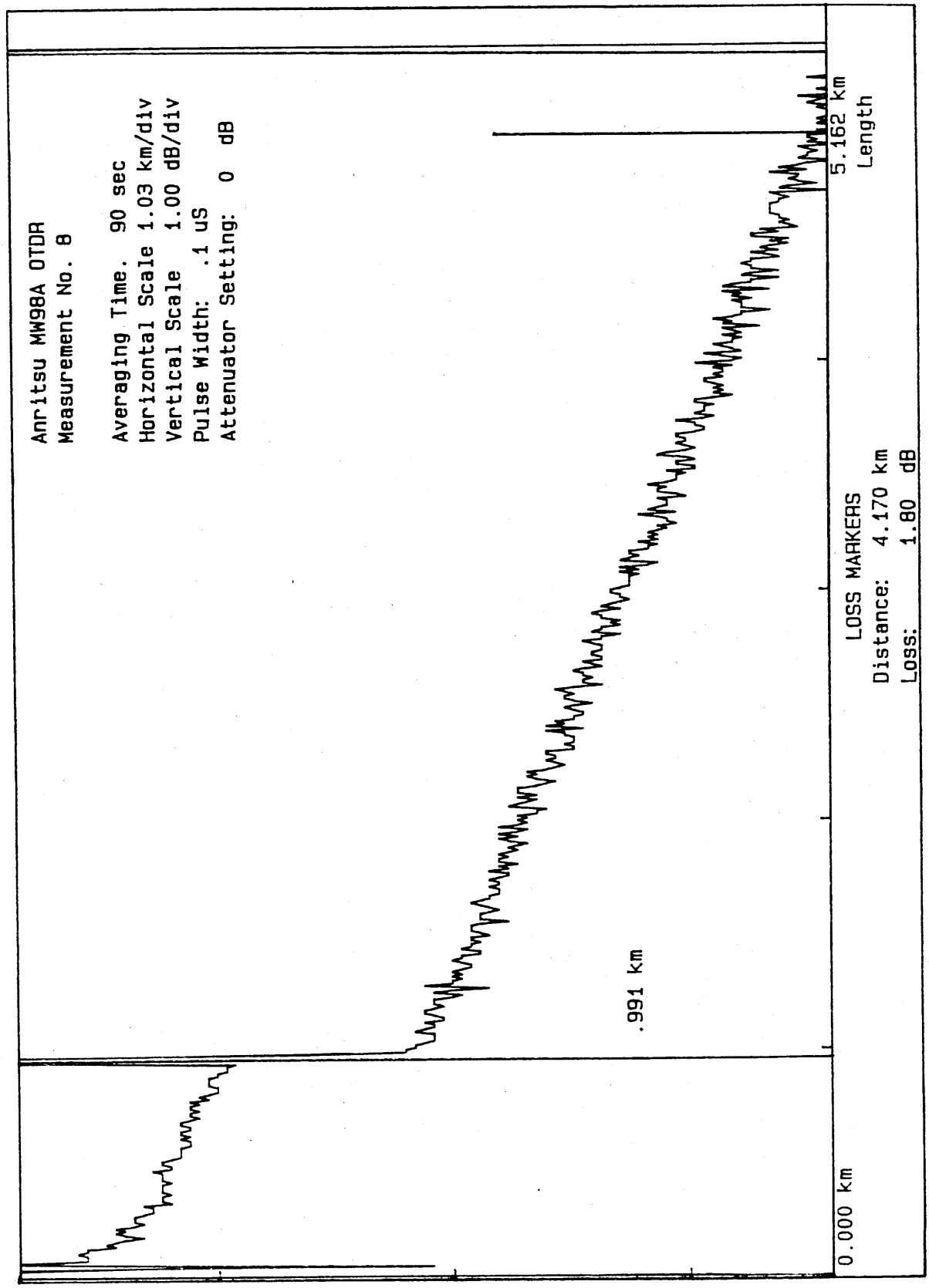
Anritsu MW98A OTDR
Measurement No. 8
Averaging Time. 90 sec
Horizontal Scale 1.03 km/div
Vertical Scale 1.00 dB/div
Pulse Width: .1 uS
Attenuator Setting: 0 dB
.991 km
LOSS MARKERS
Distance: 4.170 km
Loss: 1.80 dB
5.162 km
Length
0.000 km

Figure 45

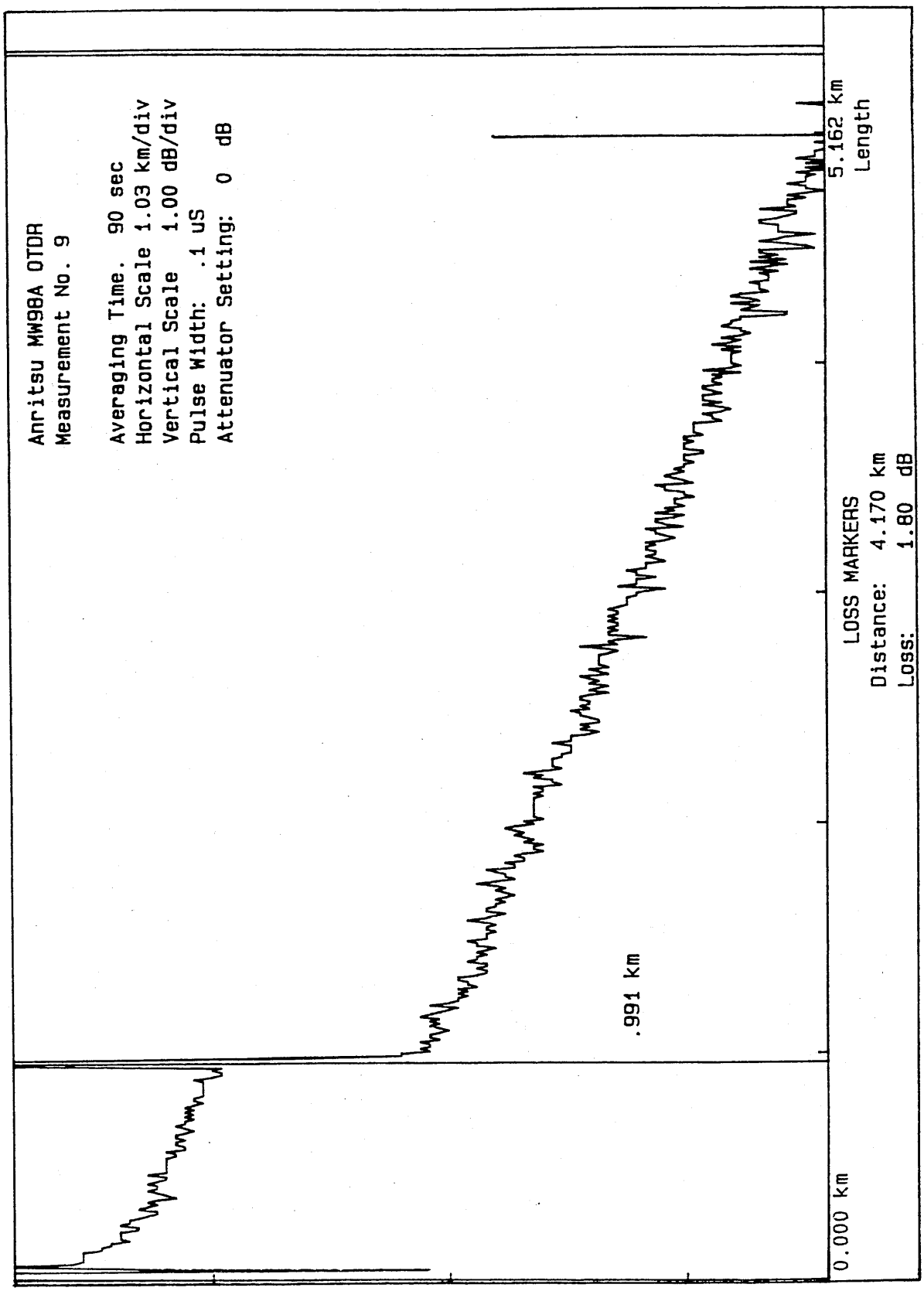
Anritsu MW98A OTDR
Measurement No. 9
Averaging Time. 90 sec
Horizontal Scale 1.03 km/div
Vertical Scale 1.00 dB/div
Pulse Width: .1 uS
Attenuator Setting: 0 dB
.991 km
0.000 km
5.162 km
Length
LOSS MARKERS
Distance: 4.170 km
Loss: 1.80 dB

Figure 46

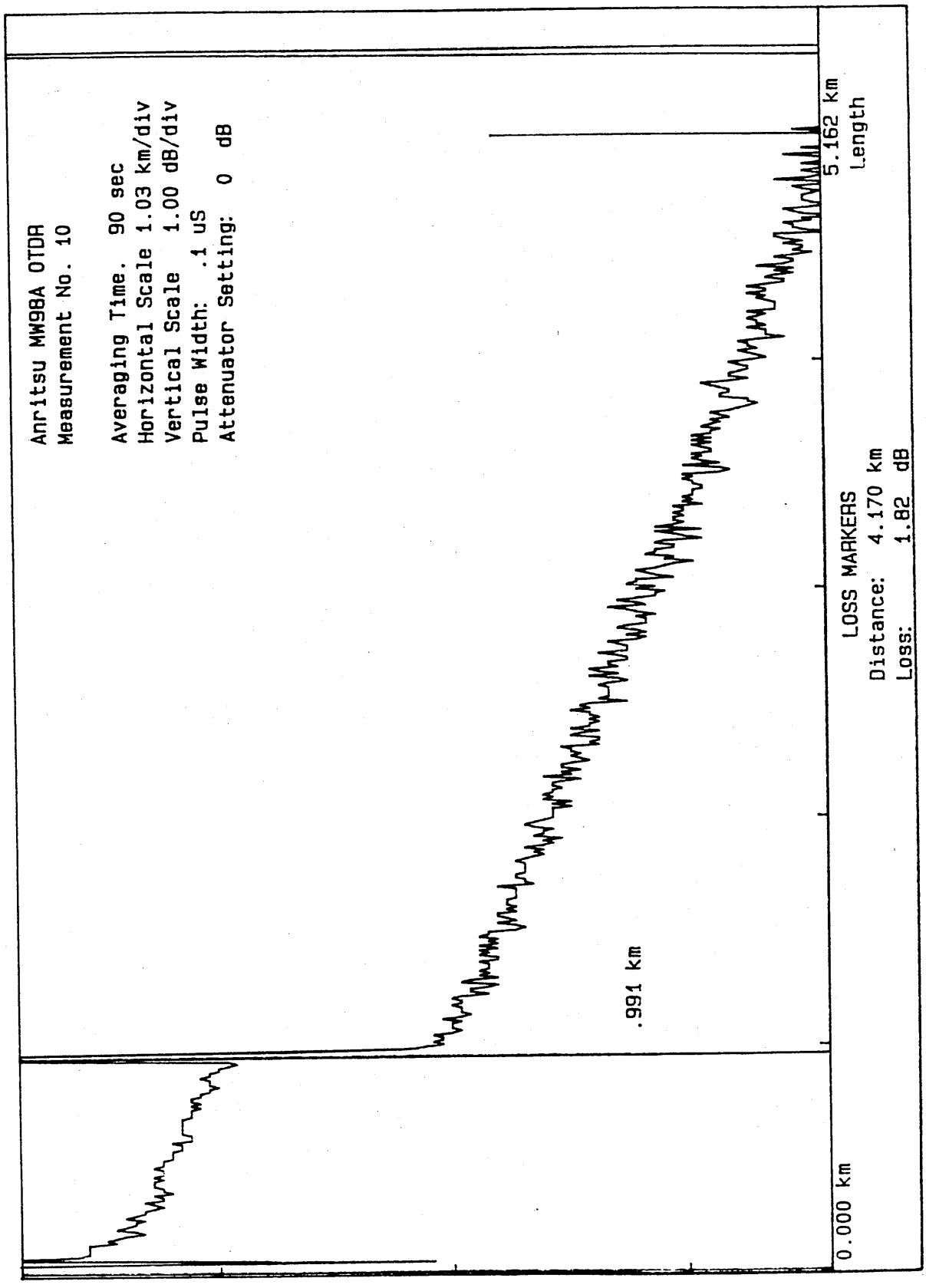
Anritsu MW98A OTDR
Measurement No. 10
Averaging Time. 90 sec
Horizontal Scale 1.03 km/div
Vertical Scale 1.00 dB/div
Pulse Width: .1 uS
Attenuator Setting: 0 dB
5.162 km
Length
LOSS MARKERS
Distance: 4.170 km
Loss: 1.82 dB
.991 km
0.000 km

Figure 47

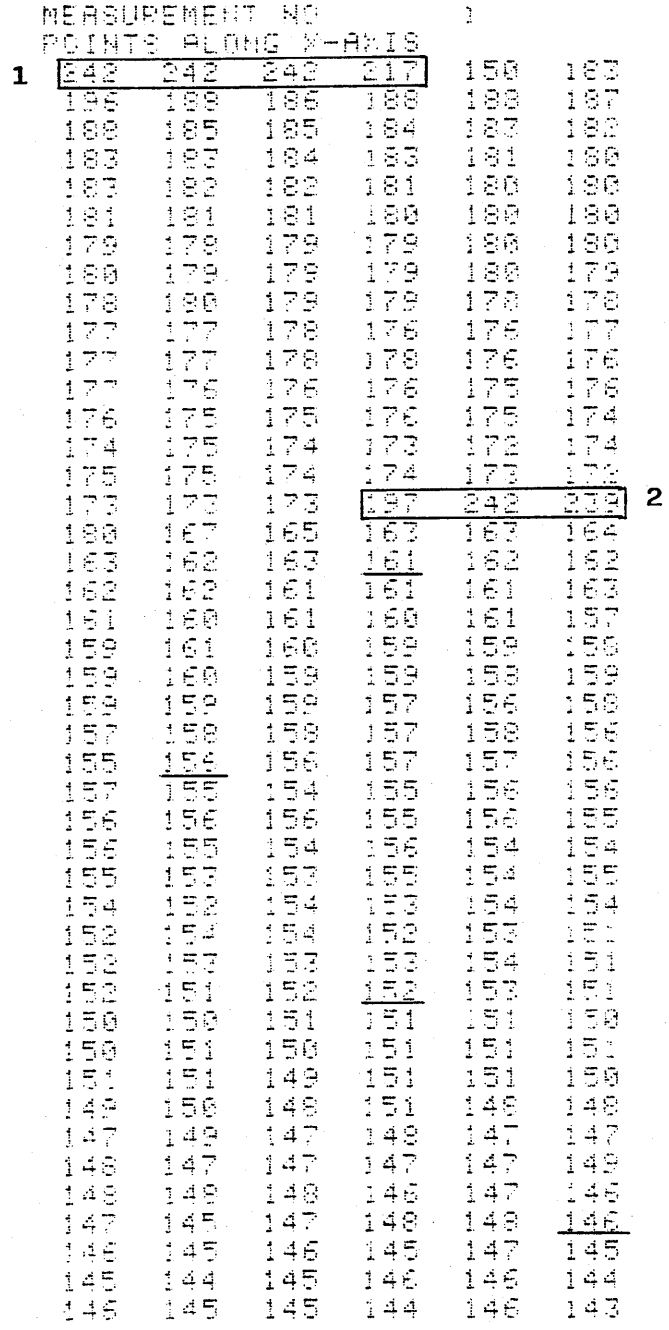

Figure 48A

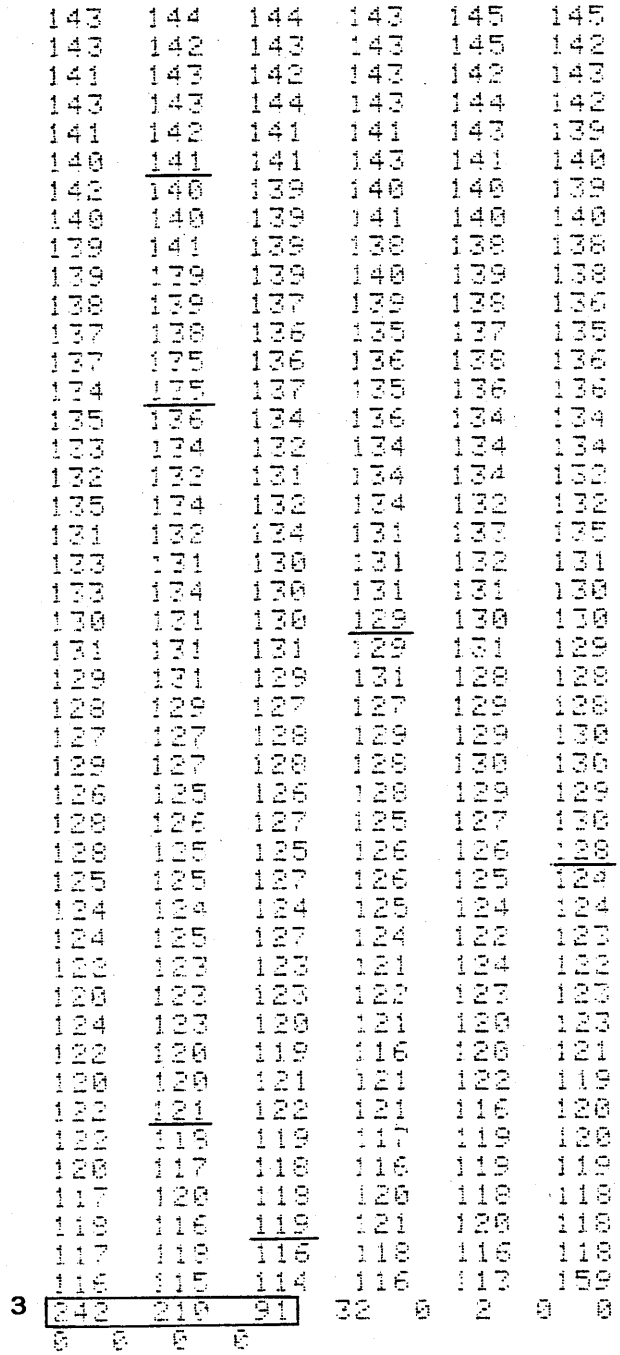

Figure 48B

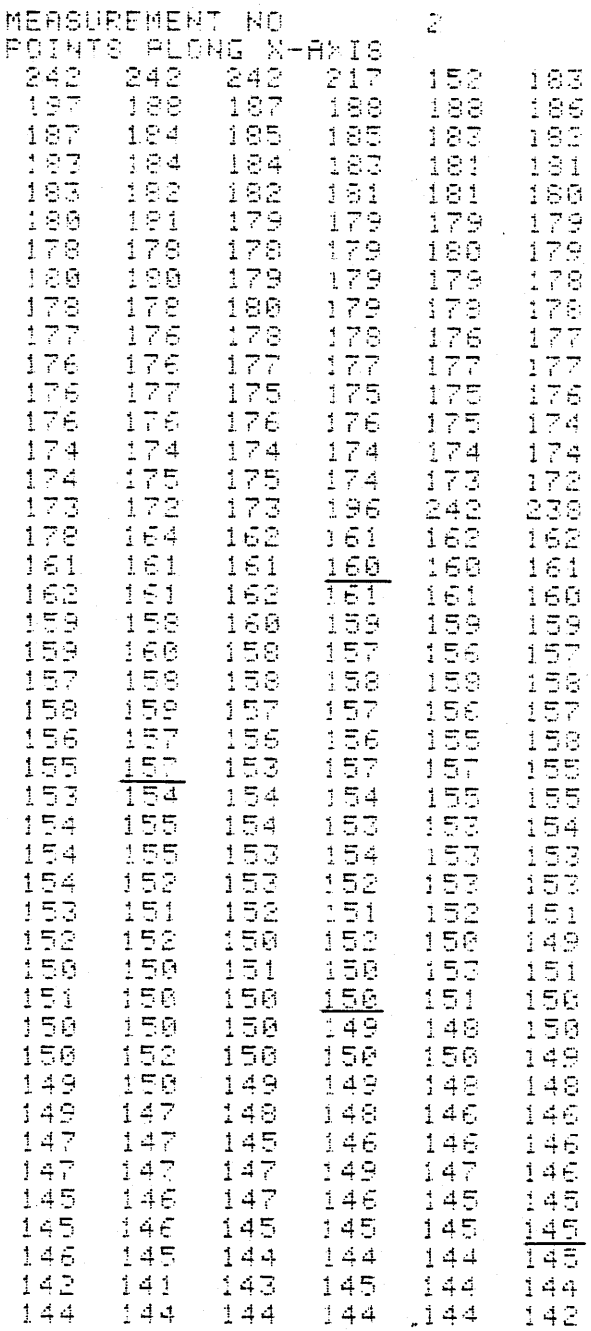

MEASUREMENT NO 2

POINTS ALONG X-AXIS

242	242	242	217	152	183
197	188	187	188	188	186
187	184	185	185	187	183
187	184	184	183	181	184
183	182	182	181	181	180
180	181	179	179	179	179
178	178	178	179	180	179
180	180	179	179	179	178
178	178	180	179	179	178
177	176	178	178	176	177
176	176	177	177	177	177
176	177	175	175	175	176
176	176	176	176	175	174
174	174	174	174	174	174
174	175	175	174	173	172
173	172	173	196	242	230
178	164	162	161	162	162
161	161	161	160	160	161
162	161	162	161	161	160
159	158	160	158	159	159
158	160	158	157	156	157
157	159	158	158	159	158
158	159	157	157	156	157
156	157	156	156	155	158
155	157	153	157	157	155
153	154	154	154	155	155
154	155	154	153	153	154
154	155	153	154	153	153
154	152	152	152	153	153
153	151	152	151	152	151
152	152	150	152	150	149
150	150	151	150	152	151
151	150	150	156	151	150
150	150	150	149	148	150
150	152	150	150	150	149
149	150	149	149	148	148
148	147	148	148	146	146
147	147	145	146	146	146
147	147	147	149	147	146
145	146	147	146	145	145
145	146	145	145	145	145
146	145	144	144	144	148
142	141	143	145	144	144
144	144	144	144	144	142

Figure 49A

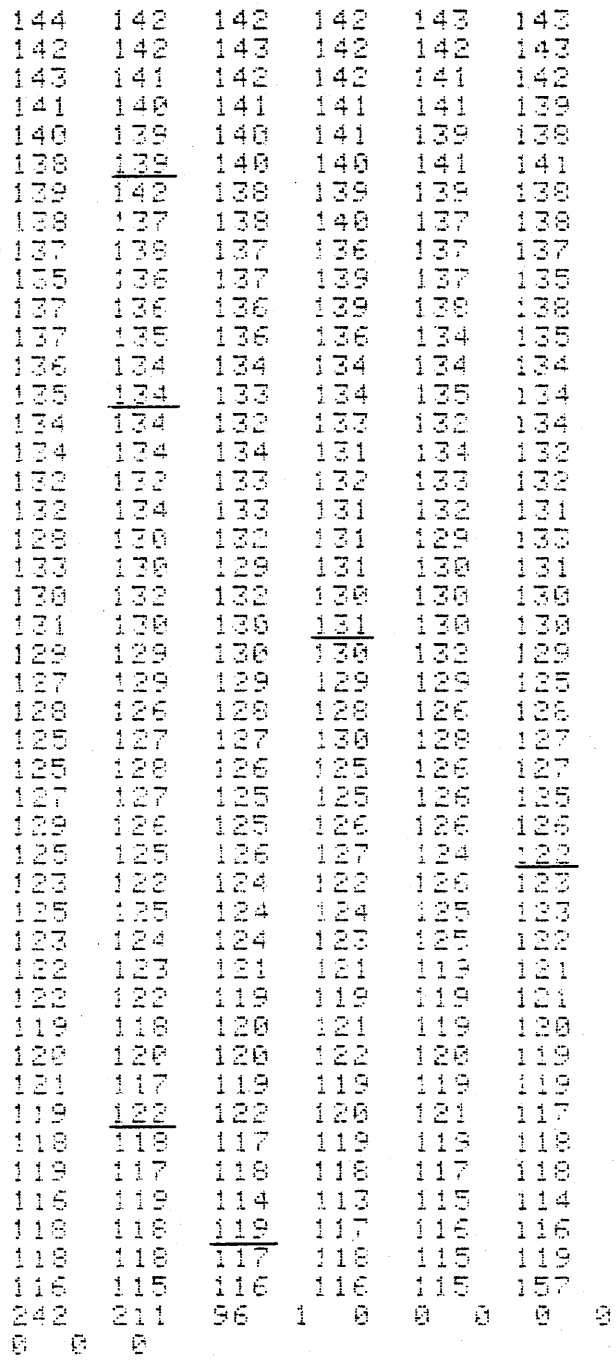

Figure 49B

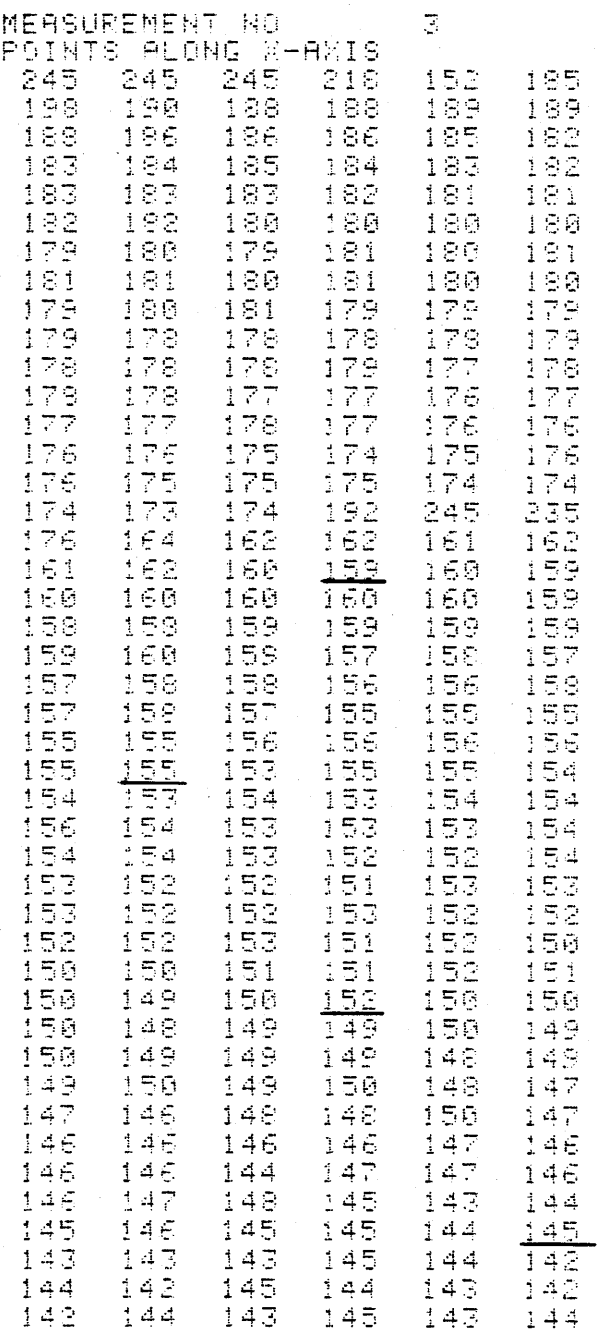

Figure 50A

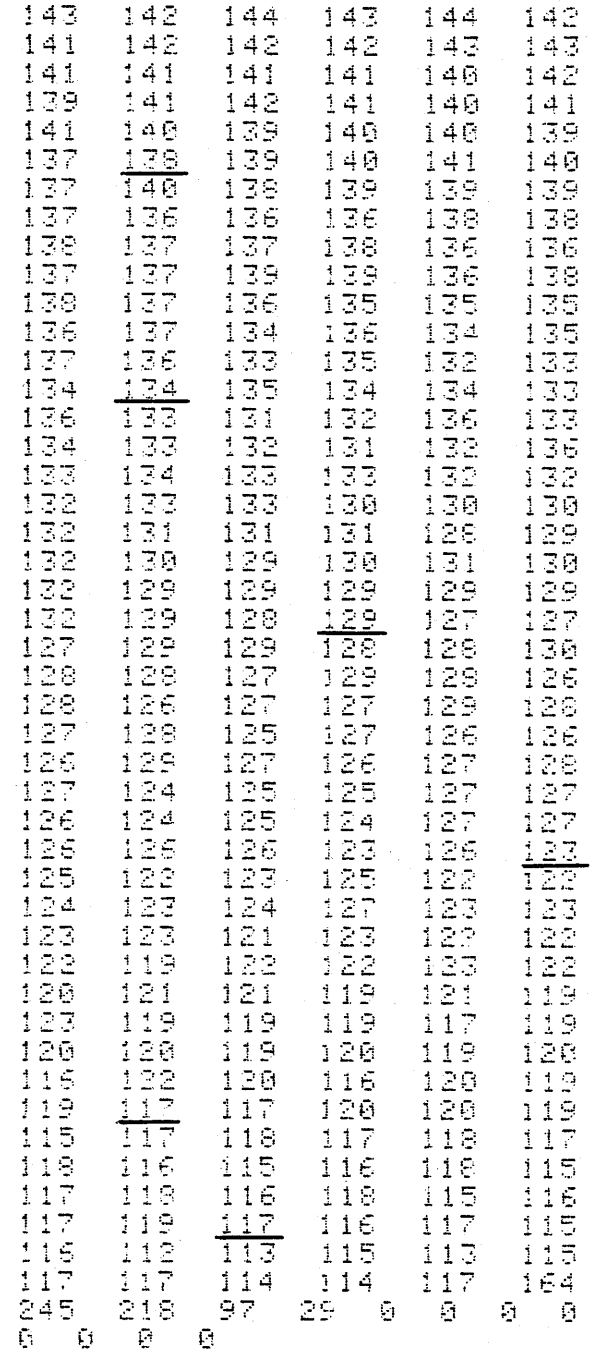

Figure 50B

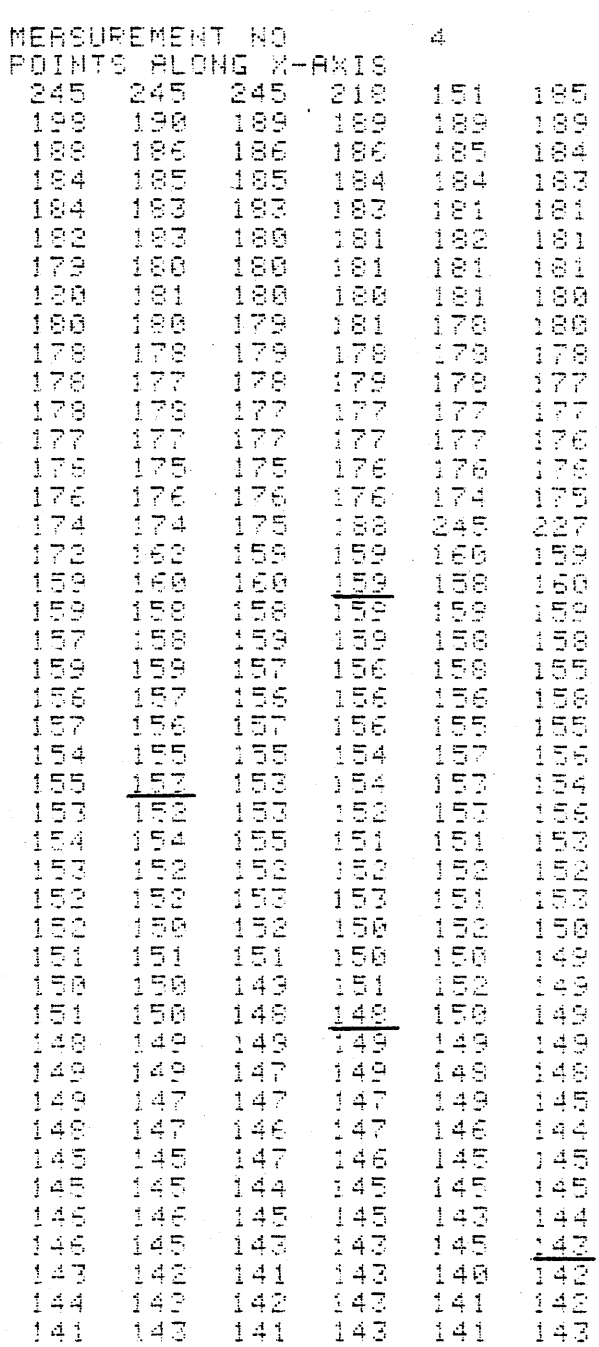

Figure 51A

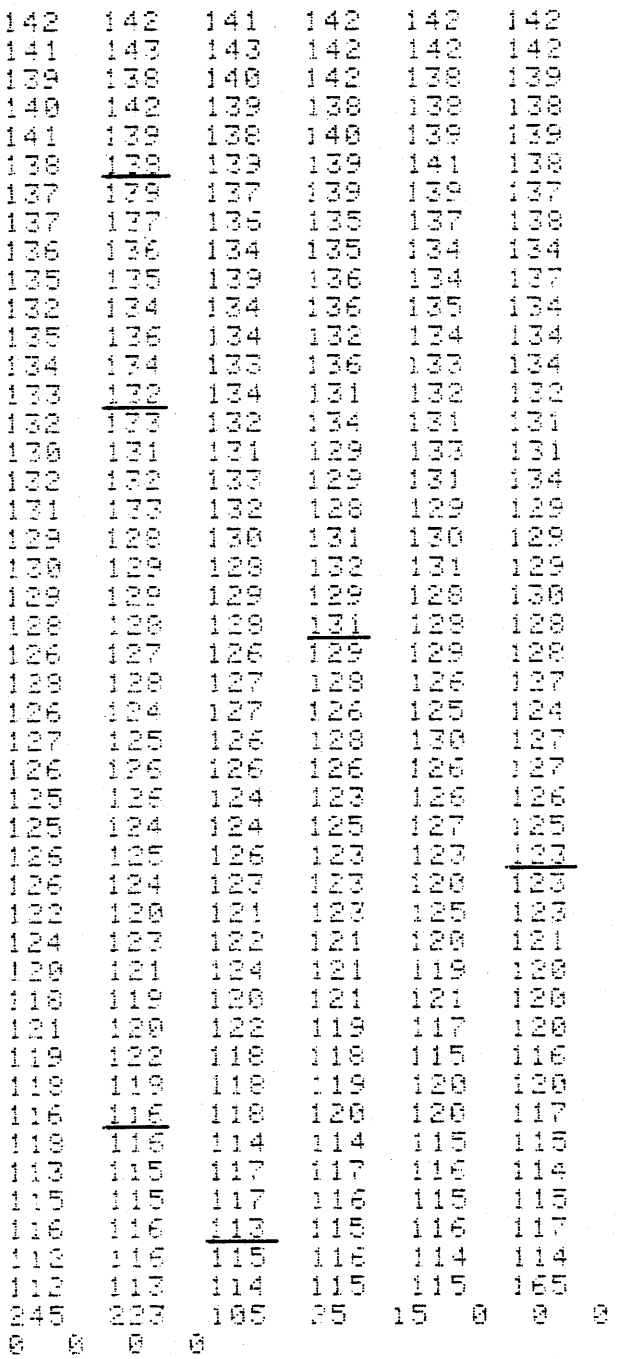

Figure 51B

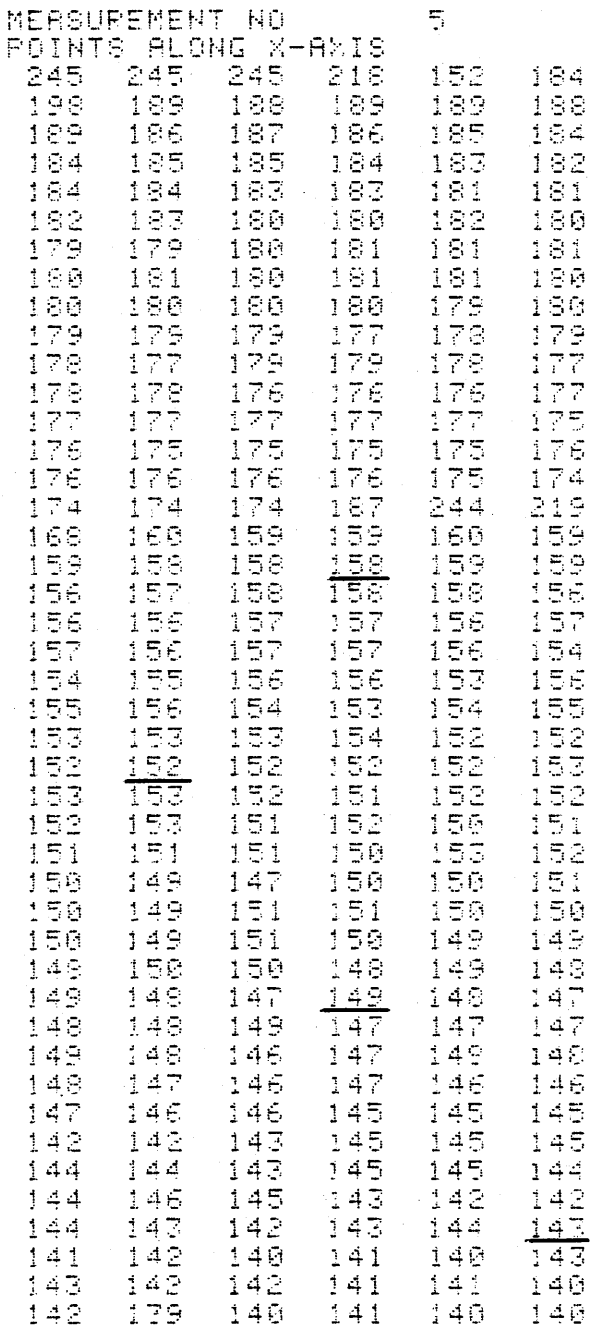

Figure 52A

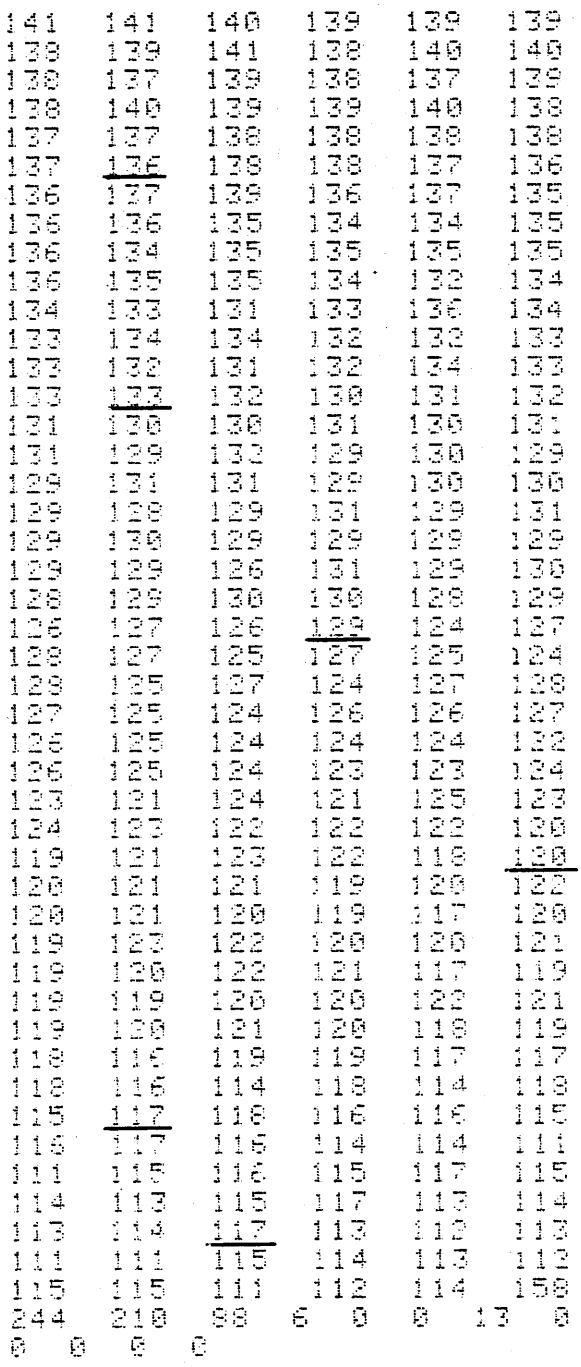

Figure 52B

MEASUREMENT NO 6

POINTS ALONG X-AXIS

245	245	245	218	152	185
198	199	188	189	189	189
188	186	186	186	185	184
184	196	185	184	183	183
187	187	183	183	181	180
182	183	182	181	182	181
179	180	180	182	182	180
182	181	180	181	182	180
180	179	180	180	179	180
180	178	179	177	178	179
178	177	179	180	178	178
179	178	178	177	177	177
177	177	177	177	176	176
175	176	175	175	176	176
176	176	177	176	175	174
174	175	175	188	244	222
169	160	159	158	158	157
159	158	157	157	156	155
155	155	157	156	155	155
156	156	156	156	155	156
154	154	154	154	156	154
154	153	152	153	153	153
152	152	151	153	152	152
153	152	151	152	152	153
151	151	152	152	151	150
150	151	152	150	150	151
151	150	150	151	151	150
150	150	148	149	148	147
149	149	149	150	150	148
147	149	149	149	148	147
148	148	147	147	146	147
149	146	147	146	149	145
148	149	148	148	147	145
146	148	147	146	147	144
146	145	145	146	146	145
144	146	145	146	147	143
144	143	145	145	144	144
143	142	141	141	142	144
142	144	144	141	142	142
141	143	143	142	140	142
141	140	140	140	141	143
141	141	141	141	140	141
142	139	138	136	139	138
140	139	139	140	139	140

Figure 53A

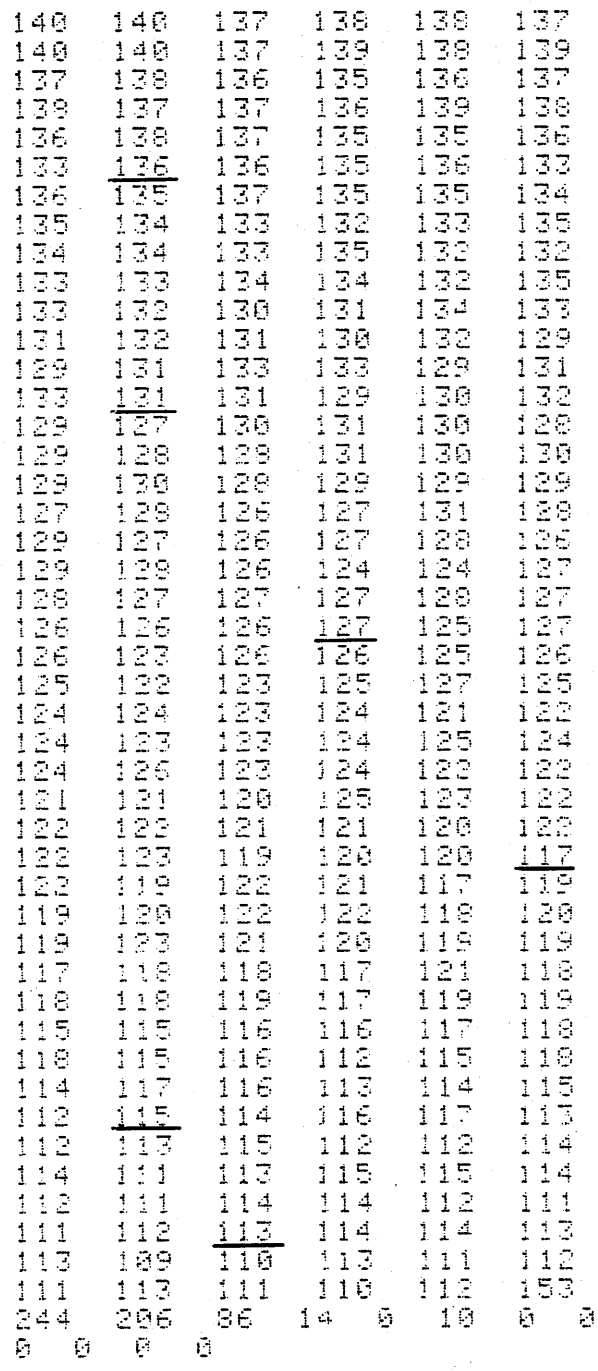

Figure 53B

MEASUREMENT NO 7

POINTS ALONG X-AXIS

245	245	245	218	152	185
198	189	189	189	189	186
188	187	188	186	185	183
185	186	185	185	183	183
185	184	184	183	182	181
182	183	180	181	181	181
181	181	181	182	182	181
182	181	181	181	182	179
181	182	181	180	179	180
180	179	179	178	179	179
179	179	180	179	178	178
179	179	179	179	178	178
177	178	178	178	177	176
176	176	175	175	175	177
176	175	176	175	175	174
174	175	175	188	244	220
167	157	157	156	155	156
155	156	155	156	154	152
154	153	155	155	153	155
155	154	155	154	153	153
153	154	154	153	153	152
154	152	152	152	152	153
151	151	150	151	151	150
152	150	152	151	150	150
152	151	152	150	149	149
149	149	150	149	149	149
148	150	148	149	150	147
147	148	148	148	148	147
148	149	148	149	147	148
145	147	147	147	145	146
147	146	148	148	144	146
145	147	145	146	146	144
144	145	145	146	145	145
144	144	145	144	144	145
145	143	143	145	145	143
144	142	144	144	144	142
142	141	143	142	142	141
142	144	143	141	141	141
143	142	142	141	140	140
140	141	139	140	140	141
139	140	141	138	139	142
140	140	139	140	139	139
140	139	139	138	139	137
139	138	138	138	138	140

Figure 54A

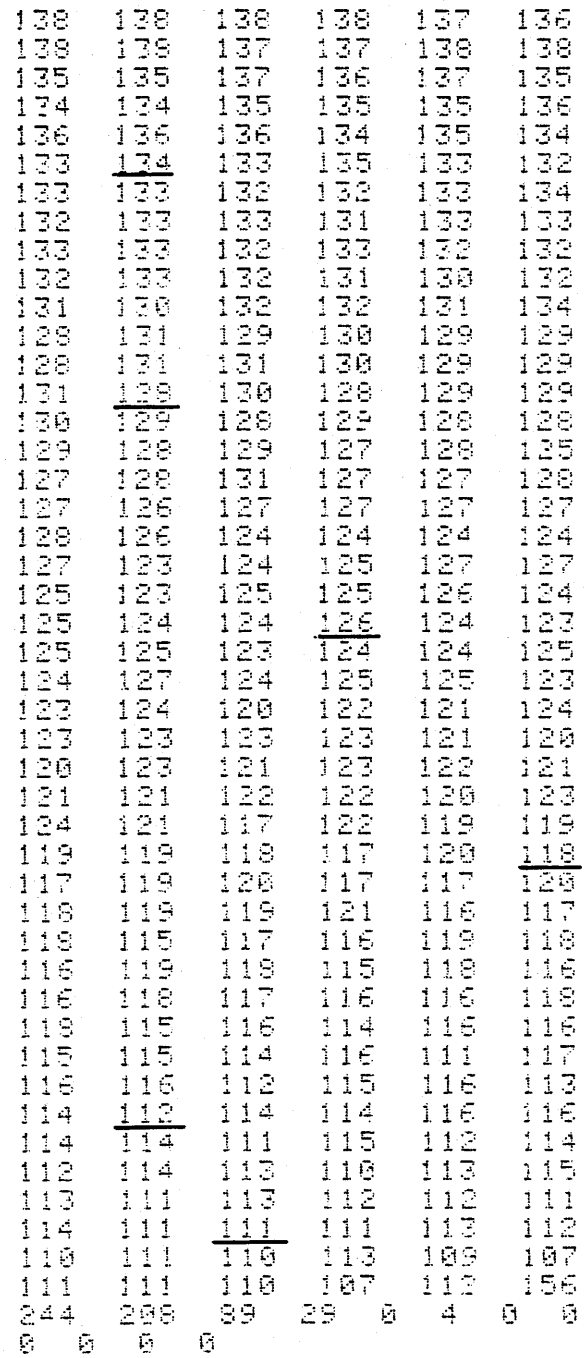

Figure 54B

MEASUREMENT NO 0

POINTS ALONG X-AXIS

245	245	245	218	152	185
199	189	189	189	190	189
189	186	187	186	185	183
185	186	185	186	184	183
184	184	184	182	182	182
182	183	180	181	181	181
180	181	181	181	181	180
181	181	181	181	182	180
180	181	181	180	179	179
179	179	179	178	178	178
179	178	179	179	178	178
179	179	178	177	178	178
177	178	178	177	178	176
177	176	175	175	175	176
176	176	176	175	175	174
174	174	173	189	244	222
166	155	155	154	154	153
152	152	152	152	154	153
152	152	153	151	151	152
153	153	152	151	152	152
152	150	149	152	150	146
153	150	150	149	150	149
150	149	148	148	149	150
149	149	147	147	149	148
148	147	148	148	146	147
148	148	148	147	144	147
147	147	146	145	146	147
148	147	146	146	145	145
145	146	145	145	146	145
144	144	146	144	145	143
145	145	144	145	144	143
144	143	142	144	145	143
145	143	142	145	143	142
143	142	143	141	141	140
144	143	142	141	143	141
143	143	143	141	140	139
141	142	141	142	140	139
138	139	140	139	139	140
140	137	137	138	137	137
137	138	138	140	136	140
138	139	137	137	136	136
137	138	137	135	137	138
138	137	138	139	137	134
136	136	135	136	136	137

Figure 55A

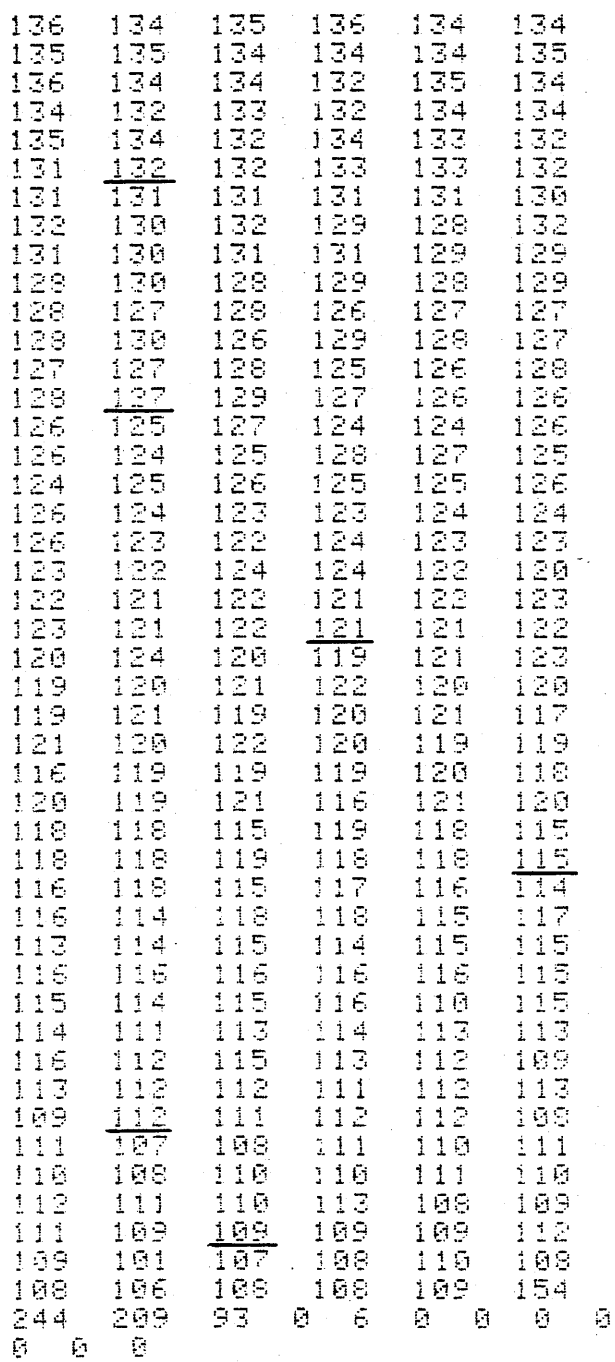
136 134 135 136 134 134
135 135 134 134 134 135
136 134 134 132 135 134
134 132 133 132 134 134
135 134 132 134 133 132
131 132 132 133 133 132
131 131 131 131 131 130
132 130 132 129 128 132
131 130 131 131 129 129
128 130 128 129 128 129
128 127 128 126 127 127
128 130 126 129 128 127
127 127 128 125 126 128
128 127 129 127 126 126
126 125 127 124 124 126
126 124 125 128 127 125
124 125 126 125 125 126
126 124 123 123 124 124
126 123 122 124 123 123
123 122 124 124 122 120
122 121 122 121 122 123
123 121 122 121 121 122
120 124 120 119 121 123
119 120 121 122 120 120
119 121 119 120 121 117
121 120 122 120 119 119
116 119 119 119 120 118
120 119 121 116 121 120
118 118 115 119 118 115
118 118 119 118 118 115
116 118 115 117 116 114
116 114 118 118 115 117
113 114 115 114 115 115
116 115 116 116 116 115
115 114 115 116 110 115
114 111 113 114 113 113
116 112 115 113 112 109
113 110 112 111 112 113
109 112 111 112 112 109
111 107 108 111 110 111
110 108 110 110 111 110
112 111 110 113 108 109
111 109 109 109 109 112
109 101 107 108 110 108
108 106 108 108 109 154
244 209 93 0 6 0 0 0 0
0 0 0

Figure 55B

MEASUREMENT NO 9

POINTS ALONG X-AXIS

245	245	245	218	152	195	
199	196	189	189	189	189	
189	197	187	186	186	184	
185	185	185	185	183	183	
185	184	184	187	182	181	
181	187	182	181	182	181	
179	180	181	182	181	181	
182	181	180	180	182	180	
180	180	180	180	180	180	
179	179	180	176	178	179	
179	178	179	179	178	177	
178	179	178	178	177	178	
177	176	177	176	177	176	
177	177	176	176	176	176	
176	176	176	177	175	174	
174	175	174	190	244	228	
157	155	155	152	153	152	
152	157	151	152	152	151	
150	151	152	151	152	151	
150	152	151	150	149	152	
149	149	149	148	149	149	
147	146	146	147	146	146	
148	147	147	146	147	146	
145	147	147	148	146	146	
146	145	146	146	145	146	
148	146	145	144	146	146	
145	145	144	145	144	147	
144	145	144	145	147	145	
143	144	144	145	146	143	
143	144	142	142	143	142	
140	141	141	140	142	141	
142	140	142	142	144	143	
141	142	140	141	141	141	
141	141	141	141	141	141	
140	141	140	140	141	138	
139	139	141	140	142	140	
138	139	139	139	139	138	
138	137	137	137	137	139	
137	137	137	135	134	136	
135	136	134	134	135	135	
136	137	135	136	135	135	
136	136	135	133	135	134	
133	135	134	135	136	133	

Figure 56A

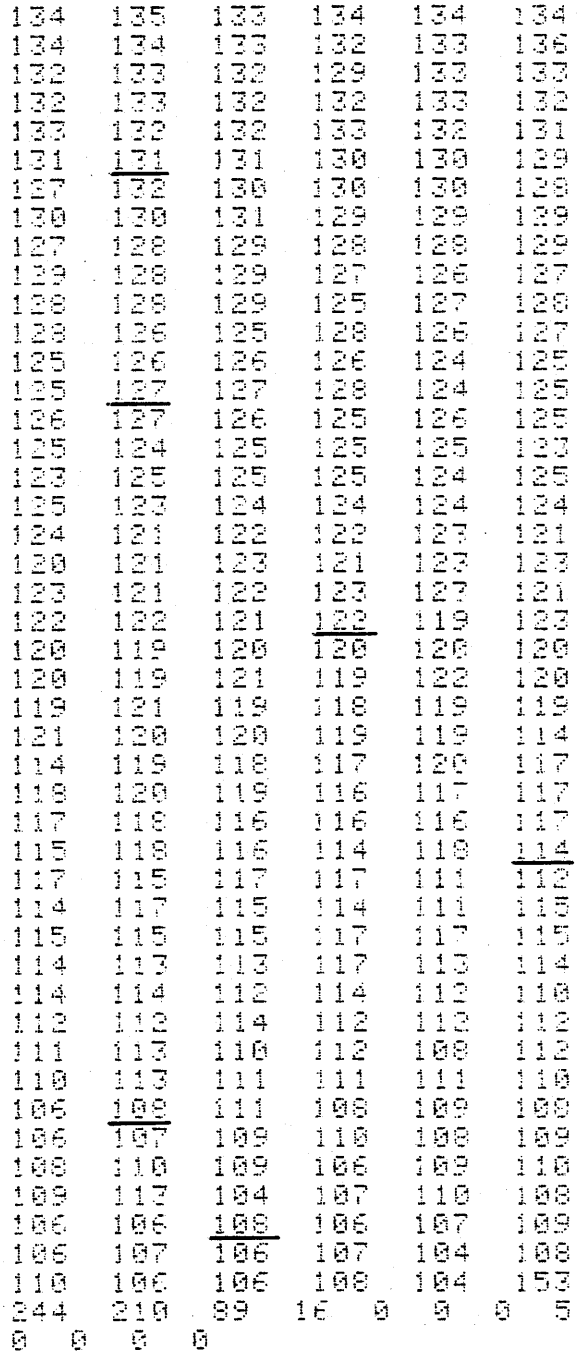

Figure 56B

MEASUREMENT NO 10

POINTS ALONG X-AXIS

245	245	245	217	152	185
199	190	189	189	189	189
189	186	187	186	185	183
184	186	185	184	184	183
185	184	183	183	182	181
182	183	181	181	182	180
181	181	182	182	182	181
182	181	181	181	182	181
181	181	180	180	180	180
179	179	179	180	178	178
178	179	179	179	179	179
179	179	178	178	178	178
177	178	177	178	178	177
177	176	176	175	176	176
176	177	176	176	175	175
174	173	174	192	245	230
168	155	153	151	152	151
151	152	150	149	150	150
150	149	151	149	148	148
149	149	150	149	149	150
149	146	148	148	146	145
149	148	145	147	146	147
146	146	146	147	145	145
147	146	147	145	147	145
146	145	147	146	146	143
142	143	145	143	144	145
145	143	144	143	144	144
144	143	143	143	143	143
145	141	142	142	143	143
142	142	143	142	142	143
142	141	140	141	140	142
140	139	140	138	141	140
140	139	141	142	141	140
139	139	139	139	139	137
139	137	140	139	140	139
139	139	139	139	138	136
140	137	138	136	138	138
137	135	136	137	136	137
137	138	134	135	134	134
137	136	134	137	135	135
134	135	134	135	135	137
135	136	135	131	134	133
133	133	133	133	134	133
131	132	135	132	134	135

Figure 57A

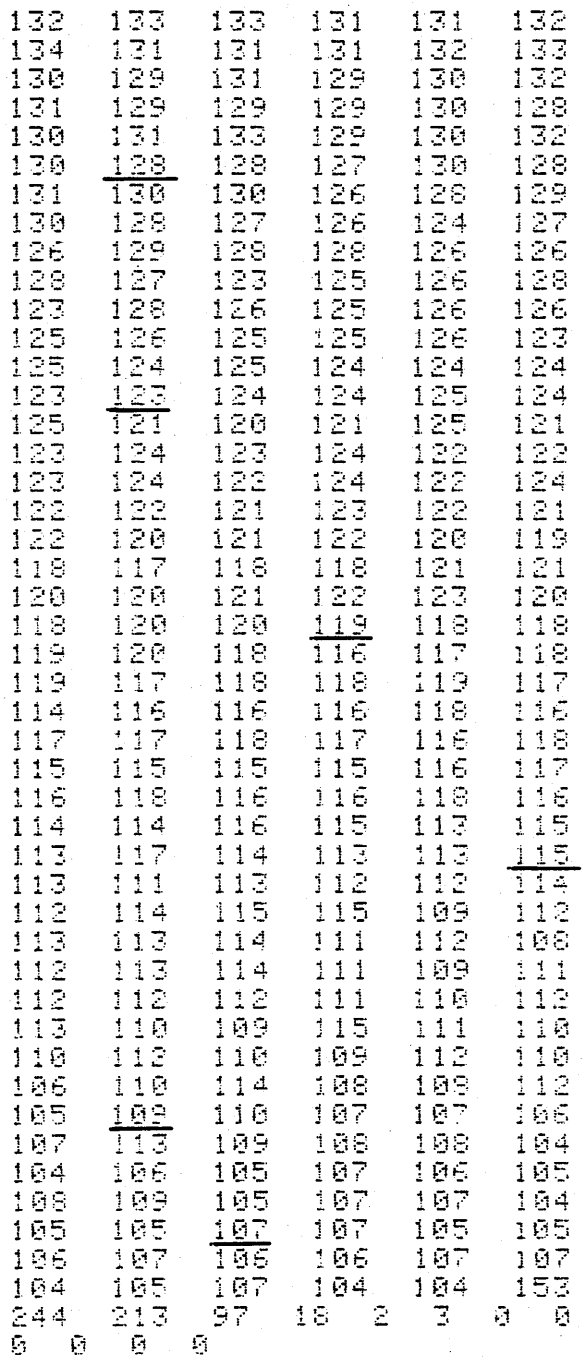
132 133 133 131 131 132
134 131 131 131 132 133
130 129 131 129 130 132
131 129 129 129 130 128
130 131 133 129 130 132
130 128 128 127 130 128
131 130 130 126 128 129
130 128 127 126 124 127
126 129 128 128 126 126
128 127 123 125 126 128
123 128 126 125 126 126
125 126 125 125 126 123
125 124 125 124 124 124
123 123 124 124 125 124
125 121 120 121 125 121
123 124 123 124 122 122
123 124 122 124 122 124
122 122 121 123 122 121
122 120 121 122 120 119
118 117 118 118 121 121
120 120 121 122 123 120
118 120 120 119 118 118
119 120 118 116 117 118
119 117 118 118 119 117
114 116 116 116 118 116
117 117 118 117 116 118
115 115 115 115 116 117
116 118 116 116 118 116
114 114 116 115 113 115
113 117 114 113 113 115
113 111 113 112 112 114
112 114 115 115 109 112
113 113 114 111 112 108
112 113 114 111 109 111
112 112 112 111 110 112
113 110 109 115 111 110
110 113 110 109 112 110
106 110 114 108 109 112
105 109 110 107 107 106
107 113 109 108 108 104
104 106 105 107 106 105
108 109 105 107 107 104
105 105 107 107 105 105
106 107 106 106 107 107
104 105 107 104 104 153
244 213 97 18 2 3 0 0
0 0 0 0

Figure 57B

In order to assess the variation between the sets of readings, ten points were chosen at random, for each set, and tabulated. Figure 58 shows the resultant table with a column headed 'Difference', this being the value of 'Set No.1' minus the value of 'Set No.10' for each point. It can be seen that the change is fairly constant for each sample point and the indication is that there is some drift occurring. However, even between adjacent sets of readings, which were taken with a separation of just a few minutes, there is sufficient change to indicate that there is little repeatability of reading when investigating fine detail and the pictorial evidence also supports this. Naturally the values are dependent on the averaging period which was a constant for each of the readings using the internal clock of the HP85B.

4.4.3 Conclusions

The following can be concluded from the above:-

a) there is a lack of measurement repeatability, however, the changes from one reading to another are unlikely to be due to temperature drift alone. If this were the case then the traces would be identical with an offset, assuming that the temperature coefficient is constant over the entire length of fibre, which is

POINT NO.	SET NO.										DIFFERENCES
	1	2	3	4	5	6	7	8	9	10	
1	161	160	159	159	158	157	156	152	152	149	12
2	156	157	155	153	152	151	151	147	147	145	11
3	152	150	152	148	149	148	146	145	143	142	10
4	146	145	145	143	143	143	143	136	136	137	9
5	141	139	138	138	136	136	134	132	131	128	13
6	135	134	134	132	133	131	128	127	127	123	12
7	129	131	129	131	129	127	126	121	122	119	10
8	128	122	123	123	120	117	118	115	114	115	13
9	121	122	117	116	117	115	112	112	108	109	12
10	119	119	117	113	117	113	111	109	108	107	12

Figure 58

feasible. The variations are therefore due to a combination of reasons, the most likely of these being differences in the point of sampling between readings, changes due to the backscattering mechanism and temperature drift in the fibre or test equipment.

b) visual evidence of OTDR measurements can be enhanced by digitising and recording numerical data. In this way comparisons can be made more easily and a pass fail criteria or 'pass band' could be introduced

if multi readings are required for a particular fibre sample. Naturally test conditions would have to be clearly stated to reduce or avoid the problems described in a) above. This suggestion and the necessary software has been passed to the fibre manufacturing unit and is currently under consideration for use in the mass production test regime.

c) the use of commercial OTDRs for this type of in depth investigation must be questioned. It is probably more appropriate to build laboratory equipment from first principles where uncompromised features can be enhanced for a particular aspect of measurement rather than employing a versatile machine with many peripheral features.

APPENDIX A

References

1. Dielectric - fibre surface waveguides for optical frequencies.
   K.C. Kao G.A. Hockham.
   Proc I.E.E. 113(7) 1966 PP 1151-1158.

2. The problem of error in deconvolution.
   A.F. Jones D.L. Missel.
   Journal of Physics Part A (General Physics).
   Vol. 3 1970, pp 462-472

3. On deconvolution using the discrete Fourier transform.
   H.F. Silverman. A.E. Pearson
   I.E.E.E. Transactions on Audio and Electro-acoustics.
   Vol. AU-21, No. 2, April 1973, pp 112-118.

4. A fibre optic time domain reflectometer.
   M.A. Nelson, et al.
   Proc. Soc. Photo-optics Inst. Eng.
   Vol. 139, March 1978, pp 93-97.

5. An optimized technique for backscatter attenuation measurements in optical fibres.
   A.J. Conduit, et al.
   Optical and Quantum Electronics
   Vol.12, No. 2, March 1980, pp 169-178.

6. Spectral and length-dependent losses in optical fibres investigated by a two-channel backscatter technique.
A.J. Conduit, et al.
I.E.E. Electronics Letters.
Vol. 16, Nos. 3, January 1980, pp 77-78.

7. Optical fibre backscatter-loss signatures: identification of features and correlation with known defects using the two-channel technique.
A.J. Conduit, et al.
6th European Conf. on Optical Communication.
York U.K. 1980, pp 152-155.

8. As assessment of the backscatter technique as a means for estimating loss in optical waveguides.
B.L. Danielson.
U.S. National Bureau of Standards, technical note.
T.N. 1018 February 1980.

9. Polarisation optical time domain reflectometry.
A.J. Rogers.
I.E.E. Electronics Letters
Vol 16. No. 13, June 1980, pp 489-90.

10. Optical Fibre impulse response using frequency domain optimal compensation deconvolution.
S.M. Riad.
Proc. Third Internation Fibre and Comm. Exposition.
San Fransisco. September 1980, pp 210-213.

11. Polarisation beat length measurement in a single mode optical fibre by backward Rayleigh scattering.
M. Nakazawa, et al.
I.E.E. Electronics Letters.
Vol 17, No. 15, July 1981, pp 513-515.

12. Sub-picosecond-time-domain reflectometry.
J.J. Fontaine, et al.
Optics Letters
Vol 6, No. 9, September 1981, pp 405-407.

13. Measurement of the insertion loss of a single micro-bend.
M.D. Rourke
Optics Letters.
Vol 6, No. 9, September 1981, pp 440-442.

14. Deconvolution of time domain waveforms in the presence of noise.
N.S. Nahman, et al.
U.S. National Bureau of Standards, technical note.
T.N. 1047 October 1981.

15. Measurement and analysis on polarisation properties of backward Rayleigh scattering for single-mode optical fibers.
M. Nakazawa, et al.
I.E.E.E. Journal of Quantum Electronics.
Vol QE-17, No. 12, December 1981, pp 2326-2334.

16. Improved dynamic-range single mode OTDR at 1.3um.
M.P. Gold. A.H. Hartog.
I.E.E. Electronic Letters.
Vol. 20, No. 7, March 1984, pp 285-287.

17. Backscattering signatures from optical fibres with differential mode attenuation.
M. Eriksrud, et al.
Journal of Lightwave Technology
Vol. LT-2, No. 2, April 1984, pp 139-145.

18. Principles of optics.
M. Born, E. Wolf.
Pergamon press, 1975.

19. Third International conference on integrated optics and optical fibre communication.
I.E.E.E. Optical Society of America.
San Francisco, April 1981.

20. OFR3, OTDR Handbook
STC Components plc.

21. OF150, OTDR Handbook
Tektronix inc.

22. Characterizing optical fibres with an OTDR.
J. Gentile.
Electro-optical Systems Design USA.
Vol. 13, No. 4, April 1981, pp 47-52.

23. Backscattering measurements in optical fibres:
separation of power decay from imperfection
contribution. P. DiVita. U. Rossi.
I.E.E. Electronics Letters.
Vol. 15, No. 15, July 1979, pp 467-469.

24. Backscatter measurements on optical fibres.
B.L. Danielson
U.S. National Bureau of Standards, technical note.
T.N. 1034 February 1981.

25. Backscatter signature simulations.
B.L. Danielson
U.,S. National Bureau of Standards, technical note.
T.N. 1050 December 1981.

26. Optical fibre characterization: backscatter, time-domain bandwidth, refracted near field, and inter-laboratory Comparisons (Volume 1).
B.L. Danielson, et al.
U.S. National Bureau of Standards, Special publication.
S.P. - 637 Vol. 1, July 1982.

27. Optical fibre diameter variations and their effect on backscatter loss measurements.
A.J. Conduit, et al.
I.E.E. Electronics letters.
Vol. 17, No. 8, April 1981, pp 308-310.

28. High-resolution measurement of diameter variations in optical fibres by the backscatter method.
A.J. Conduit, et al.
I.E.E. Electronics Letters.
Vol. 17, No. 20, October 1981, pp 742-744.

29. Determination of Structural parameter variations in single mode optical fibres by time-domain reflecto-metry.
M.P. Gold. A.H. Hartog.
I.E.E. Electronics Letters.
Vol. 18, No. 12, June 1982, pp 489-490.

30. On the theory of backscattering in single-mode optical fibres.
A.H. Hartog, M.P. Gold
Journal of Lightwave Technology.
Vol. LT-2, No. 2, April 1984, pp 76-81.

31. Operation Manual - optical pulse echo tester, M.W 97A/98A.
Anritsu Electric Company Ltd.

32. Coherent OTDR for fault location in long wavelength Optical Systems
D.F. Smith, et al.
Conference paper.
International Conference on 'Measurements for Telecommunication Transmission Systems'
London 27-28 November 1985.-

```
 10 ! DECLARE ARRAY SIZES
 15 DIM S(4),M(4)
 20 DIM Y(1000)
 25 DIM A$[32],B$[32],C$[32],D$[
    10],E$[32],T$[10]
 30 A1=708
 35 !
 40 ! ## ## ## ## ## ## ## ##
 45 ! ON ERROR GOTO 6000
 50 GCLEAR
 55 CLEAR
 60 DISP "  Anritsu MW98A OTDR P
    rogram"
 65 DISP
 70 ! START OF MAIN PROGRAM
 75 ! SELECT I/P DEVICE
 80 DISP "SELECT SOURCE OF DATA"
 85 DISP "[1] OTDR"
 90 DISP "[2] TAPE"
 95 DISP "[3] DISC"
100 INPUT S2
105 IF S2<1 OR S2>3 THEN 80
110 DISP "Select plotter"
115 DISP "[1] Plotter"
120 DISP "[2] CRT (no hard copy"
125 DISP "[3] CRT (with hard cop
    y)"
130 DISP "[4] No output plotted"
135 INPUT P4
140 IF P4<1 OR P4>4 THEN 110
145 IF S2=2 OR S2=3 THEN 500
200 ! OTDR ROUTINE HERE
205 GOSUB 5000 ! GET USER DATA
210 S1=1  ! DEFAULT STORAGE
215 DISP "Select the storage med
    ia for    data files"
220 DISP "[1] Internal tape cart
    ridge "
225 DISP "[2] External disc driv
    e "
230 DISP "[3] OTDR data is not s
    aved"
235 INPUT S1
240 IF S1<1 OR S1>3 THEN 215
242 IF S1=3 THEN 265
245 DISP "Enter the base filenam
    e"
250 DISP "Max no. of 6 character
    s ";
255 INPUT F$
260 IF LEN(F$)<1 OR LEN(F$)>6 TH
    EN 250
```

Figure 21

```
255 DISP "Enter the averaging ti
    me in seconds";
270 INPUT D4
275 DISP "Enter the measurement
    no. ";
280 INPUT E$
285 IF VAL(E$)<1 OR VAL(E$)>999
    THEN 275
290 DISP "Enter the no. of measu
    rements "
295 INPUT M2
300 IF M2<1 OR M2>999 THEN 290
302 IF M2=1 THEN T4=0
303 IF M2=1 THEN 350
305 DISP "Enter the time period
    between each measurement"
310 DISP "Enter hours ";
315 INPUT T1
320 DISP "Enter minutes ";
325 INPUT T2
330 DISP "Enter seconds ";
335 INPUT T3
340 T4=(T1*3600+T2*60+T3)*1000
350 GOSUB 7500
355 GOSUB 7700
360 GOSUB 1500 ! GET OTDR DATA
362 GCLEAR 10
365 OUTPUT A1 USING "K,/" ; "AVR
    0"
370 LOCAL A1
375 IF S1=1 OR S1=2 THEN G$=F$&E
    $
380 IF S1=1 OR S1=2 THEN GOSUB 3
    000
385 E$=VAL$(VAL(E$)+1)
390 ! PLOT OUTPUT
395 IF P4=1 THEN GOSUB 2000
400 IF P4=2 OR P4=3 THEN GOSUB 4
    000
405 IF P4=2 OR P4=3 THEN GOSUB 4
    500
410 IF M2=1 THEN 40
412 GOSUB 7500
413 GOSUB 7800
415 M2=M2-1 ! DEC NO OF MEAS.LEF
    T
420 GOTO 350 ! TAKE ANOTHER MEAS
    UREMENT
500 ! DISC & TAPE ROUTINE HERE
505 S1=S2-1
510 IF S1=1 THEN MASS STORAGE IS
     ":T"
515 IF S1=2 THEN MASS STORAGE IS
     ":D700"
520 CAT
525 DISP "Enter base filename to
     be read"
530 INPUT F$
535 IF LEN(F$)<1 OR LEN(F$)>6 TH
    EN 525
```

Figure 22

```
540 DISP "Enter the measurement
    no range "
545 DISP "Start no. ";
550 INPUT S3
555 DISP "Stop no. ";
560 INPUT S4
565 FOR J=S3 TO S4
570 G$=F$&VAL$(J)
575 GOSUB 3500
580 IF P4=1 THEN GOSUB 2000
585 IF P4=2 OR P4=3 THEN GOSUB 4
    000
590 IF P4=2 OR P4=3 THEN GOSUB 4
    500
595 NEXT J
600 GOTO 40 ! RETURN TO START
800 ! ************************
805 ! PROGRAM VARIABLES
810 ! A1. ..OTDR ADDRESS..708
815 ! A2....ATTEN SETTING DB
820 ! M(0-4) MARKER POS 0-500/10
825 ! S(0-4) MARKER POSITION km
830 ! Y(0-1000) SCREEN DATA
835 ! A$ TITLE
840 ! B$ ROUTE
845 ! C$ OPERATOR
850 ! D$ DATE
855 ! T$ TIME
860 ! E$ MEASUREMENT NO.
865 ! D1 DIST. RANGE CODE
870 ! H1 HORIZ. SCALE CODE
875 ! P0 PULSE WIDTH CODE
880 ! H2 HORIZ. SHIFT (km)
885 ! M1 MASK POS. (km)
890 ! I1 REFRACTIVE INDEX
895 ! A2 APPROX. METHOD CODE
900 ! V1 VERT. SCALE CODE
905 ! L1 LOSS MARKER DIFF. (km)
910 ! L2 TOTAL LOSS (dB)
915 ! L3 LOSS (dB/km)
920 ! L4 SPLICE VALUE (dB)
925 ! U1 PLUG-IN UNIT CODE
930 ! F1 FUNCTION CODE
935 ! M CURSOR NO.
940 ! M(0-4) MARKER POS. (0-500/
    1000)
945 ! P1 NO. OF POINTS ACROSS SC
    REEN
950 ! I FOR..NEXT LOOP COUNTER
955 ! X GENERAL PURPOSE VARIABLE
960 ! P2 PLOTTER GP-IB ADDRESS
965 ! D2 SCALING FACTOR
970 ! U$ PLUG-IN UNIT
975 ! H4 HORIZ. SCALE (km/div)
980 ! V2 VERTICAL SCALE (dB)
985 ! F$ FILENAME FOR FILES
990 ! T1 TIMER VALUE (HRS)
995 ! T2 TIMER VALUE (MINS)
1000 ! T3 TIMER VALUE (SECS)
1005 ! T4 TIMER VALUE (mS)
```

Figure 23

```
1010 ! H3 HORZ.SCALE
1015 ! V2 VERTICAL SCALE (dB)
1020 ! D DATE CONVERTED TO SECS.
1025 ! S1 MASS STORAGE SELECT
1030 ! D4 AVERAGING TIME (Sec)
1035 ! S2 I/P DEVIICE CODE
1040 ! P4 PLOTTER/CRT & H.COPY S
     ELECT
1045 ! G$ CONCATENATED FILENAME
     OF F$+E$
1050 ! S3 MEASUREMENT START NO F
     OR FILENAME SUFFIX
1055 ! S4 MEASUREMENT STOP NO FO
     R FILENAME SUFFIX
1060 ! J FILE READIN LOOP VAR
1065 ! X$ GP VARIABLE
1070 ! P9 P.WIDTH SBRT LOCAL VAR
1075 ! **********************
1080 !
1500 ! ************************
1505 ! * ROUTINE TO GRAB ALL   *
1510 ! * THE DATA FROM THE OTDR*
1515 ! ************************
1520 OUTPUT A1 USING "K,/" ; "HL
     D1"
1525 ! ATTENUATOR SETTING
1530 OUTPUT A1 USING "K,/" ; "AT
     TR"
1535 ENTER A1 ; A2
1540 ! DISTANCE RANGE
1545 OUTPUT A1 USING "K,/" ; "DS
     RR"
1550 ENTER A1 ; D1
1555 ! HORIZONTAL SCALING
1560 OUTPUT A1 USING "K,/" ; "HS
     CR"
1565 ENTER A1 ; H1
1570 ! PULSE WIDTH
1575 OUTPUT A1 USING "K,/" ; "PL
     SR"
1580 ENTER A1 ; P0
1585 ! HORIZ SHIFT
1590 OUTPUT A1 USING "K,/" ; "HI
     FR"
1595 ENTER A1 ; H2
1600 ! MASK
1605 OUTPUT A1 USING "K,/" ; "MI
     KR"
1610 ENTER A1 ; M1
1615 ! REFRACTIVE INDEX
1620 OUTPUT A1 USING "K,/" ; "IO
     RR"
1625 ENTER A1 , I1
1630 ! APPROX METHOD
1635 OUTPUT A1 USING "K,/" ; "AP
     RR"
1640 ENTER A1 ; A3
1645 ! VERT SCALE
1650 OUTPUT A1 USING "K,/" ; "VS
     CR"
```

Figure 24

```
1655 ENTER A1 ; V1
1660 ! LOSS DATA
1665 OUTPUT A1 USING "K,/" ; "LS
     DR"
1670 ENTER A1 ; L1,L2,L3,L4
1675 ! TYPE OF PLUG IN
1680 OUTPUT A1 USING "K,/" ; "UN
     TR"
1685 ENTER A1 ; U1
1690 ! FUNCTION
1695 OUTPUT A1 USING "K,/" ; "FN
     CR"
1700 ENTER A1 ; F1
1705 ! MARKERS
1710 OUTPUT A1 USING "K,/" ; "MK
     SR"
1715 ENTER A1 ; M
1720 OUTPUT A1 USING "K,/" ; "MI
     MR"
1725 ENTER A1 ; M(0)
1730 OUTPUT A1 USING "K,/" ; "MI
     1R"
1735 ENTER A1 ; M(1)
1740 IF F1=0 THEN 1775 ! ONLY 2
     MARKERS FOR LOSS FUNCTION
1745 OUTPUT A1 USING "K,/" ; "MI
     2R"
1750 ENTER A1 ; M(2)
1755 OUTPUT A1 USING "K,/" ; "MI
     3R"
1760 ENTER A1 ; M(3)
1765 OUTPUT A1 USING "K,/" ; "MI
     4R"
1770 ENTER A1 ; M(4)
1775 P1=500 ! POINTS ACROSS SCRE
     EN
1780 IF H1>=0 AND H1<=2 OR H1=5
     THEN P1=1000
1785 OUTPUT A1 USING "K,/" ; "DA
     DR"
1790 FOR I=1 TO P1
1795 ENTER A1 ; X,Y(I)
1800 NEXT I
1805 OUTPUT A1 USING "K,/" ; "HL
     D0"
1810 RETURN
2000 ! ************************
2005 ! * OTDR PLOT TO PLOTTER  *
2010 ! * AT ADDRESS A1         *
2015 ! ************************
2020 GCLEAR
2025 CLEAR
2030 BEEP
2035 DISP "Make sure there is pa
     per in the plotter."
2040 DISP "Press END LINE when r
     eady."
2045 INPUT X$
2050 P2=705
2055 PLOTTER IS P2
```

Figure 25

```
2060 GCLEAR
2065 ! PLOT TO EXTERNAL PLOTTER
2070 LOCATE 0,1.8*RATIO*100,10,1
     55
2075 ! DRAW SCALES
2080 SCALE 0,499,110,249
2085 LINETYPE 1
2090 XAXIS 110,50,0,499
2091 YAXIS 0,25,0,249
2095 FRAME
2100 !
2105 ! PLOT OUT SCATTER TRACE
2110 ! D2=1 IF P1=500, D2=2,P1=1
     000
2115 D2=1
2120 IF P1=1000 THEN D2=2
2125 PENUP
2130 FOR I=1 TO P1
2135 PLOT (I-1)/D2,Y(I)
2140 NEXT I
2145 PENUP
2150 ! MAIN MARKER POSITION
2155 LORG 5
2160 S(0)=FNA(M(0))
2165 S(1)=FNA(M(1))
2170 IF F1=0 THEN 2190
2175 S(2)=FNA(M(2))
2180 S(3)=FNA(M(3))
2185 S(4)=FNA(M(4))
2190 MOVE S(0),Y(INT(S(0)+11.5)*
     D2)
2196 PLOT S(0),0
2197 PLOT S(0),145
2200 MOVE S(1),Y(INT(S(1)+1.5)*D
     2)
2210 IF F1=0 THEN 2235
2215 FOR I=2 TO 4
2220 MOVE S(I),Y(INT(S(I)+100)*D
     2)
2230 NEXT I
2235 PENUP
2240 PLOT S(M),0
2245 PLOT S(M),249
2250 PENUP
2255 IF S(M)<400 THEN LORG 1 ELS
     E LORG 7
2260 MOVE S(M),130
2265 LABEL USING "DD.DDD,K" ; M(
     M)," km"
2270 LOCATE  65*RATIO*100,RATIO*
     100,10,100
2280 SCALE 0,32,0,24
2285 LORG 1
2290 MOVE 1,23
2295 LABEL "Anritsu MW98A OTDR"
2300 GOTO 2330
2301 GOTO 2330
2305 LABEL "Title: ";A$
2310 LABEL "Route: ";B$
2315 LABEL "Operator: ";C$
```

Figure 26

```
2320 IF S2=1 THEN LABEL "Date: "
     ;DATE$;"  Time: ";TIME$
2325 IF S2=2 OR S2=3 THEN LABEL
     "Date: ";D$;"  Time: ";T$
2330 LABEL "Measurement No. ";E$
2331 LABEL
2332 LABEL "Averaging Time. ";D4
     ;"sec"
2334 GOTO 2355
2335 GOSUB 8060 ! PLUG IN TYPE
2340 LABEL U$
2345 LABEL "Distance Range: ";18
     *2^D1;"km"
2350 LABEL
2355 H4=FNH(H1)
2360 IF H4<1 THEN 2375
2365 LABEL USING "K,D.DD,K" ; "H
     orizontal Scale ",H4," km/d
     iv"
2370 GOTO 2380
2375 LABEL USING "K,DDDD,K" ; "H
     orizontal Scale ",H4*1000,"
      m/div"
2380 V3=FNV(V1)
2385 LABEL USING "K,D.DD,K" ; "V
     ertical Scale   ";V3;" dB/d
     iv"
2386 GOTO 2450
2390 LABEL
2395 IF F1=1 THEN 2430
2400 ! LOSS MODE
2405 LABEL "LOSS MARKERS"
2410 LABEL USING "K,DD.DDD,K" ;
     "Distance: ",L1," km"
2415 LABEL USING "K,DD.DD,X,K" ;
      "Loss:      ",L2," dB"
2416 GOTO 2560
2420 LABEL USING "K,DD.DD,X,K" ;
      "Loss/km:   ",L3," dB/km"
2425 GOTO 2445
2430 !
2435 ! SPLICE MODE
2440 LABEL USING "K,MDD.DD,K" ;
     "Splice:    ",L4," dB"
2445 IF A3=0 THEN LABEL "Two Poi
     nt Approximation" ELSE LABE
     L "Least Squares Approximat
     ion"
2450 ! PULSE WIDTH
2455 LABEL USING "K,D.D,K" ; "Pu
     lse Width: ";FNP(P0);" uS"
2456 GOTO 2485
2460 ! REF INDEX
2465 LABEL
2470 LABEL "Refractive Index: ";
     I1
2475 ! ATT SETTING
2480 LABEL
2485 LABEL "Attenuator Setting:
     ";A2;" dB"
```

Figure 27

```
2490 LOCATE 0,100*RATIO,0,10
2495 FRAME
2500 LOCATE 0,180*RATIO,0,10
2505 SCALE 0,500,0,10
2510 MOVE 0,8
2515 LORG 1
2520 LABEL USING "DD.DDD,K" ; H2
     ;" km"
2525 MOVE 250,8
2530 LORG 4
2535 LABEL USING "DD.DDD,K" ; H2
     +5*FNH(H1)," km"
2550 MOVE 250,5
2555 LABEL "Length"
2556 MOVE 155,6.5
2557 GOTO 2405
2560 IF M1=0 THEN 2580
2565 MOVE FNA(M1),1
2570 LORG 1
2575 LABEL "MASK"
2580 RETURN
2585 !
3000 ! ********************
3005 ! * CURRENT SCREEN *
3010 ! * SAVE TO DISC   *
3015 ! ********************
3016 ALPHA 14,1
3018 DISP "SAVING DATA NOW"
3019 OFF CURSOR
3020 IF S1=1 THEN MASS STORAGE I
     S ":T"
3025 IF S1=2 THEN MASS STORAGE I
     S ":D700"
3030 !
3035 G$=F$&E$
3040 CREATE G$,36
3045 ASSIGN# 1 TO G$
3050 PRINT# 1 ; A$,B$,C$,DATE$,T
     IME$,E$,D4
3055 PRINT# 1 ; A2,D1,H1,P0,H2
3060 PRINT# 1 ; M1,I1,A3,V1,U1
3065 PRINT# 1 ; L1,L2,L3,L4
3070 PRINT# 1 ; F1,P1,M,M()
3075 PRINT# 1 ; Y()
3080 ASSIGN# 1 TO *
3085 RETURN
3090 !
3500 ! ***********************
3505 ! * READ SCREEN DATA *
3510 ! * FROM DISC        *
3515 ! ***********************
3517 CRT OFF
3520 IF S1=1 THEN MASS STORAGE I
     S ":T"
3525 IF S1=2 THEN MASS STORAGE I
     S ":D700"
3530 ASSIGN# 1 TO G$
3535 READ# 1 ; A$,B$,C$,D$,T$,E$
     ,D4
3540 READ# 1 ; A2,D1,H1,P0,H2
```

Figure 28

```
3545 READ# 1 ; M1,I1,A3,V1,U1
3550 READ# 1 ; L1,L2,L3,L4
3555 READ# 1 ; F1,P1,M,M()
3560 READ# 1 ; Y()
3565 ASSIGN# 1 TO *
3567 CRT ON
3570 RETURN
3575 !
4000 ! **********************
4005 ! * PLOT SCREEN DATA *
4010 ! * TO CRT GRAPHICS  *
4015 ! * & ALPHA SCREEN   *
4020 ! **********************
4025 ! PLOT OUT GRAPHICS
4030 P2=1
4035 PLOTTER IS P2
4040 GCLEAR
4045 ! LOCATE 0,RATIO*100,15,100
4050 LOCATE 10,RATIO*90,15,90
4055 SCALE 0,499,0,249
4060 AXES 50,25
4065 FRAME
4070 !
4075 ! PLOT OUT SCATTER TRACE
4080 ! D2=1 IF P1=500, D2=2 IF P
     1=1000
4085 D2=1
4090 IF P1=1000 THEN D2=2
4095 PENUP
4100 FOR I=1 TO P1
4105 PLOT (I-1)/D2,Y(I)
4110 NEXT I
4115 PENUP
4120 ! MAIN MARKER POSITION
4125 LORG 5
4130 S(0)=FNA(M(0))
4135 S(1)=FNA(M(1))
4140 IF F1=0 THEN 4160
4145 S(2)=FNA(M(2))
4150 S(3)=FNA(M(3))
4155 S(4)=FNA(M(4))
4160 MOVE S(0),Y(INT(S(0)+1.5)*D
     2)
4165 LABEL "*"
4170 MOVE S(1),Y(INT(S(1)+1.5)*D
     2)
4175 LABEL "X"
4180 IF F1=0 THEN 4205
4185 FOR I=2 TO 4
4190 MOVE S(I),Y(INT(S(I)+1.5)*D
     2)
4195 LABEL "X"
4200 NEXT I
4205 PENUP
4210 PLOT S(M),0
4215 PLOT S(M),249
4220 PENUP
4225 IF S(M)<400 THEN LORG 1 ELS
     E LORG 7
4230 MOVE S(M),25
```

Figure 29

```
4235 LABEL USING "DD.DDD,K" ; M(
     M)," km"
4240 LOCATE 0,100*RATIO,0,15
4245 FRAME
4250 SCALE 0,500,0,10
4255 MOVE 0,9
4260 LORG 3
4265 LABEL USING "DD.DDD,K" ; H2
     ," km"
4270 MOVE 250,9
4275 LORG 6
4280 LABEL USING "DD.DDD,K" ; H2
     +5*FNH(H1)," km"
4285 MOVE 490,9
4290 LORG 9
4295 LABEL USING "DD.DDD,K" ; H2
     +10*FNH(H1)," km"
4300 MOVE 250,6
4305 LORG 6
4310 LABEL "Length"
4315 IF M1=0 THEN 4335
4320 MOVE FNA(M1),1
4325 LORG 1
4330 LABEL "Mask"
4335 IF P4=3 THEN COPY
4340 RETURN
4345 !
4500 ! ******************
4505 ! * PRINTOUT DATA *
4510 ! * TO CRT        *
4515 ! ******************
4520 !
4525 PLOTTER IS 1
4530 GCLEAR
4535 LOCATE 0,RATIO*100,0,100
4540 FRAME
4545 SCALE 0,32,0,24
4550 MOVE 1,22
4555 LORG 1
4560 LABEL "Anritsu MW98A OTDR
          Page 1"
4565 LABEL
4570 LABEL "Title: ";A$
4575 LABEL "Route: ";B$
4580 LABEL "Operator: ";C$
4585 IF S2=1 THEN LABEL "Date:";
     DATE$;" Time:";TIME$
4590 IF S2=2 OR S2=3 THEN LABEL
     "Date:";D$;" Time:";T$
4595 !
4600 LABEL "Measurement No. ";E$
4602 LABEL "Averaging Time. ";D4
     ;"sec"
4610 GOSUB 8060 ! PLUG IN TYPE
4615 LABEL U$
4620 LABEL "Distance Range: ";18
     *2^D1;"km"
4625 H4=FNH(H1)
4630 IF H4<1 THEN 4645
4635 LABEL USING "K,D.DD,K" ; "H
     orizontal Scale ",H4," km/d
     iv"
```

Figure 30

```
4640 GOTO 4650
4645 LABEL USING "K,DDDDD,K" ; "
     Horizontal Scale ",H4*1000,
     " m/div"
4650 V3=FNV(V1)
4655 LABEL USING "K,D.DD,K" ; "V
     ertical Scale   ";V3;" dB/d
     iv"
4660 IF F1=0 THEN 4685
4665 ! SPLICE MODE
4670 LABEL
4675 LABEL USING "K,MDD.DD,K" ;
     "Splice:       ",L4,"dB"
4680 IF A3=0 THEN LABEL "Two Poi
     nt Approximation" ELSE LABE
     L "Least Squares Approximat
     ion"
4685 IF P4=3 THEN COPY
4690 GCLEAR
4695 LOCATE 0,RATIO*100,0,100
4700 FRAME
4705 SCALE 0,32,0,24
4710 MOVE 25,22
4715 LABEL "Page 2"
4720 MOVE 1,22
4725 IF F1=1 THEN 4760
4730 ! LOSS MODE
4735 LABEL "LOSS MARKERS"
4740 LABEL USING "K,DD.DDD,K" ;
     "Distance: ",L1," km"
4745 LABEL USING "K,DD.DD,X,K" ;
      "Loss:      ",L2," dB"
4750 LABEL USING "K,DD.DD,X,K" ;
      "Loss/km:   ",L3," dB/km"
4755 IF A3=0 THEN LABEL "Two Poi
     nt Approximation" ELSE LABE
     L "Least Squares Approximat
     ion"
4760 ! PULSE WIDTH
4765 LABEL
4770 LABEL USING "K,D.D,K" ; "Pu
     lse Width: ";FNP(P0);" uS"
4775 ! REF INDEX
4780 LABEL
4785 LABEL "Refractive Index: "
     I1
4790 ! ATT SETTING
4795 LABEL
4800 LABEL "Attenuator Setting:
     ";A2;" dB"
4805 IF P4=3 THEN COPY
4810 RETURN
4815 !
5000 ! ************************
5005 ! * INPUT MEASUREMENT(S) *
5010 ! * RELATED INFORMATION  *
5015 ! ************************
5020 CLEAR
5025 DISP "Input measurement tit
     le";
```

Figure 31

```
5030 INPUT A$
5035 DISP "Enter route name ";
5040 INPUT B$
5045 DISP "Enter operators name
     ";
5050 INPUT C$
5055 DISP "Date set is ";DATE$;"
      Do you wish to change it?"
5060 DISP "Enter Y or N then pre
     ss ENDLINE"
5065 INPUT X$
5070 IF X$="Y" OR X$="y" THEN 50
     75 ELSE 5090
5075 DISP "Enter date ";
5080 DISP "e.g 05/17/1986 for 17
      May 1986"
5085 INPUT D$
5090 DISP "Time set is ";TIME$;"
      Do you wish to change it?"
5095 DISP "Enter Y or N then pre
     ss ENDLINE"
5100 INPUT X$
5105 IF X$="Y" OR X$="y" THEN 51
     10 ELSE 5140
5110 DISP "Enter current time ";
5115 DISP "e.g 14:22:07 for 2:22
     :07 pm"
5120 INPUT T$
5125 D=MDY(D$)-MDY("12/31/1985")
5130 D=86*1000+D
5135 SETTIME HMS(T$),D
5140 CLEAR
5145 RETURN
5150 !
6000 ! ********************
6005 ! * DISC ERROR SBRT *
6010 ! ********************
6015 BEEP
6020 WAIT 200
6025 BEEP
6030 IF ERRN=60 THEN DISP "Disc
     is write protected, change
     write protect tab on disc"
6035 IF ERRN=62 THEN DISP "Tape
     cartridge out, Please inser
     t a tape correctly"
6040 IF ERRN=63 THEN DISP "File
     already exists with that na
     me, please use a different
     name"
6045 IF ERRN=65 THEN DISP "Tape
     full, replace with new tape
     "
6050 IF ERRN=67 THEN DISP G$," D
     oes not exist on selected d
     evice,try different filenam
     e"
6055 IF ERRN=73 THEN DISP "Bad t
     ape or tape not initialized
     , only use initialized tape
     s"
```

Figure 32

```
6060 IF ERRN=124 THEN DISP "Disc
      file directory full"
6065 IF ERRN=126 THEN DISP "Plot
     ter is not connected to
      computer"
6070 IF ERRN=128 THEN DISP "Disc
      is full, change disc"
6075 IF ERRN=129 THEN DISP "Stor
     age device damaged, replace
      tape/disc"
6080 IF ERRN=130 THEN DISP "Disc
      is not initialized or disc
      not inserted properly ";
6085 IF ERRN=130 THEN DISP "or d
     isc drive is not present"
6090 DISP "Press END LINE when r
     eady to    continue"
6095 INPUT X$
6100 !
6105 IF ERRN=60 THEN 3000
6110 IF ERRN=62 AND ERRL<3000 TH
     EN 500
6115 IF ERRN=62 AND ERRL<3000 TH
     EN 500
6120 IF ERRN=62 THEN 3500
6125 IF ERRN=63 AND ERRL>3000 TH
     EN 245
6130 IF ERRN=65 AND ERRL>3000 TH
     EN 3000
6135 IF ERRN=67 THEN 525
6140 IF ERRN=124 OR ERRN=128 THE
     N 3000
6145 IF ERRN=126 THEN 2000
6150 IF ERRN=129 AND ERRL=530 TH
     EN 520
6155 IF ERRN=129 AND ERRL>3000 A
     ND ERRL<3200 THEN 3000
6160 IF ERRN=129 AND ERRL>3200 A
     ND ERRL<4000 THEN 3500
6165 IF ERRN=130 AND ERRL>500 AN
     D ERRL<900 THEN 500
6170 IF ERRN=130 AND ERRL>3000 A
     ND ERRL<3200 THEN 3000
6175 IF ERRN=130 AND ERRL>3200 A
     ND ERRL<4000 THEN 3500
6180 DISP "Error cannot be overc
     ome"
6185 !
6190 !
6500 PAUSE
7000 ! AVERAGE TIME WAIT SBRT
7500 ! MEASUREMENT RUN DATA
7515 OFF CURSOR
7516 ALPHA 1,1
7517 CLEAR
7520 DISP "Date: ";DATE$
7525 DISP "Measurement Title: ";
     A$
7530 DISP "Route: ";B$
7535 DISP "Operators Name: ";C$
```

Figure 33

```
7540 IF D4>0 THEN DISP "Meas. Av
     erage time: ";D4;"secs"
7545 DISP "Meas. No: ";E$;"  Mea
     s. left: ";M2
7560 IF T4=0 THEN 7590
7565 DISP "Time between"
7570 DISP "measurements: ";T1;"h
     r"
7575 DISP "               ";T2;"m
     in"
7580 DISP "               ";T3;"s
     ec"
7590 IF S1=1 THEN DISP "Data sto
     red on tape cartridge"
7595 IF S1=2 THEN DISP "Data sto
     red on disc"
7600 IF S1=1 OR S1=2 THEN DISP "
     Base Filename: ";F$
7602 OFF CURSOR
7605 RETURN
7700 ! AVERAGE TIME WAIT SBRT
7702 IF D4=0 THEN 7740
7705 OUTPUT A1 USING "K,/" ; "AV
     R1"
7710 ON TIMER# 3,D4*1000 GOTO 77
     35
7715 !
7720 ALPHA 14,1
7725 DISP "  AVERAGING  TIME LEF
     T:";INT(D4+.5-READTIM(3));"
     sec"
7726 OFF CURSOR
7730 GOTO 7720
7735 OFF TIMER# 3
7740 !
7745 ALPHA 14,1
7750 DISP "  DATA READ IN PROGRE
     SS"
7752 OFF CURSOR
7755 RETURN
7800 ! INTERMEASUREMENT WAIT SBR
     T
7805 OFF CURSOR
7810 ON TIMER# 3,T4 GOTO 7860
7815 ALPHA 14,1
7825 DISP "TIME BEFORE NEXT MEAS
     UREMENT:-"
7826 OFF CURSOR
7830 T5=T4/1000-READTIM(3)
7835 T6=INT(T5/3600)
7840 T7=INT((T5-T6*3600)/60)
7845 T8=INT(T5-T6*3600-T7*60)
7850 DISP T6;"HR ";T7;"MIN ";T8;
     "SEC"
7852 OFF CURSOR
7855 GOTO 7815
7860 OFF TIMER# 3
7870 ALPHA 14,1
7875 DISP
7876 OFF CURSOR
```

Figure 34

```
7880 RETURN
8000 ! FUNCTION TO CONVERT HSCAL
     ING TO KM
8005 DEF FNH(X)
8010 IF X=0 THEN H3=4
8015 IF X=1 THEN H3=2
8020 IF X=2 THEN H3=1
8025 IF X=3 THEN H3=.5
8030 IF X=4 THEN H3=.25
8035 IF X=5 THEN H3=.1
8040 IF X=6 THEN H3=.05
8045 IF X=7 THEN H3=.025
8050 FNH=H3*1.5/I1 ! CORRECT FOR
      REFRACTIVE INDEX
8055 FN END
8060 IF U1=1 THEN U$="0.85um Mul
     ti Mode"
8065 IF U1=2 THEN U$="1.3um Mult
     i Mode"
8070 IF U1=3 THEN U$="1.3um Sing
     le Mode"
8075 IF U1=4 THEN U$="1.55um Sin
     gle Mode"
8080 RETURN
8085 DEF FNV(X) ! VERT SCALE
8090 IF X=0 THEN V2=2.5
8095 IF X=1 THEN V2=1
8100 IF X=2 THEN V2= 5
8105 IF X=3 THEN V2=.25
8110 FNV=V2
8115 FN END
8120 DEF FNP(X) ! PULSE WIDTH
8125 IF X=0 THEN P9=.1
8130 IF X=1 THEN P9=.5
8135 IF X=2 THEN P9=2
8140 FNP=P9
8145 FN END
8150 DEF FNA(X) = (X-H2)/(10*FNH
     (H1))*499
8155 END
```

Figure 35

```
 10 OPTION BASE 1
 20 DIM S(4),M(4)
 30 DIM Y(1000)
 40 DIM E$[32]
 50 DISP "WHAT IS FILE NAME"
 60 INPUT F$
 70 DISP "ENTER THE MEAS NO.RANG
    E"
 80 DISP "START NO. ";
 90 INPUT S3
100 DISP "STOP NO. ";
110 INPUT S4
120 FOR J=S3 TO S4
130 G$=F$&VAL$(J)
140 ASSIGN# 1 TO G$
150 READ# 1 ; A$,B$,C$,D$,T$,E$,
    D4
160 READ# 1 ; A2,D1,H1,P0,H2
170 READ# 1 ; M1,I1,A3,V1,U1
180 READ# 1 ; L1,L2,L3,L4
190 READ# 1 ; F1,P1,M,M()
200 READ# 1 ; Y()
205 ASSIGN# 1 TO *
210 PRINT "MEASUREMENT NO",E$
220 PRINT "POINTS ALONG X-AXIS"
230 FOR X=5 TO 550
240 PRINT Y(X);
250 NEXT X
255 PRINT
260 END
```

Figure 36

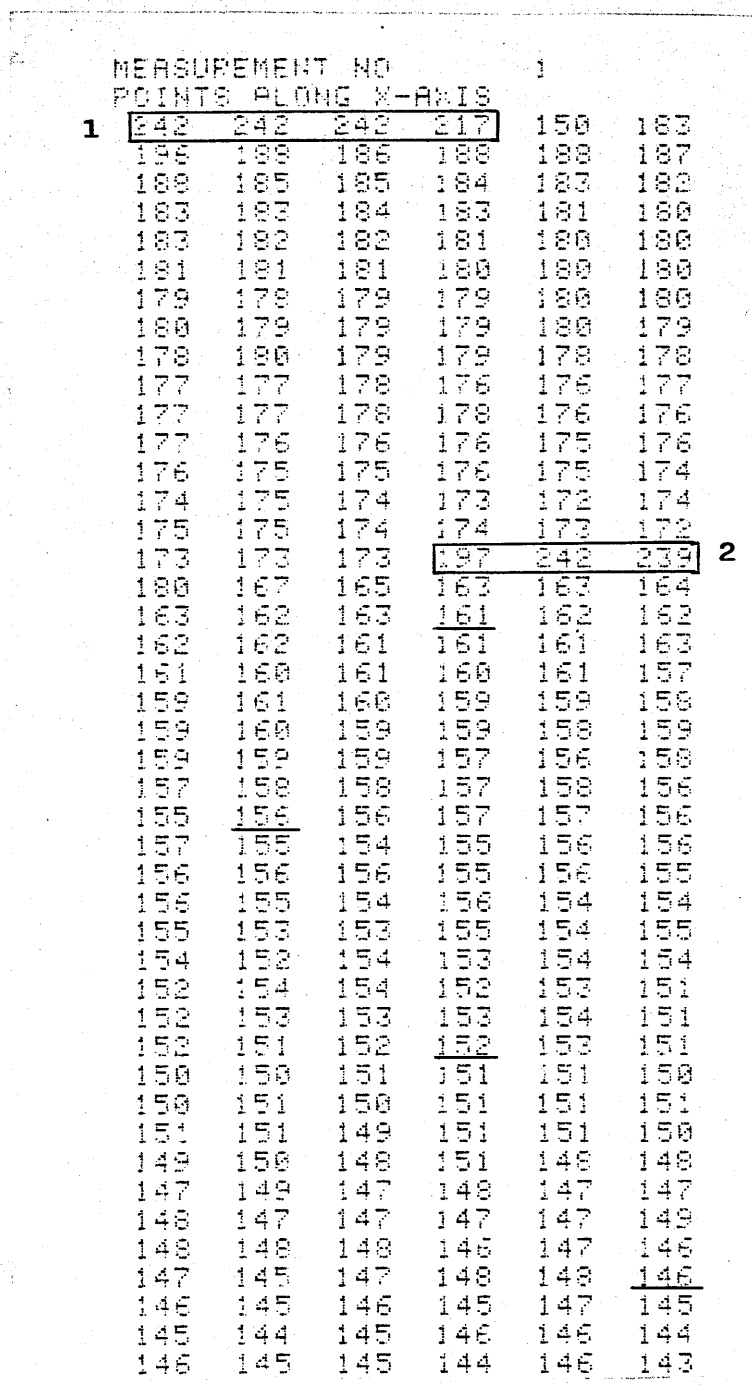
MEASUREMENT NO 1
POINTS ALONG X-AXIS
1
242 242 242 217 150 183
198 199 186 188 188 187
188 185 185 184 183 182
183 182 184 183 181 180
183 182 182 181 180 180
181 181 181 180 180 180
179 178 179 179 180 180
180 179 179 179 180 179
178 180 178 179 178 178
177 177 178 176 176 177
177 177 178 178 176 176
177 176 176 176 175 176
176 175 175 176 175 174
174 175 174 173 172 174
175 175 174 174 173 172
173 173 173 197 242 239
2
180 167 165 163 163 164
163 162 163 161 162 162
162 162 161 161 161 163
161 160 161 160 161 157
159 161 160 159 159 158
159 160 159 159 158 159
159 159 159 157 156 158
157 158 158 157 158 156
155 156 156 157 157 156
157 155 154 155 156 156
156 156 156 155 156 155
156 155 154 156 154 154
155 153 153 155 154 155
154 152 154 153 154 154
152 154 154 152 153 151
152 153 153 153 154 151
152 151 152 152 153 151
150 150 151 151 151 150
150 151 150 151 151 151
151 151 149 151 151 150
149 150 148 151 148 148
147 149 147 148 147 147
148 147 147 147 147 149
148 148 148 146 147 146
147 145 147 148 148 146
146 145 146 145 147 145
145 144 145 146 145 144
146 145 145 144 146 143

Figure 48A

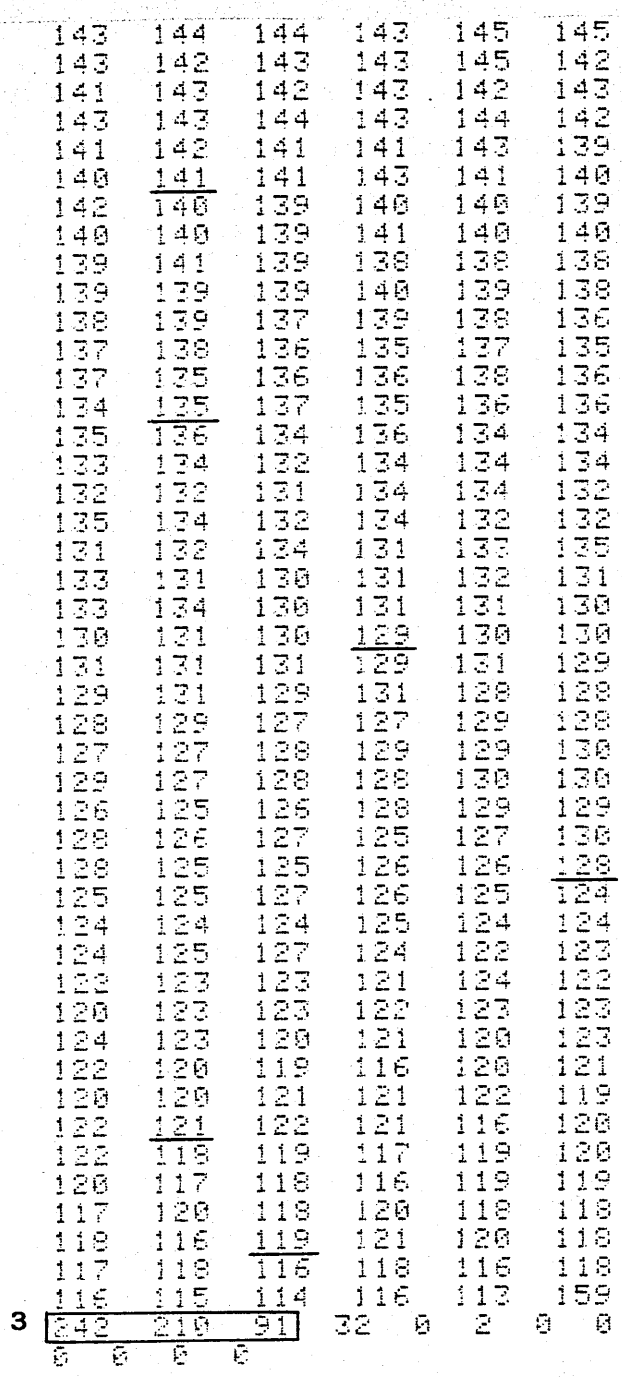
143 144 144 143 145 145
143 142 143 143 145 142
141 143 142 143 142 143
143 143 144 143 144 142
141 142 141 141 143 139
140 141 141 143 141 140
142 140 139 140 140 139
140 140 139 141 140 140
139 141 139 138 138 138
139 139 139 140 139 138
138 139 137 139 138 136
137 138 136 135 137 135
137 135 136 136 138 136
134 135 137 135 136 136
135 136 134 136 134 134
133 134 132 134 134 134
132 132 131 134 134 132
135 134 132 134 132 132
131 132 134 131 133 135
133 131 130 131 132 131
133 134 130 131 131 130
130 131 130 129 130 130
131 131 131 129 131 129
129 131 128 131 128 128
128 129 127 127 129 128
127 127 128 129 129 130
129 127 128 128 130 130
126 125 126 128 129 129
128 126 127 125 127 130
128 125 125 126 126 128
125 125 127 126 125 124
124 124 124 125 124 124
124 125 127 124 122 123
123 123 123 121 124 122
120 123 123 122 123 123
124 123 120 121 120 123
122 120 119 116 120 121
120 120 121 121 122 119
122 121 122 121 116 120
122 118 119 117 119 120
120 117 118 116 119 119
117 120 118 120 118 118
118 116 119 121 120 118
117 118 116 118 116 118
116 115 114 116 112 159
3 242 210 91 32 0 2 0 0
0 0 0 0

Figure 48B

MEASUREMENT NO 2

POINTS ALONG X-AXIS

242	242	242	217	152	183
197	188	187	188	188	186
187	184	185	185	183	183
183	184	184	183	181	181
183	182	182	181	181	180
180	181	179	179	179	179
178	178	178	179	180	179
180	180	179	179	179	178
178	178	180	179	178	178
177	176	178	178	176	177
176	176	177	177	177	177
176	177	175	175	175	176
176	176	176	176	175	174
174	174	174	174	174	174
174	175	175	174	173	172
173	172	173	196	242	238
178	164	162	161	162	162
161	161	161	160	160	161
162	161	162	161	161	160
159	158	160	159	159	159
159	160	158	157	156	157
157	158	158	158	158	158
158	159	157	157	156	157
156	157	156	156	155	158
155	157	153	157	157	155
153	154	154	154	155	155
154	155	154	153	153	154
154	155	153	154	153	153
154	152	153	152	153	153
153	151	152	151	152	151
152	152	150	152	150	149
150	150	151	150	153	151
151	150	150	150	151	150
150	150	150	149	148	150
150	152	150	150	150	149
149	150	149	149	148	148
149	147	148	148	146	146
147	147	145	146	146	146
147	147	147	149	147	146
145	146	147	146	145	145
145	146	145	145	145	145
146	145	144	144	144	145
142	141	143	145	144	144
144	144	144	144	144	142

Figure 49A

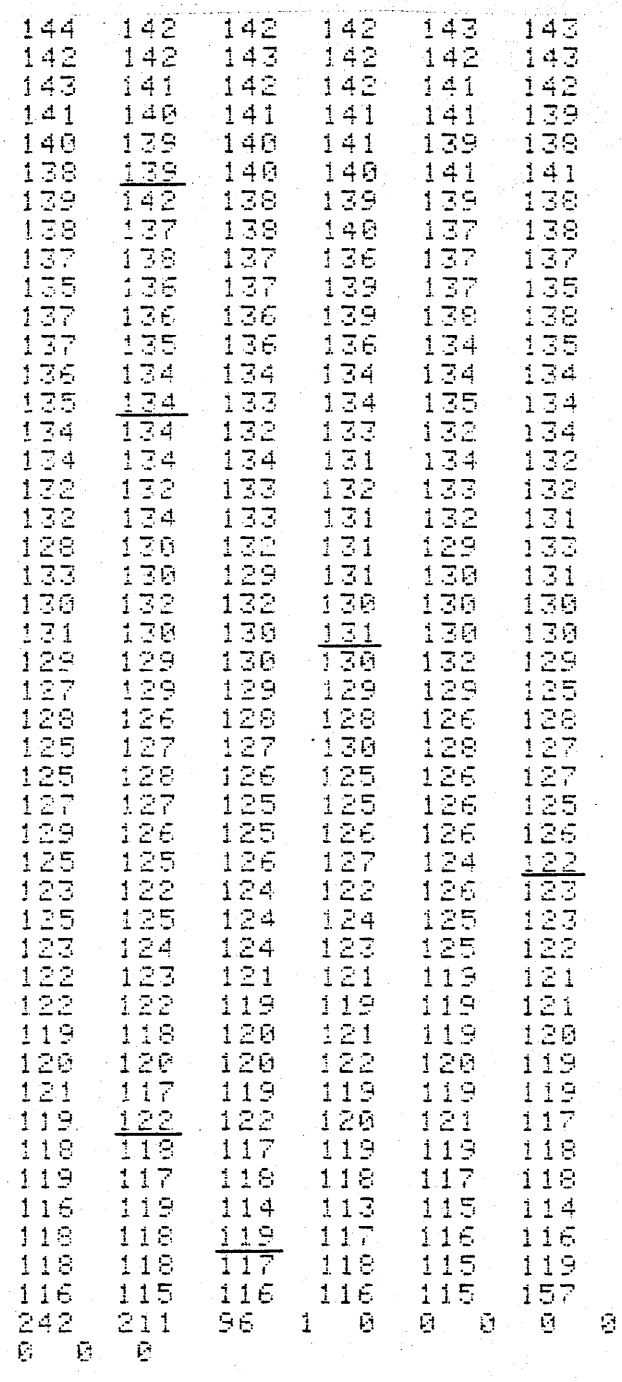
144 142 142 142 143 143
142 142 143 142 142 143
143 141 142 142 141 142
141 140 141 141 141 139
140 139 140 141 139 138
138 139 140 140 141 141
139 142 138 139 139 138
138 137 138 140 137 138
137 138 137 136 137 137
135 136 137 139 137 135
137 136 136 139 138 138
137 135 136 136 134 135
136 134 134 134 134 134
135 134 133 134 135 134
134 134 132 133 132 134
134 134 134 131 134 132
132 132 133 132 133 132
132 134 133 131 132 131
130 130 132 131 129 133
133 130 129 131 130 131
130 132 132 130 130 130
131 130 130 131 130 130
129 129 130 130 132 129
127 129 129 129 129 125
128 126 128 128 126 128
125 127 127 130 128 127
125 128 126 125 126 127
127 127 125 125 126 125
129 126 125 126 126 125
125 125 126 127 124 122
123 122 124 122 126 123
125 125 124 124 125 123
123 124 124 123 125 122
122 123 121 121 119 121
122 122 119 119 119 121
119 118 120 121 119 120
120 120 120 122 120 119
121 117 119 119 119 119
119 122 122 120 121 117
118 119 117 119 119 118
119 117 118 118 117 118
116 119 114 113 115 114
118 118 119 117 116 116
118 118 117 118 115 119
116 115 116 116 115 157
242 211 96 1 0 0 0 0 0
0 0 0

Figure 49B

MEASUREMENT NO 3

POINTS ALONG X-AXIS

245	245	245	216	152	185
198	190	188	188	189	189
189	186	186	186	185	182
183	184	185	184	183	182
183	183	183	182	181	181
182	182	180	180	180	180
179	180	179	181	180	181
181	181	180	181	180	180
179	180	181	179	179	179
179	178	178	178	178	179
178	178	178	179	177	178
179	178	177	177	176	177
177	177	178	177	176	176
176	176	175	174	175	176
176	175	175	175	174	174
174	173	174	192	245	235
176	164	162	162	161	162
161	162	160	159	160	159
160	160	160	160	160	159
158	158	159	159	159	159
159	160	159	157	158	157
157	158	158	156	156	158
157	158	157	155	155	155
155	155	156	156	156	156
155	155	153	155	155	154
154	153	154	153	154	154
156	154	153	153	153	154
154	154	153	152	152	154
153	152	152	151	153	153
153	152	152	153	152	152
152	152	153	151	152	150
150	150	151	151	152	151
150	149	150	152	150	150
150	148	149	149	150	149
150	149	149	149	148	149
149	150	149	150	148	147
147	146	148	148	150	147
146	146	146	146	147	146
146	146	144	147	147	146
146	147	148	145	143	144
145	146	145	145	144	145
143	143	143	145	144	142
144	142	145	144	143	142
142	144	143	145	143	144

Figure 50A

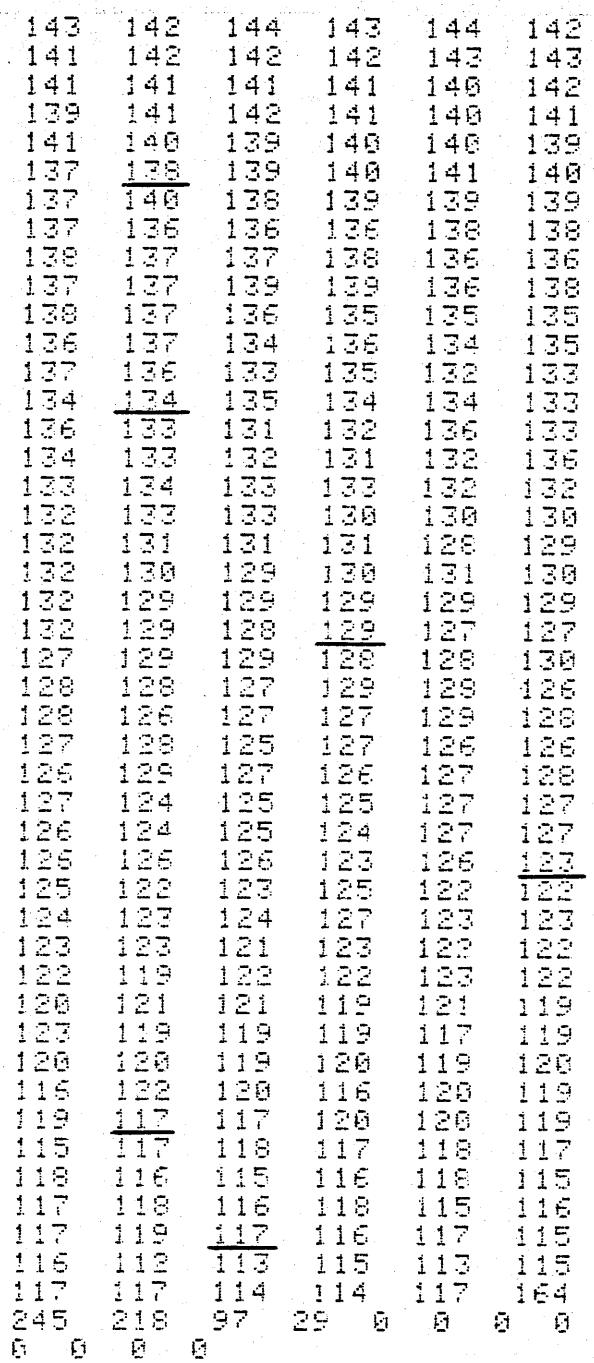
143 142 144 143 144 142
141 142 142 142 142 143
141 141 141 141 140 142
139 141 142 141 140 141
141 140 139 140 140 139
137 138 139 140 141 140
137 140 138 139 139 139
137 136 136 136 138 138
138 137 137 138 136 136
137 137 139 139 136 138
138 137 136 135 135 135
136 137 134 136 134 135
137 136 133 135 132 133
134 134 135 134 134 133
136 133 131 132 136 133
134 133 132 131 132 136
133 134 133 133 132 132
132 132 133 130 130 130
132 131 131 131 128 129
132 130 129 130 131 130
132 129 129 129 129 129
132 129 128 129 127 127
127 129 129 128 128 130
128 128 127 129 129 126
128 126 127 127 129 128
127 128 125 127 126 126
126 129 127 126 127 128
127 124 125 125 127 127
126 124 125 124 127 127
126 126 126 123 126 123
125 122 123 125 122 122
124 127 124 127 123 123
123 123 121 123 122 122
122 119 122 122 123 122
120 121 121 119 121 119
127 119 119 119 117 119
120 120 119 120 119 120
116 122 120 116 120 119
119 117 117 120 120 119
115 117 118 117 118 117
118 116 115 116 116 115
117 118 116 118 115 116
117 119 117 116 117 115
116 112 113 115 113 115
117 117 114 114 117 164
245 218 97 29 0 0 0 0
0 0 0 0

Figure 50B

MEASUREMENT NO 4

POINTS ALONG X-AXIS

245	245	245	218	151	185
199	190	189	189	189	189
188	186	186	186	185	184
184	185	185	184	184	183
184	183	183	183	181	181
182	183	180	181	182	181
179	180	180	181	181	181
180	181	180	180	181	180
180	180	179	181	178	180
179	178	179	178	178	178
178	177	178	179	178	177
179	179	177	177	177	177
177	177	177	177	177	176
176	175	175	176	176	176
176	176	176	176	174	175
174	174	175	188	245	227
172	162	159	159	160	159
159	160	160	159	158	160
159	158	158	159	159	159
157	158	159	159	158	158
159	159	157	156	158	155
156	157	156	156	156	158
157	156	157	156	155	155
154	155	155	154	157	156
155	153	153	154	153	154
153	152	157	152	153	156
154	154	155	151	151	153
153	152	152	152	152	152
152	152	153	153	151	153
152	150	152	150	152	150
151	151	151	150	150	149
150	150	149	151	152	149
151	150	148	148	150	149
148	149	149	149	149	149
149	149	147	149	148	148
149	147	147	147	149	145
148	147	146	147	146	144
145	145	147	146	145	145
145	145	144	145	145	145
146	146	145	145	143	144
146	145	143	143	145	142
143	142	141	143	140	142
144	142	142	143	141	142
141	143	141	143	141	143

Figure 51A

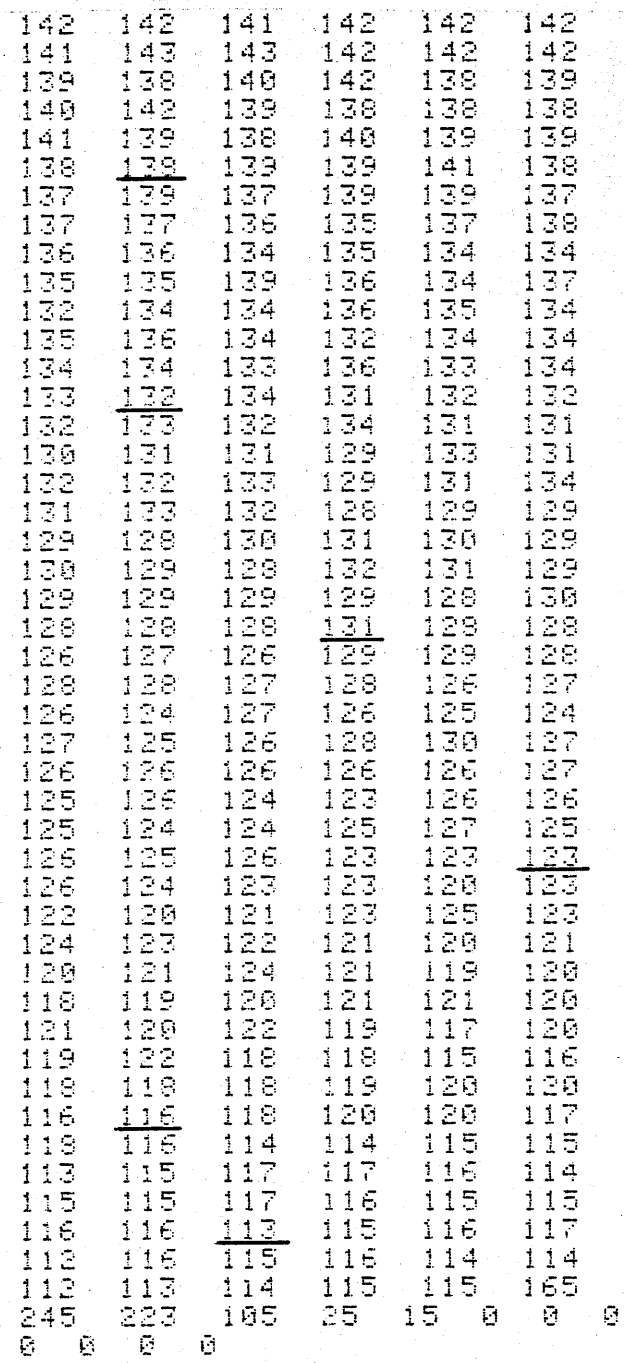
142 142 141 142 142 142
141 143 143 142 142 142
139 138 140 142 138 139
140 142 139 138 138 138
141 139 138 140 139 139
138 138 139 139 141 138
137 139 137 139 139 137
137 137 136 135 137 138
136 136 134 135 134 134
135 135 139 136 134 137
132 134 134 136 135 134
135 136 134 132 134 134
134 134 133 136 133 134
133 132 134 131 132 132
132 133 132 134 131 131
130 131 131 129 133 131
132 132 133 129 131 134
131 133 132 128 129 129
129 130 130 131 130 129
130 129 129 132 131 129
129 129 129 129 120 130
128 128 128 131 128 128
126 127 126 129 129 128
128 128 127 128 126 127
126 124 127 126 125 124
127 125 126 128 130 127
126 126 126 126 126 127
125 126 124 123 126 126
125 124 124 125 127 125
126 125 126 123 123 127
126 124 123 123 120 123
122 120 121 123 125 123
124 123 122 121 120 121
120 121 124 121 119 120
118 119 120 121 121 120
121 120 122 119 117 120
119 122 118 118 115 116
118 118 118 119 120 120
116 116 118 120 120 117
119 115 114 114 115 115
113 115 117 117 116 114
115 115 117 116 115 115
116 116 113 115 116 117
112 116 115 116 114 114
112 113 114 115 115 165
245 223 105 35 15 0 0 0
0 0 0 0

Figure 51B

MEASUREMENT NO 5

POINTS ALONG X-AXIS

245	245	245	216	152	184
190	189	188	189	189	188
189	186	187	186	185	184
184	185	185	184	183	182
184	184	183	182	181	181
182	183	180	180	182	180
179	179	180	181	181	181
180	181	180	181	181	180
180	180	180	180	179	180
179	179	179	177	178	179
178	177	179	179	178	177
178	178	176	176	176	177
177	177	177	177	177	175
176	175	175	175	175	176
176	176	176	176	175	174
174	174	174	187	244	219
168	160	159	159	160	159
159	158	158	158	159	159
156	157	158	156	158	156
156	156	157	157	156	157
157	156	157	157	156	154
154	155	156	156	153	156
155	156	154	153	154	155
153	153	153	154	152	152
152	152	152	152	152	153
153	153	152	151	152	152
152	153	151	152	150	151
151	151	151	150	153	152
150	149	147	150	150	151
150	149	151	151	150	150
150	149	151	150	149	149
149	150	150	148	149	148
149	148	147	149	148	147
148	148	149	147	147	147
149	148	146	147	149	148
148	147	146	147	146	146
147	146	146	145	145	145
142	142	143	145	145	145
144	144	143	145	145	144
144	146	145	143	142	142
144	143	142	143	144	143
141	142	140	141	140	143
143	143	142	141	141	140
142	179	140	141	140	140

Figure 52A

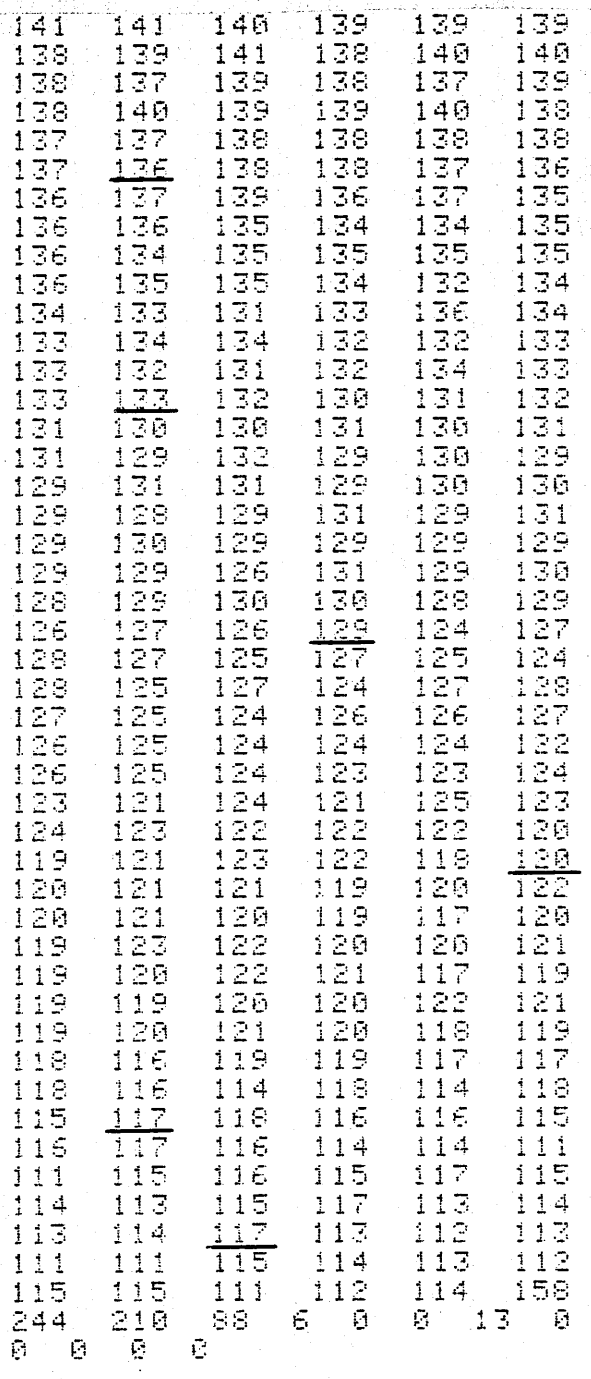
141 141 140 139 139 139
138 139 141 138 140 140
138 137 139 138 137 139
138 140 139 139 140 138
137 137 138 138 138 138
137 134 138 138 137 136
136 137 139 136 137 135
136 136 135 134 134 135
136 134 135 135 135 135
136 135 135 134 132 134
134 133 131 133 136 134
133 134 134 132 132 133
133 132 131 132 134 132
133 133 132 130 131 132
131 130 130 131 130 131
131 129 132 129 130 129
129 131 131 129 130 130
129 128 129 131 129 131
129 130 129 129 129 129
129 129 126 131 129 130
128 129 130 130 128 129
126 127 126 129 124 127
128 127 125 127 125 124
128 125 127 124 127 128
127 125 124 126 126 127
126 125 124 124 124 122
126 125 124 123 123 124
123 121 124 121 125 123
124 123 122 122 122 120
119 121 123 122 118 120
120 121 121 119 120 122
120 121 120 119 117 120
119 123 122 120 120 121
118 120 122 121 117 119
119 119 120 120 122 121
119 120 121 120 118 119
118 116 119 119 117 117
118 116 114 118 114 118
115 117 118 116 116 115
116 117 116 114 114 111
111 115 116 115 117 115
114 113 115 117 113 114
113 114 117 113 112 113
111 111 115 114 113 112
115 115 111 112 114 158
244 210 88 6 0 0 13 0
0 0 0 0

Figure 52B

MEASUREMENT NO 6

POINTS ALONG X-AXIS

245	245	245	218	152	185
198	189	188	189	189	189
188	186	186	186	185	184
184	186	185	184	183	183
182	183	183	183	181	180
182	183	182	181	182	181
179	180	180	182	182	180
182	181	180	181	182	180
180	179	180	180	179	180
180	178	179	177	178	179
178	177	179	180	178	178
179	178	178	177	177	177
177	177	177	177	178	176
176	176	175	175	176	176
176	176	177	176	175	174
174	175	175	188	244	222
169	160	159	158	158	157
158	158	157	157	156	155
155	155	157	156	155	155
156	156	156	156	155	156
154	154	154	154	156	154
154	153	152	153	153	153
152	152	151	153	152	152
153	152	151	152	152	153
151	151	152	152	151	150
150	151	152	150	150	151
151	150	150	151	151	150
150	150	148	149	148	147
149	149	149	150	150	148
147	149	149	149	148	147
148	148	147	147	146	147
149	146	147	146	149	145
148	149	148	148	147	145
146	148	147	146	147	144
146	145	145	146	146	145
144	146	145	146	147	143
144	143	145	145	144	144
143	142	141	141	142	144
142	144	144	141	142	142
141	143	143	142	140	142
141	140	140	140	141	143
141	141	141	141	140	141
142	139	138	138	139	138
140	139	139	140	139	140

Figure 53A

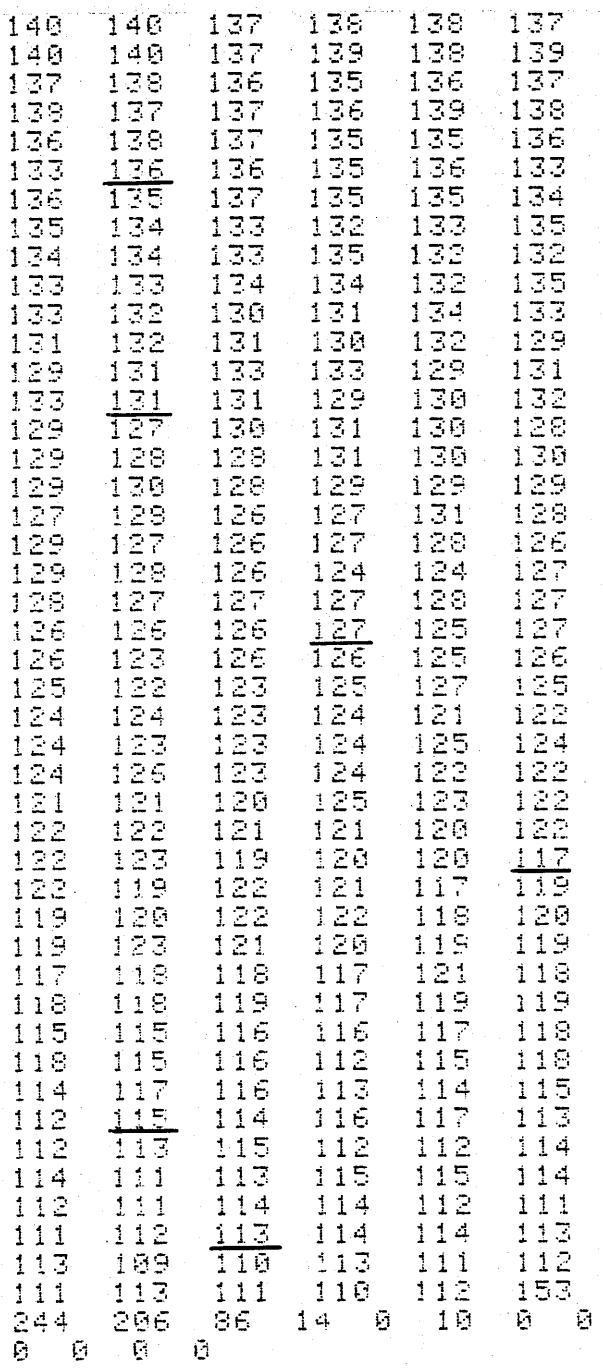
140 140 137 138 138 137
140 140 137 139 138 139
137 138 136 135 136 137
139 137 137 136 139 138
136 138 137 135 135 136
133 136 136 135 136 133
136 135 137 135 135 134
135 134 133 132 133 135
134 134 133 135 132 132
133 133 134 134 132 135
133 132 130 131 134 133
131 132 131 130 132 129
129 131 133 133 129 131
133 131 131 129 130 132
129 127 130 131 130 128
129 128 128 131 130 130
129 130 128 129 129 129
127 129 126 127 131 128
129 127 126 127 128 126
129 128 126 124 124 127
128 127 127 127 128 127
126 126 126 127 125 127
126 123 126 126 125 126
125 122 123 125 127 125
124 124 123 124 121 122
124 123 123 124 125 124
124 126 123 124 122 122
121 121 120 125 123 122
122 122 121 121 120 122
122 123 119 120 120 117
122 119 122 121 117 119
119 120 122 122 118 120
119 123 121 120 119 119
117 118 118 117 121 118
118 118 119 117 119 119
115 115 116 116 117 118
118 115 116 112 115 118
114 117 116 113 114 115
112 115 114 116 117 113
112 113 115 112 112 114
114 111 113 115 115 114
112 111 114 114 112 111
111 112 113 114 114 113
113 109 110 113 111 112
111 113 111 110 112 153
244 206 86 14 0 10 0 0
0 0 0 0

Figure 53B

MEASUREMENT NO 7

POINTS ALONG X-AXIS

245	245	245	218	152	185
198	189	189	189	189	188
188	187	188	186	185	183
185	186	185	185	183	183
185	184	184	183	182	181
182	183	180	181	181	181
181	181	181	182	182	181
182	181	181	181	182	179
181	182	181	180	179	180
180	179	179	178	179	179
179	179	180	179	178	178
179	179	179	179	178	178
177	178	178	178	177	176
176	176	175	175	175	177
176	175	176	175	175	174
174	175	175	188	244	220
167	157	157	156	155	156
155	156	155	156	154	152
154	153	155	155	153	155
155	154	155	154	153	153
152	154	154	153	153	152
154	152	152	152	152	153
151	151	150	151	151	150
152	150	152	151	150	150
152	151	152	150	149	149
149	149	150	149	149	149
148	150	148	149	150	147
147	148	148	148	146	147
148	149	148	149	147	146
145	147	147	147	145	146
147	146	146	146	144	146
145	147	145	146	146	144
144	145	145	146	145	145
144	144	145	144	144	145
145	143	143	145	145	143
144	142	144	144	144	142
142	141	143	142	142	141
142	144	143	141	141	141
143	142	142	141	140	140
140	141	139	140	140	141
139	140	141	138	139	142
140	140	139	140	139	139
140	139	139	138	139	137
139	138	138	138	138	140

Figure 54A

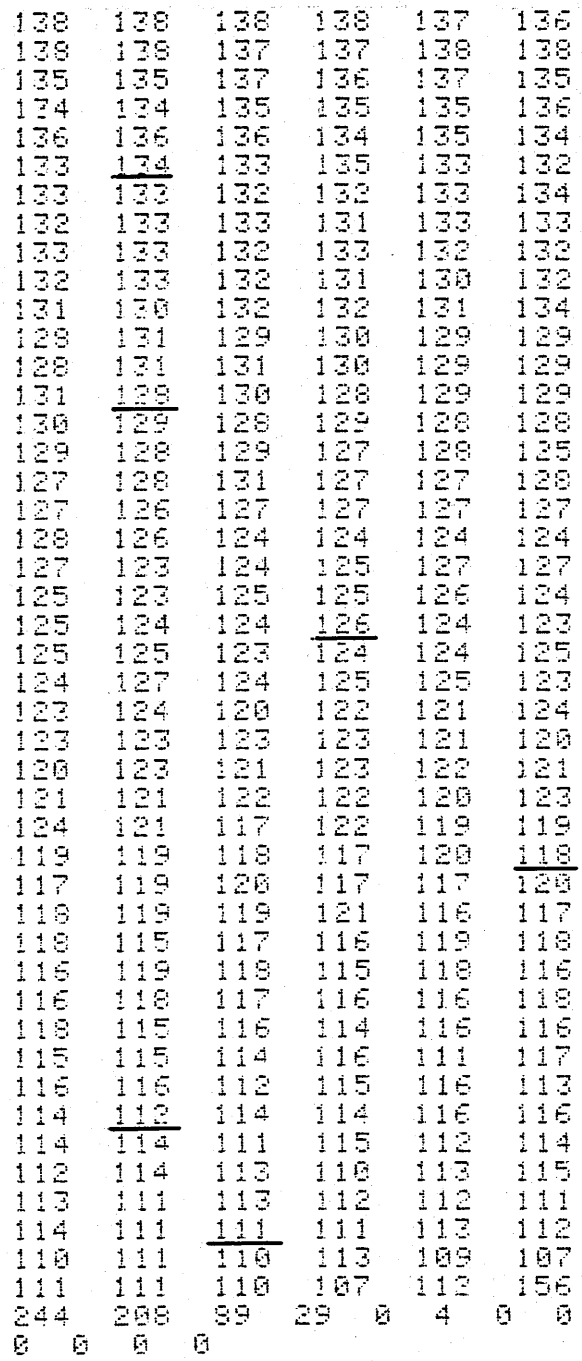

138	138	138	138	137	136
139	139	137	137	138	138
135	135	137	136	137	135
134	134	135	135	135	136
136	136	136	134	135	134
133	134	133	135	133	132
133	133	132	132	133	134
132	133	133	131	133	133
133	133	132	133	132	132
132	133	132	131	130	132
131	130	132	132	131	134
129	131	129	130	129	129
128	131	131	130	129	129
131	128	130	128	129	129
130	129	128	129	128	128
129	128	129	127	128	125
127	128	131	127	127	128
127	126	127	127	127	127
128	126	124	124	124	124
127	123	124	125	127	127
125	123	125	125	126	124
125	124	124	126	124	123
125	125	123	124	124	125
124	127	124	125	125	123
123	124	120	122	121	124
123	123	123	123	121	120
120	123	121	123	122	121
121	121	122	122	120	123
124	121	117	122	119	119
119	119	118	117	120	118
117	119	120	117	117	120
118	119	119	121	116	117
119	115	117	116	119	118
115	119	118	115	118	116
116	118	117	116	116	118
118	115	116	114	116	116
115	115	114	116	111	117
116	116	112	115	116	113
114	113	114	114	116	116
114	114	111	115	112	114
112	114	113	110	113	115
113	111	113	112	112	111
114	111	111	111	113	112
110	111	110	113	109	107
111	111	110	107	112	156
244	208	89	29	0 4	0 0
0	0	0	0		

Figure 54B

MERSUREMENT NO 0

POINTS ALONG X-AXIS

245	245	245	216	152	185
199	189	189	189	190	189
189	186	187	186	185	183
185	186	185	186	184	183
184	184	184	183	182	182
182	183	180	181	181	181
180	181	181	181	181	180
181	181	181	181	182	180
180	181	181	180	179	179
179	179	179	178	178	178
179	178	179	179	178	178
179	179	178	177	178	178
177	178	178	177	178	176
177	176	175	175	175	176
176	176	176	175	175	174
174	174	173	189	244	222
166	155	155	154	154	153
152	152	152	152	154	153
152	152	153	151	151	152
153	153	152	151	152	152
152	150	149	152	150	146
153	150	150	149	150	149
150	149	148	148	149	150
149	149	147	147	149	148
148	147	148	148	146	147
148	148	148	147	144	147
147	147	146	145	146	147
148	147	146	146	145	145
145	146	145	145	146	145
144	144	146	144	145	143
145	145	144	145	144	142
144	143	142	144	145	143
145	143	142	145	143	142
143	142	143	141	141	140
144	143	142	141	142	141
143	143	143	141	140	139
141	142	141	142	140	139
138	139	140	139	139	140
140	137	137	138	137	137
137	138	138	140	136	140
138	139	137	137	136	136
137	138	137	135	137	138
138	137	138	139	137	134
136	136	135	136	136	137

Figure 55A

136	134	135	136	134	134
135	135	134	134	134	135
136	134	134	132	135	134
134	132	133	132	134	134
135	134	132	134	133	132
131	132	132	133	133	132
131	131	131	131	131	130
132	130	132	129	128	132
131	130	131	131	129	129
128	130	128	129	128	129
128	127	128	126	127	127
128	130	126	129	128	127
127	127	128	125	126	128
128	127	129	127	126	126
126	125	127	124	124	126
126	124	125	128	127	125
124	125	126	125	125	126
126	124	123	123	124	124
126	123	122	124	123	123
123	122	124	124	122	120
122	121	122	121	122	123
123	121	122	121	121	122
120	124	120	119	121	123
119	120	121	122	120	120
119	121	119	120	121	117
121	120	122	120	119	119
116	119	119	119	120	118
120	119	121	116	121	120
118	118	115	119	118	115
118	118	119	118	118	115
116	118	115	117	116	114
116	114	118	118	115	117
113	114	115	114	115	115
116	116	116	116	116	115
115	114	115	116	110	115
114	111	113	114	113	113
116	112	115	113	112	109
113	112	112	111	112	113
109	112	111	112	112	108
111	107	108	111	110	111
110	108	110	110	111	110
112	111	110	113	108	109
111	109	109	109	109	112
109	101	107	108	110	108
108	106	108	108	109	154
244	209	93	0 6	0 0	0 0
0	0 0				

Figure 55B

MEASUREMENT NO 9

POINTS ALONG X-AXIS

245	245	245	218	152	185
199	190	189	189	189	189
189	197	187	186	186	184
185	185	185	185	183	183
185	184	184	183	182	181
181	183	182	181	182	181
179	180	181	182	181	181
182	181	180	180	182	180
180	180	180	180	180	180
179	179	180	178	178	179
179	178	179	179	178	177
178	179	178	178	177	178
177	178	177	178	177	176
177	177	176	176	176	176
176	176	176	177	175	174
174	175	174	190	244	202
167	155	155	152	153	152
152	157	151	152	152	151
150	151	152	151	152	151
153	152	151	150	149	152
150	149	149	148	149	148
149	147	148	148	149	149
147	146	146	147	146	146
148	147	147	146	147	146
145	147	147	148	146	146
146	145	146	146	145	146
148	146	145	144	146	146
145	145	144	145	144	142
144	145	144	145	147	145
143	144	144	145	146	143
143	144	142	142	143	142
140	141	141	140	142	141
142	143	142	143	144	143
141	142	140	141	141	141
141	141	141	141	141	141
140	141	140	140	141	138
139	139	141	140	142	140
138	139	139	139	139	138
138	137	137	137	137	139
137	137	137	135	134	136
135	136	134	134	135	136
136	137	135	136	135	135
136	136	135	133	135	134
133	135	134	135	136	133

Figure 56A

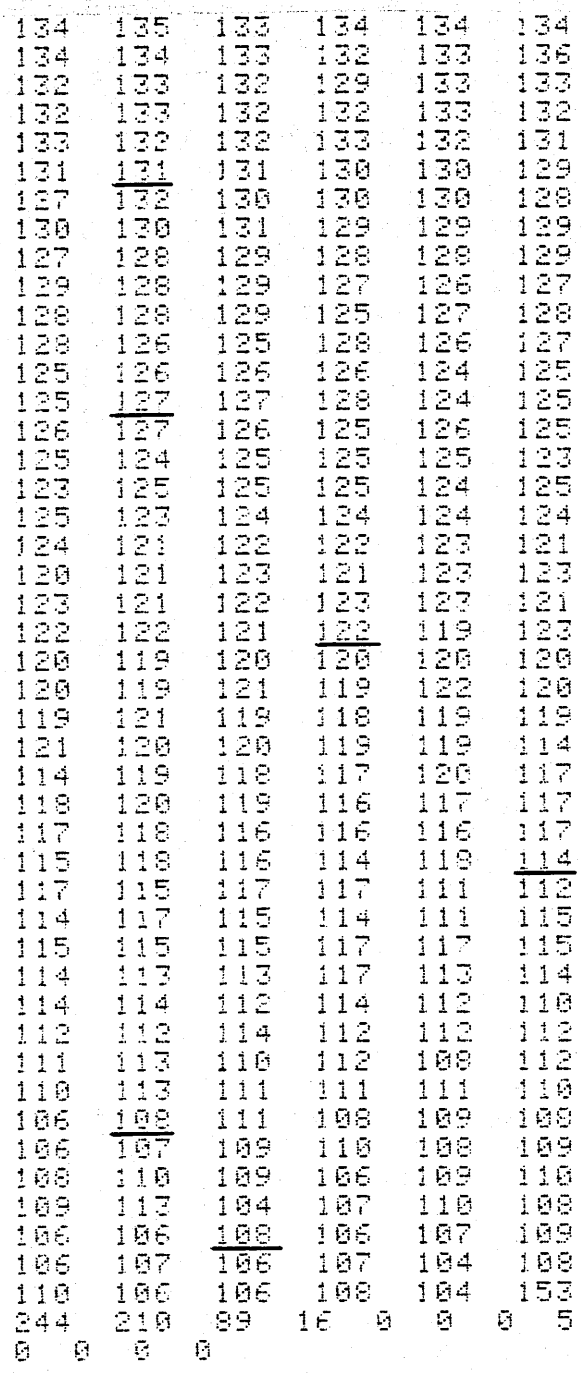

Figure 56B

MEASUREMENT NO 10

POINTS ALONG X-AXIS

245	245	245	217	152	185
199	190	189	189	189	189
189	186	187	186	185	183
184	186	185	184	184	183
185	184	183	183	182	181
182	183	181	181	182	180
181	181	182	182	182	181
182	181	181	181	182	181
181	181	180	180	180	180
179	179	179	180	178	178
178	179	179	179	179	179
179	179	178	178	178	178
177	178	177	178	178	177
177	176	176	175	176	176
176	177	176	176	175	175
174	173	174	192	245	230
168	155	153	151	152	151
151	152	150	149	150	150
150	149	151	149	148	149
149	149	150	149	149	150
149	146	148	148	146	145
149	148	145	147	146	147
146	146	146	147	145	145
147	146	147	145	147	145
146	145	147	146	146	143
142	143	145	143	144	145
145	143	144	143	144	144
144	143	143	143	143	143
145	141	142	142	143	143
142	142	142	142	142	143
142	141	140	141	140	142
140	139	140	138	141	140
140	139	141	142	141	140
139	139	139	139	139	137
139	137	140	139	140	139
139	138	139	139	138	136
140	137	138	136	138	138
137	135	136	137	136	137
137	138	134	135	134	134
137	136	134	137	135	135
134	135	134	135	135	137
135	136	135	131	134	133
133	133	133	133	134	133
131	132	135	132	134	135

Figure 57A

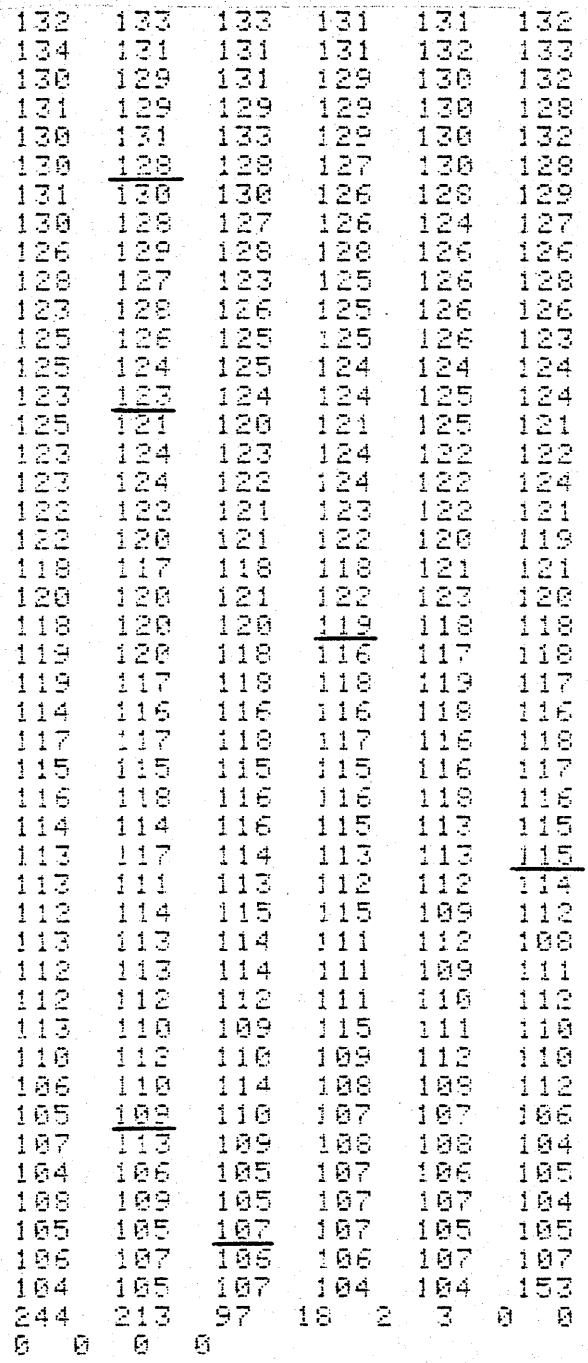
132 133 133 131 131 132
134 131 131 131 132 133
130 129 131 129 130 132
131 129 129 129 130 128
130 131 133 129 130 132
130 128 128 127 130 128
131 130 130 126 128 129
130 128 127 126 124 127
126 129 128 128 126 126
128 127 123 125 126 128
123 128 126 125 126 126
125 126 125 125 126 123
125 124 125 124 124 124
123 123 124 124 125 124
125 121 120 121 125 121
123 124 123 124 122 122
123 124 122 124 122 124
122 122 121 123 122 121
122 120 121 122 120 119
118 117 118 118 121 121
120 120 121 122 123 120
118 120 120 119 118 118
119 120 118 116 117 118
119 117 118 118 119 117
114 116 116 116 118 116
117 117 118 117 116 118
115 115 115 115 116 117
116 118 116 116 118 116
114 114 116 115 113 115
113 117 114 113 113 115
113 111 113 112 112 114
112 114 115 115 109 112
113 113 114 111 112 108
112 113 114 111 109 111
112 112 112 111 110 112
113 110 109 115 111 110
110 112 110 109 112 110
106 110 114 108 109 112
105 109 110 107 107 106
107 113 109 108 108 104
104 106 105 107 106 105
108 109 105 107 107 104
105 105 107 107 105 105
106 107 106 106 107 107
104 105 107 104 104 153
244 213 97 18 2 3 0 0
0 0 0 0

Figure 57B